12-15-2014

Modeling Mussel Mortality: Investigating the Importance of Swash and the Potential Implications of Changing Wave Environments

Shadow Leigh Gulledge
University of South Carolina - Columbia

MODELING MUSSEL MORTALITY: INVESTIGATING THE IMPORTANCE OF SWASH AND THE POTENTIAL IMPLICATIONS OF CHANGING WAVE ENVIRONMENTS

by

Shadow Leigh Gulledge

Bachelor of Science
University of South Carolina, 2012

Submitted in Partial Fulfillment of the Requirements

For the Degree of Master of Earth and Environmental Resources Management in

Earth and Environmental Resources Management

College of Arts and Sciences

University of South Carolina

2014

Accepted by:

Jean Taylor Ellis, Director of Thesis

Brian Helmuth, Reader

John Kupfer, Reader

Joe Quattro, Reader

Lacy Ford, Vice Provost and Dean of Graduate Studies

DEDICATION

This thesis is dedicated to my dad, Daniel Fockler, who passed away on June 5, 2014, while I was preparing this manuscript. Thank you for supporting me and pushing me to achieve my goal. You helped in so many different ways which made this process much easier to get through. I am now and will always be grateful to you. I am blessed to have had such an incredible father. I love you so much and will miss you greatly. May you rest in peace.

ACKNOWLEDGEMENTS

I am extremely grateful to my advisors, Brian Helmuth and Jean Ellis, for their guidance, expertise and support throughout my graduate studies. I am also grateful that I had John Kupfer and Joe Quattro on my committee to provide advice and encouragement during my time as a graduate student. I would like to thank past and present members of the Helmuth lab (Allison Matzelle, Mackenzie Zippay, Cristián Monaco, Nicole Kish, Nick Colvard & Josie Iacarella) for their effort, support and friendship. My thanks also go out to April South who always had a teaching position for me in Biology 102 Lab.

There were also several people outside of USC that were responsible for helping me succeed. I would like to thank my best friend, Jesselyn West, for all of her support and for helping me during my times of great stress. Your friendship is invaluable and greatly appreciated. I would like to thank my mom, Sheila Gross, my stepdad, Kevin Gross, my father-in-law, William Gulledge, my dad, Daniel Fockler, and my brother, Joe Boyes, for their encouragement and kindness. Also, I would like to thank my family in Winnsboro, Ohio, and Florida as well as my husband's family all over South Carolina for their support and understanding. To everyone who played a part in helping me succeed, your love was tremendously helpful and I am lucky to have such an amazing family.

Finally, I would like to acknowledge my husband, Alex Gulledge. You are my guiding light and the reason I have been able to be so successful. I am exceptionally fortunate to have someone who supports and loves me as much as you do. Thank you for everything you have done for me. I love you.

ABSTRACT

Rising sea level and increases in temperature are causing biogeographic shifts in intertidal zones and can also lead to shifts in the local vertical zonation of organisms due to changes in body temperature during aerial exposure during low tide. Swash is an important determinant of aerial body temperatures, and vulnerability of intertidal zones to changes in climate could potentially depend on how much and how often animals are cooled by waves. While wave heights (and thus swash) are generally expected to increase with climate change, anthropogenic physical structures, such as breakwaters and wave energy converters, can decrease wave height and swash. Here I explore the ability of a simple biophysical model of aerial body temperature to predict how changing wave climates might affect intertidal zones in California. A key limitation is that biophysical models frequently rely on input data from weather stations that are limited in their spatial coverage. An attractive alternative is to use larger-scale reanalyzed data with global coverage, but the accuracy of the models that use these data has not been evaluated in the context of sensitivity to swash.

This study examines the sensitivity of mussel (*Mytilus californianus*) aerial body temperature to changing atmospheric, oceanographic, and morphological parameters. Specifically, it compares model predictions using coarse gridded weather data from NOAA NCEP Climate Forecast System Reanalysis (CFSR), versus local weather station data as environmental inputs. A sensitivity analysis was conducted to determine whether

precise details of mussel morphology and site topography are needed, or whether more generic estimates can be used. The model was used to explore the potential impacts of changing wave climates on mussel temperatures by considering current and potential future wave heights at four locations in California (Bodega Bay, Hopkins, Alegria and Coal Oil Point). In all cases model results were ground-truthed against *in situ* measurements of temperature made using biomimetic sensors using both standard measures of error (average absolute difference and RMSE) as well as metrics of physiological state based on mussel performance curves.

Model results demonstrated that body temperatures predicted using rough estimates of mussel absorptivity, mussel size, cloud cover, absolute shore level (ASL), effective shore level (ESL) slope and ASL plus ESL slope were very close to those generated using organism- and site-specific parameters. At Bodega Bay, the model successfully predicted maximum daily aerial body temperatures to within a few degrees using both *in situ* weather station (average absolute error 3.2°C) and CFSR data (error 3.3°C). Model error using CFSR data for the other locations was considerably higher (error: Hopkins Marine Station, 6.8°C; Alegria, 6.5°C; Coal Oil Point, 8.5°C). Physiologically, the model ran cold at Bodega and Hopkins but ran hot at Alegria and Coal Oil Point. Sensitivity analyses suggested that mussel temperatures were most sensitive to changes in the nearshore wave climate at Bodega Bay and Hopkins and least sensitive at Alegria and Coal Oil Point. Due to the overall inaccuracy of this model when using CFSR data, the use of this method by decision makers should be approached with caution. This study suggests that additional analyses using a tailored site-specific model are required.

TABLE OF CONTENTS

LIST OF TABLES

LIST OF FIGURES

CHAPTER 1

INTRODUCTION

1.1. BACKGROUND

The rocky intertidal zone has been a focus of extensive study, in part due to the presence of steep environmental gradients created by the rise and fall of the tide. Intertidal organisms are often assumed to live at or near their thermal limits of heat tolerance for survival and reproduction (Denny et al. 2011; Foster 1969; Jones et al. 2009; Jost and Helmuth 2007; Somero 2002; Tomanek and Helmuth 2002), especially at the upper, landward edges of their intertidal distributions (Smith 2010). It has also been shown that behavioral ecology (Wolcott 1973) and microclimate-influenced phenotypic plasticity (Davenport and Davenport 2005) can limit the upper boundaries for some invertebrate species. Organisms within this habitat are typically marine in their evolutionary history (Harley 2007). However, due to emersion during low tide, they must also contend with stressful abiotic factors associated with terrestrial conditions (Jones et al. 2009; Mislan et al. 2011; Pincebourde et al. 2012; Smith 2010; Stillman 2002). Aerial exposure can cause desiccation and extreme changes in body temperature (Denny 2006). Therefore, the timing of extreme (spring) low tides can have major implications for the growth, survival and reproduction of intertidal invertebrates and algae (Dayton 1971; Harley 2008; Stillman and Somero 1996).

Vertical zonation in the intertidal – the replacement of one dominant species by another along a vertical gradient from the sea to the land – has been attributed to multiple

environmental factors, including wave exposure, substrate characteristics, and tidal regime (Harley and Helmuth 2003), coupled with characteristics of the organism such as mobility and physiological tolerances (McNeill 2010). A central concept that has emerged over decades of study is that the upper vertical limit of intertidal species is set by physical factors associated with terrestrial conditions, such as solar radiation and wave-exposure, and the lower vertical limit is set by biological factors, such as competition and predation (Connell 1972; Harley 2007; McNeill 2010; Raimondi 1988; Stillman 2002; Wethey 1983; Wolcott 1973).

Vertical zonation patterns have been described using different approaches. Stephenson and Stephenson (1949) introduced a universally applicable zonation system based on the distribution of dominant species; i.e. biologically-defined zonation. They defined the most terrestrial margin of the intertidal the supralittoral zone; moving successively closer to the water they defined the supralittoral fringe, midlittoral zone, infralittoral fringe and infralittoral zone. The midlittoral zone is frequently defined as the region dominated by mussels (Stephenson and Stephenson 1949). An alternative approach is to define zonation based on the physical characteristics as driven by the tidal cycle. The concept of critical tide factors was introduced by Doty (1946). He divided the intertidal into eight zones based on how tidal cycles drive exposure time: below lowest lower low water, LLLW – mean lower low water, MLLW – lowest higher low water, LHLW – highest higher low water, HHLW – lowest lower high water, LLHW – lowest higher high water, LHHW – highest higher high water, and above HHHW (see Fig. 1.1) (Doty 1946; Doty and Archer 1950). The division of these zones, as defined by Doty (1946), is based on tidal benchmarks approximating the temporal distribution of emersion

and submersion time. Doty and Archer (1950) designated these tidal stages as “critical” because with only a slight increase in vertical height an organism may have an abrupt two- or three-fold change in its exposure time to terrestrial or marine conditions.

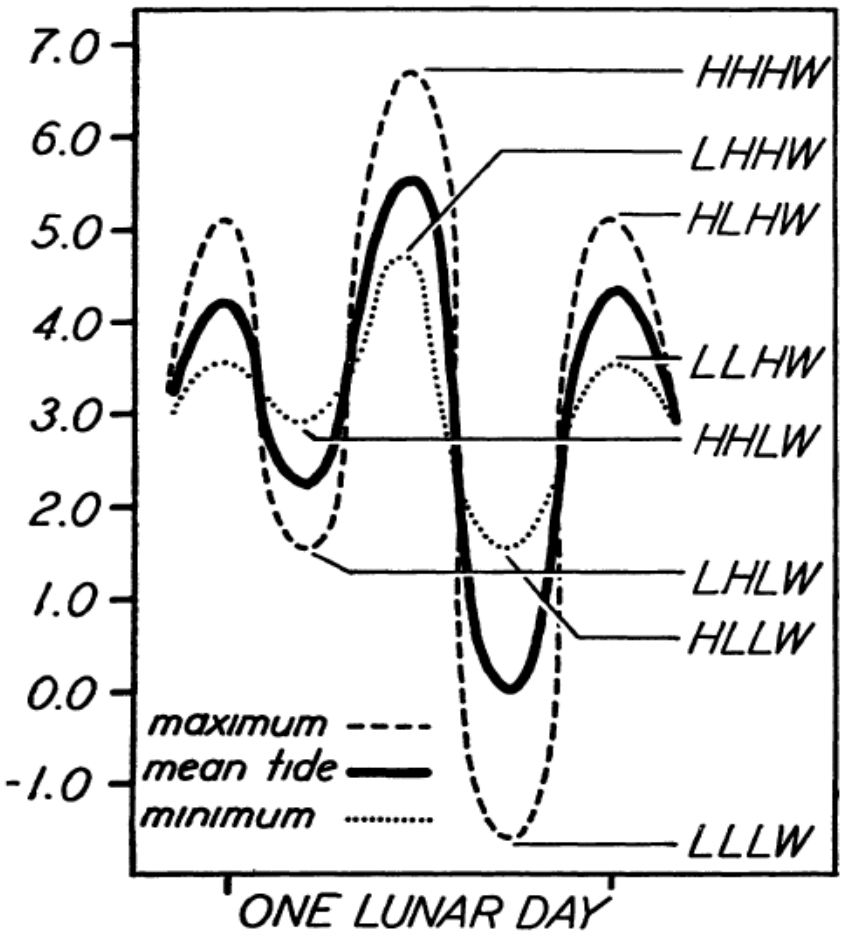

Figure 1.1 Illustration of critical tide factors as defined by Doty (1946). Figure shows the tidal elevation levels in feet relative to mean lower low water (MLLW) for San Francisco, CA on 06/19/1945. Figure source: Doty and Archer (1950).

Perhaps the biggest modifier of the effects of aerial exposure, and one that confounds patterns of zonation both within and among shores, is swash, which is also referred to as wave run-up (Burrows et al. 1954; Colman 1933; Underwood 1972, 1978, 1981, 2000; Underwood and Jernakoff 1984; Wolcott 1973). The physical impacts of waves on organisms have been extensively examined (e.g. Burrows et al. 2008; Denny

1995, 2006; Doty 1946; Gaylord 1999; Harger 1970; Harley 2007; Lawson 1957; Leigh et al. 1987; Smith 2010), and comparisons between "wave protected" and "wave exposed" shores abounds in the literature (Blanchette 1997; Boulding 1990; Boulding and VanAlstyne 1993; Brown and Quinn 1988; Connell 1972; Denny et al. 2006; Etter 1989; Fitzhenry et al. 2004; Harley and Helmuth 2003; Helmuth et al. 2006a; Pincebourde et al. 2012). Although methods for quantifying the effects of swash, and potential changes in swash, on intertidal temperatures are rare, such studies do exist (i.e. Gilman et al. 2006a; Harley and Helmuth 2003; Smith 2010).

The Pacific Ocean has a large fetch length that has the potential for large waves to be generated that can deliver 300 Watts of power over a 0.01 m portion of intertidal zone, producing an estimated 2,100 TWh of energy (Denny 2006; Leigh et al. 1987; MMS 2006). While high onshore wave heights can be detrimental to intertidal organisms (Connell 1972; Dayton 1971; Denny 1995; Leigh et al. 1987; Smith 2010; Sousa 1979), the associated swash, which runs up the rocks and cools organisms during aerial exposure at low tide (Fitzhenry et al. 2004; Harley and Helmuth 2003; Smith 2010), also benefits many organisms (Denny 2006). Any change in wave height is therefore potentially a concern because decreased swash could lead to increases in aerial body temperature that could potentially alter mortality and physiological performance (Helmuth et al. 2011). Conversely, increases in swash can theoretically mitigate increases in stress caused by higher air temperatures (Helmuth et al. 2011).

The Bureau of Ocean Energy Management (BOEM) is working with the Pacific Coast states of the U.S. to determine optimal locations for wave energy farms (MMS 2006; Paasch et al. 2012). These wave energy farms are expected to provide a source of

clean renewable energy (MMS 2006). Depending on how and where such farms are emplaced, they could cause a reduction in nearshore wave height (Boehlert and Gill 2010; MMS 2006; Millar et al. 2007; Paasch et al. 2012; Palha et al. 2010; Smith et al. 2012); however, the extent to which the waves will be reduced as well as the effects on intertidal organisms have not yet been determined (MMS 2006).

The goal of this project is to create a modeling framework that will inform policy decisions for wave energy farms by quantitatively examining the role of swash on the survival of California mussels. An eventual goal is to combine the model with a physiological model, such as a dynamic energy budget (DEB) model (i.e. Sarà et al. 2013), so that changes in growth and reproduction can be calculated (Kearney et al. 2010), and to develop similar models for other intertidal species. The objective is to use a biophysical heat budget model (adapted from Helmuth et al. 2011) to examine how swash affects the survival of *Mytilus californianus*, and to use these data to determine which sites are most sensitive to changing wave climates. These data can influence where wave energy farms should be placed to have minimal effect on intertidal organisms. It will also inform the likely impacts of climate change as the zonation of rocky intertidal organisms is affected by changes in temperature and sea level rise. Determining how the sensitivity of rocky intertidal organisms to swash varies along the coastline is important for informing decision makers of the implications of installing wave energy farms.

1.2. Ecology of the Study Organism

The model organism for this study is the California ribbed mussel, *Mytilus californianus*. This filter-feeding mussel on the west coast of North America ranges from the Aleutian Islands (Alaska) to southern Baja California (Mislan and Wethey 2011;

Zippay and Helmuth 2012). This species resides in the low to mid intertidal zone on exposed shores and because California mussels tend to outgrow their competitors, they are competitive dominants for space (Dayton 1971; Menge 1976; Paine 1966, 1974). Individuals typically live in a habitat with heavy wave action and, to protect themselves in this environment, they aggregate together and create dense homogeneous beds (Zippay and Helmuth 2012) that provide structure and stability to the ecosystem (Jones et al. 2010). Mussel beds serve as a habitat and refuge for other organisms, such as algae, microinvertebrates, and fish (Kanter 1977; Smith et al. 2006; Suchanek 1979). The mussels also provide food to sea stars, drilling whelks, crabs and lobsters (Menge et al. 1994; Sanford 2002; Jubb et al. 1983; Robles et al. 1990). These characteristics make them an integral part of the rocky intertidal ecosystem creating a unique community of plants and animals.

California mussels often compete for space in the mid-intertidal zone with barnacles, such as *Balanus* spp., *Mitella* spp. (Paine 1966) and *Chthamalus anisopoma* (Raimondi 1988). Mussels endure a predator-prey relationship with sea stars, *Pisaster* spp., and the predation by the sea stars sets the lower vertical limit of mussels (Leigh et al. 1987; Paine 1966; Sanford et al. 2003). Organismal body temperatures tend to be highest during aerial exposure (Jones et al. 2009; Mislan and Wethey 2011) on warm, sunny days when low tide occurs in the middle of the day and there is a low amount of wave splash (Helmuth 2002; Wolcott 1973). During this time the organism's body temperature can change more than 20°C (Helmuth 1998; Mislan and Wethey 2011). Hence, temperature and desiccation are typically assumed to be the two factors that limit

most organisms' upper vertical limits, including the California mussel (Connell 1972; McNeill 2010; Wolcott 1973).

Many intertidal animals regularly experience temperatures close to their lethal temperature during summer months (Jones et al. 2010; Smith 2010), although recent evidence suggests that near lethality may occur at fewer sites than previously assumed (Mislan et al. 2014). Thus, if wave energy farms cause a reduction of wave height and swash, the organisms' maximum aerial body temperature may reach lethal levels. At sites where aerial body temperature is closely tied to a decrease in upper zonation limits (Harley and Helmuth 2003; Mislan et al. 2014), a decrease in potential swash could cause a reduction in the upper zonation limit and, consequently, the abundance of *Mytilus californianus*.

Mussels are intricately intertwined with the organisms of the intertidal habitat, playing a key role in the stability of this ecosystem (Berlow 1999; Bernhardt and Leslie 2013; Connell 1972; Lively et al. 1993; Menge 1976; Paine 1966, 1974; Pincebourde et al. 2008). Dense mussel beds enhance the overall biodiversity of the intertidal zone by creating a microhabitat for a variety of organisms (Cimberg 1975; Kanter 1977, 1980; Menge et al. 1994; Suchanek 1979). However, researchers have found that this community of squatters is rapidly declining in abundance and diversity (Smith et al. 2006). For example, there are approximately 4,000 individual porcelain crabs per square meter living within mussel beds (Stillman 2002). Therefore, if mussel density is decreased, there is a consequent effect of a decrease in porcelain crab density. The overall outcome is a loss of biodiversity (Jones et al. 2010), which will inevitably change population dynamics (Wootton 2010).

A reduction in California mussels may cause cascading impacts on the entire rocky intertidal ecosystem (Berlow 1999; Wootton 2010). If a prominent (engineering) intertidal species such as mussels disappear, there is a higher risk of other species invading the area causing a change in the ecosystem structure, and subsequently, ecosystem function (Jones et al. 2010). Overexpansion of an existing species in the intertidal zone is another possible outcome (Tsuchiya 1983). Wootton (2010) found that with the removal of *Mytilus californianus* there was a change in mid intertidal space dominance, with the new champion being the algae, *Corallina vancouveriensis*. Reduced wave height could result in a decrease in mussel density due to mussels surpassing their lethal temperatures. From this it can be surmised that temperature may indirectly impact community structure and function (Tomanek and Helmuth 2002).

1.3. Methods of Calculating Swash

Swash is related to effective shore level (ESL) (Fitzhenry et al. 2004; Gilman et al. 2006a) and absolute shore level (ASL) (Gilman et al. 2006a; Harley and Helmuth 2003; Helmuth et al. 2011; Mislan et al. 2011; Wolcott 1973). The ESL is the still-water tidal elevation at which the organism is first wetted by water, usually detected by a decrease in body temperature (Harley and Helmuth 2003). The ASL is the height of an organism above the still-water chart datum (i.e. MLLW), which is always static in reference to the organism (Gilman et al. 2006a), and is a measure independent of swash. Subtraction of the ESL from the ASL provides an estimate of swash (Harley and Helmuth 2003), i.e. the vertical distance that waves effectively "move" the still tide level (Fig. 1.2).

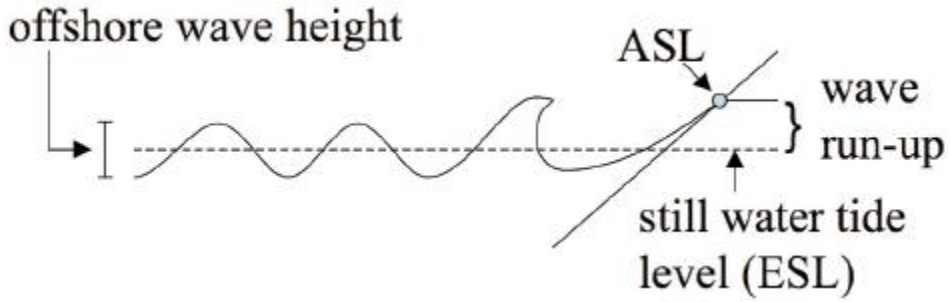

Figure 1.2 Relationship between ASL, ESL and a point on the shore (circle). "Wave run-up" represents the swash. Figure source: Gilman et al. (2006a).

Several studies have used ESL to understand the effects of swash on mussel body temperatures (Gilman et al. 2006a; Mislan et al. 2011; Smith 2010). Harley and Helmuth (2003) presented a method to estimate ESL through temperature drops and used ESL as a measure of examining the vertical zonation limit of the California mussel and the barnacle species *Balanus glandula*. They found that ESL is an indicator of swash (termed "wave splash" in their publication) and is a reliable predictor of where these organisms will be vertically located on the shore. Gilman et al. (2006a) related ESL and swash through an ESL regression calculation technique and plotted the difference between ASL and ESL as a function of significant wave height. The slope of the regression equation, which is unique to a site and depends on factors such as steepness of the substratum, allows one to directly compare swash among different sites (Gilman et al. 2006a) using significant wave heights.

1.4. Research Questions

In this study, a simple biophysical heat budget model (Porter and Gates 1969; Helmuth 1999) was used to understand the likely effects of changing wave climates on intertidal mussel body temperatures. The model was adapted from Helmuth et al. (2011), and verified against *in situ* biomimetic sensors called "robomussels" or "robologgers"

(hereafter loggers; more detail provided in *Section 2.5*) (Fitzhenry et al. 2004; Helmuth et al. 2006a). While more complicated models exist (Wethey et al. 2011a), this model is relatively simple in input requirements and therefore is quite user-friendly for researchers without a modeling background. The original model was designed to use local weather station data as inputs; its effectiveness using more widely-available but more coarsely gridded data remains untested.

Because the availability of local weather station data in coastal zones is limited (Mislan and Wethey 2011), the ability to accurately predict intertidal mussel body temperatures using a data source with continuous spatial coverage, the NOAA National Centers for Environmental Prediction (NCEP) Climate Forecast System Reanalysis (CFSR), was tested (Saha et al. 2010). Only one extensive study has been completed to compare model accuracy using different sources of input data (Mislan and Wethey 2011). This study found that CFSR data, with a grid size of 32km, was a better predictor of mussel daily maximum body temperature than the four global data sets with larger grid sizes that were tested (Mislan and Wethey 2011). However, Mislan and Wethey (2011) determined CFSR was not as effective as using local weather station data.

The research presented here addresses the following questions: (1) will a model tailored to a specific site produce more accurate results than a general model using estimated parameters that can be used for multiple locations; (2) can CFSR data be used to predict aerial mussel body temperatures in place of local weather station data; and (3) how will changes in wave climate due to wave energy farms coupled with local-scale climate change affect survival and zonation of mussels, and how does sensitivity vary with wave exposure and site topography?

CHAPTER 2

METHODS

2.1. STUDY LOCATIONS

Four locations on the coast of California were selected based on local weather station (LWS) data availability and differences in nearshore oceanographic features: Bodega Bay (38.3185°N, 123.0739°W), Hopkins (36.6219°N, 121.9053°W), Alegria (34.4672°N, 120.2770°W) and Coal Oil Point (34.4067°N, 119.8783°W) (Fig. 2.1). Point Conception (34.4481°N, 120.4714°W) marks the transition from strong upwelling, high wave exposure and colder water on the northern coast to weak seasonal upwelling, low wave exposure, and warmer water on the southern coast. These varying oceanographic conditions affect the recruitment and survival of *Mytilus californianus* from site to site (Blanchette et al. 2007). Bodega Bay and Hopkins are north of Point Conception and are wave-exposed whereas Alegria and Coal Oil Point are to the south and are wave-protected.

2.2. GENERAL MODEL STRUCTURE

The model was adapted from the biophysical heat budget model presented in Helmuth et al. (2011), which is based on a model that was originally presented by Helmuth in 1999. This is a steady-state model of heat flux that assumes the study organism (*M. californianus*) will reach equilibrium within one hour of becoming either submerged in water or exposed to air. It uses physiological,

meteorological and oceanographic data to predict hourly body temperatures by calculating the surface temperature of uniformly sized mussels within a horizontal bed (Helmuth et al. 2011). The model uses significant wave heights and tidal stage predictions to estimate species emersion and swash (Harley and Helmuth 2003; Gilman et al. 2006a).

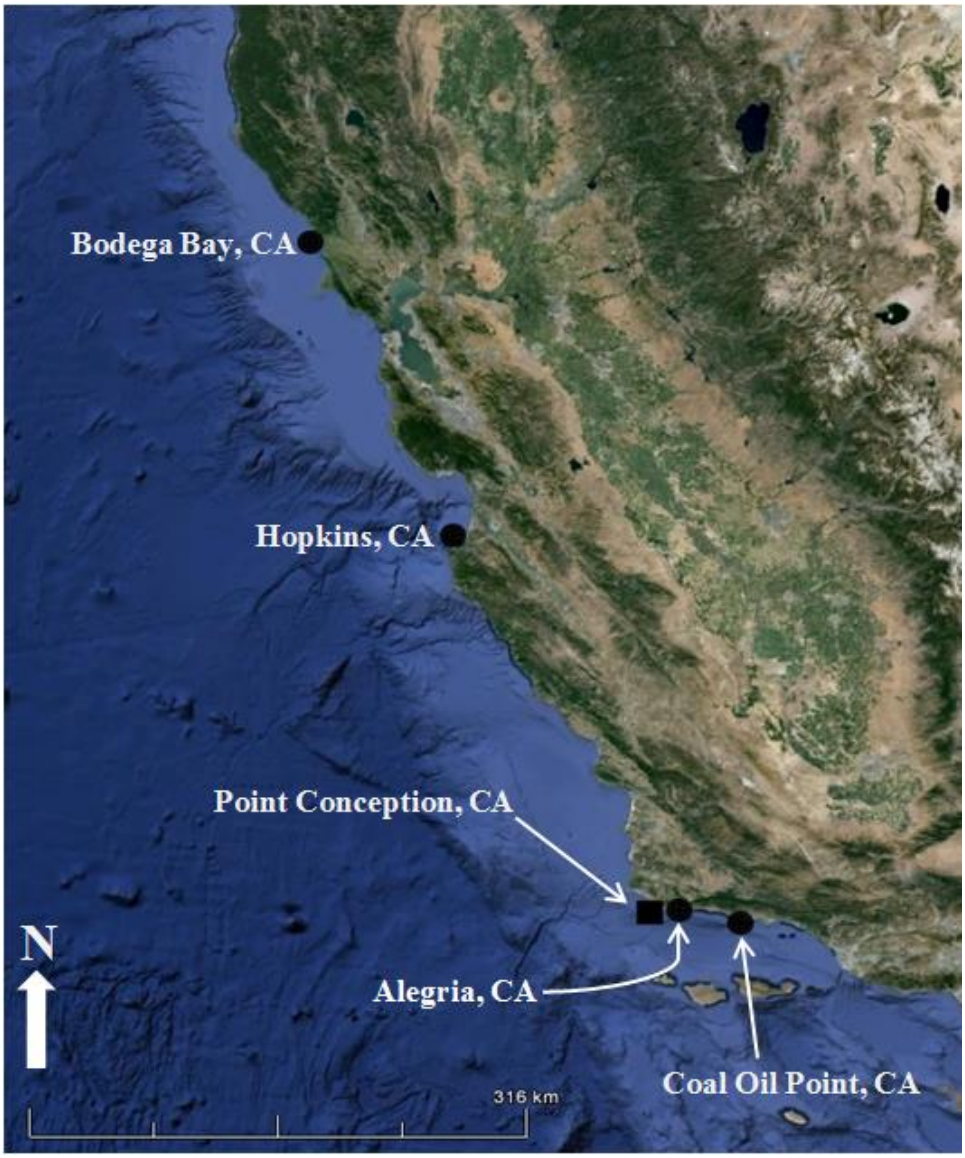

Figure 2.1 Location of study sites on the California coast. Each study site is marked with a black circle and Point Conception is marked with a square for reference. Basemap is from Google Earth (obtained June 14, 2014).

2.3. DATA COLLECTION

Six weather variables were obtained: water temperature, significant wave height, tidal stage, air temperature, solar radiation and wind speed. Historical water temperature and significant wave height data were obtained from NOAA National Data Buoy Center (Table 2.1; NDBC 2013). Tidal stage data were obtained from XTide (Table 2.1; WWW Tide and Current Predictor 2013). XTide has been used by many researchers (Gilman et al. 2006b; Harley and Helmuth 2003; Helmuth et al. 2011; Mislan et al 2011; Smith 2010; Wethey et al. 2011a) and was selected here because it is easy to use and it estimates tidal heights at fixed time intervals (Flater 2013). Other weather data (air temperature, solar radiation and wind speed) were obtained either from a local weather station or from NOAA NCEP CFSR (NOMADS Data Access 2013). The model was run using local weather station data (Table 2.1) or CFSR data for Bodega Bay and Hopkins Marine Station in Pacific Grove. Predictions for Alegria and Coal Oil Point only used CFSR weather data. For all study sites the minimum wind speed was set to 0.25 m/s to account for free convection, i.e., the assumption that coastal air is never truly still. Any negative solar radiation values were removed from the analysis. All cloud cover values were set to 0.60, which equates to an intermediate amount of cloud cover.

When the model was run using CFSR data air temperature, solar radiation and wind speed were obtained from NOAA NCEP CFSR. The 'high resolution' option was chosen when gathering the data for each variable using a bounding box of 32°S, 42°N, -129°W and -118°E. Additional processing of these data narrowed the geographic range to each study site. The temporal duration for this study was determined to ensure continuous study periods across all sites, which is required for accuracy assessment (Table 2.1).

Table 2.1 Location of weather data sources for all study sites. Local weather station data were not obtained for Alegria or Coal Oil Point.

	Bodega Bay	Hopkins	Alegria	Coal Oil Point
Time Frame	7/9/04 – 12/31/08	7/1/00 – 6/30/05	10/1/00 – 9/30/09	11/1/03 – 10/31/09
NOAA Buoy Number	46013	46042	46054	46053
NOAA Buoy Coordinates	38.24°N, 123.30°W	36.79°N, 122.47°W	34.27°N, 120.48°W	34.26°N, 119.88°W
Distance of NOAA Buoy from Study Site (km)	22.02	54.11	29.15	16.67
X-Tide Location	Bodega Harbor Entrance	Monterey	Gaviota	Santa Barbara
X-Tide Coordinates	38.30°N, -123.05°W	36.61°N, -121.89°W	34.47°N, -120.22°W	34.41°N, -119.69°W
Distance of X-Tide Location from Study Site (km)	2.82	2.09	5.49	17.48
Local Weather Station	BOON[1]	HMS[2]		

[1]Bodega Ocean Observing Node maintained by the University of California – Davis (http://bml.ucdavis.edu/boon/data_access.html)
[2]Hopkins Marine Station (Stanford) maintained by Dr. Mark Denny (http://mlo.stanford.edu/wdataarchive.htm)

2.4. Sensitivity Analyses

Sensitivity analyses were conducted for the Bodega Bay site to examine the separate influences of changes in mussel size, mussel absorptivity, absolute shore level (ASL), effective shore level (ESL) slope and cloud cover, and the interactive influences

of changes in ASL and ESL slope on *M. californianus* body temperature. Local weather station data were used for the sensitivity analyses (Table 2.2).

Logger ASLs, regression ASLs and regression ESLs (Table 2.2) were calculated using the method described in Gilman et al. (2006a). In brief, rapid temperature drops are used as indicators of when a logger is first splashed by waves. The estimated still tidal level at the first temperature drop is the "ESL" on that day. By plotting these ESLs versus significant wave height, the ESL of any logger is estimated as a function of significant wave heights. Higher slope values of this regression indicate that for each meter of wave height, the swash is greater. This approach can also be used to estimate the ASL by recording the y-intercept of the regression, i.e. when wave heights are zero. This latter approach is not as accurate as direct measurements using surveying equipment, but provides a means of estimating ASL and ESL from temperature data (Gilman et al. 2006a).

To complete the regression the logger recorded temperatures and the significant wave height in 10 minute intervals were run through SiteParser (described in Gilman et al. 2006a). This program provides the daily tide heights at which the logger's temperature drops by 2.5°C (indicating the logger being splashed by waves). Regression analysis was completed to compare the daily tide heights provided by SiteParser (y-axis) versus the daily maximum significant wave height (x-axis). The y-intercept value of this regression equation provides the ASL and values of ESL are determined as a function of significant wave height, with steeper slopes indicating a greater sensitivity of swash to wave height (Gilman et al. 2006a). The term "ESL slope" used here refers to the slope values that

were either estimated to be 0.25 m or calculated using the regression technique, rather than the ESL, per se.

The Logger ASLs are different from the regression ASLs because of the different time frames used. The logger ASL was obtained using several different years of data (not reported here) and the regression ASL was obtained using data from 7/9/2004 – 7/9/2005, one year that was included in the time frame used for all Bodega Bay analyses. This also explains why the predicted high intertidal zone ASL values are similar to, or in some cases, lower than the mid intertidal zone loggers (Table A.4). Both values were determined using the regression technique however different time frames were used. Although the logger temperatures led to rather low ASL estimates it should be noted that the logger ASL does increase from the mid intertidal zone to the high intertidal zone (1.36 m to 1.56 m) as does the regression ASL (1.13 m to 1.27 m).

Table 2.2 Values used in the model for the sensitivity analyses for Bodega Bay. All models use local weather station data instead of CFSR data. The *general* model is the model that is used in the accuracy assessments (with CFSR and LWS data) as well as in the models with changing wave climates (with CFSR data). The low intertidal zone is MLLW + 0.5 m, the mid intertidal zone is MLLW + 1.5 m, and the high intertidal zone is MLLW + 2.5 m. The total number of days (N) used for the model simulations with each change in variable are indicated in the first column. This applies to all sensitivity analyses unless otherwise stated within the table or figure caption. In the ASL and ESL Slope columns, G is for the ASL and ESL slope of the general model, L is for the logger ASL, and R is for the regression ASL and ESL slope.

Variable Being Changed	Mussel Absorptivity	ASL (m)	ESL slope (m)	Mussel Size (m)	Cloud Cover
General Model	0.85	0.5, 1.5, or 2.5 LWS or CFSR	0.25	0.075	0.6
Mussel Absorptivity N = 1,450	0.8	1.5	0.25	0.075	0.6
	0.825	1.5	0.25	0.075	0.6
	0.85	1.5	0.25	0.075	0.6

Variable Being Changed	Mussel Absorptivity	ASL (m)	ESL slope (m)	Mussel Size (m)	Cloud Cover
	0.875	1.5	0.25	0.075	0.6
	0.9	1.5	0.25	0.075	0.6
Mussel Size (m) N = 1,450	0.85	1.5	0.25	0.05	0.6
	0.85	1.5	0.25	0.06	0.6
	0.85	1.5	0.25	0.07	0.6
	0.85	1.5	0.25	0.075	0.6
	0.85	1.5	0.25	0.08	0.6
	0.85	1.5	0.25	0.09	0.6
	0.85	1.5	0.25	0.10	0.6
	0.85	1.5	0.25	0.11	0.6
	0.85	1.5	0.25	0.12	0.6
	0.85	1.5	0.25	0.13	0.6
	0.85	1.5	0.25	0.14	0.6
	0.85	1.5	0.25	0.15	0.6
	0.85	1.5	0.25	0.175	0.6
	0.85	1.5	0.25	0.20	0.6
	0.85	1.5	0.25	0.225	0.6
	0.85	1.5	0.25	0.25	0.6
Cloud Cover N = 1,447	0.85	1.5	0.25	0.075	0.6
	0.85	1.5	0.25	0.075	Norm.
ASL (m) Low N = 524 Mid N = 1,386 High N = 1,345	0.85	0.5	0.25	0.075	0.6
	0.85	1.5	0.25	0.075	0.6
	0.85	2.5	0.25	0.075	0.6
	0.85	0.69 L. Low	0.25	0.075	0.6
	0.85	1.36 L. Mid	0.25	0.075	0.6
	0.85	1.56 L. High	0.25	0.075	0.6
	0.85	0.43 R. Low	0.25	0.075	0.6
	0.85	1.13 R. Mid	0.25	0.075	0.6
	0.85	1.27 R. High	0.25	0.075	0.6
ESL slope (m) Low N = 637 Mid N = 1,450 High N = 1,375	0.85	0.5	0.25	0.075	0.6
	0.85	1.5	0.25	0.075	0.6
	0.85	2.5	0.25	0.075	0.6
	0.85	0.5	0.06 R. Low	0.075	0.6
	0.85	1.5	0.16 R. Mid	0.075	0.6

Variable Being Changed	Mussel Absorptivity	ASL (m)	ESL slope (m)	Mussel Size (m)	Cloud Cover
	0.85	2.5	0.12 R. High	0.075	0.6
ASL (m) & ESL slope (m) Low N = 637 Mid N = 1,446 High N = 1,371	0.85	0.5 G. Low	0.25 G. Low	0.075	0.6
	0.85	1.5 G. Mid	0.25 G. Mid	0.075	0.6
	0.85	2.5 G. High	0.25 G. High	0.075	0.6
	0.85	0.69 L. Low	0.06 R. Low	0.075	0.6
	0.85	1.36 L. Mid	0.16 R. Mid	0.075	0.6
	0.85	1.56 L. High	0.12 R. High	0.075	0.6
	0.85	0.43 R. Low	0.06 R. Low	0.075	0.6
	0.85	1.13 R. Mid	0.16 R. Mid	0.075	0.6
	0.85	1.27 R. High	0.12 R. High	0.075	0.6

Table 2.3 Number of loggers (N) used for the sensitivity analyses and accuracy assessments for each intertidal zone within each study site. The low intertidal zone is MLLW + 0.5 m, the mid intertidal zone is MLLW + 1.5 m, and the high intertidal zone is MLLW + 2.5 m.

Intertidal Zone	Bodega Bay Loggers	Hopkins Loggers	Alegria Loggers	Coal Oil Point Loggers
Low	1	1	1	2
Mid	3	3	3	2
High	1	1	1	2

2.5. Accuracy Assessment

Tests were performed for the four study sites to determine how accurate the models were at predicting mussel body temperatures during aerial exposure. These accuracy assessments were performed using LWS and CFSR data for Bodega Bay and Hopkins, and only CFSR data for Alegria and Coal Oil Point. For these analyses the tide heights used were MLLW + 0.5 m, MLLW + 1.5 m, and MLLW + 2.5 m for the low, mid

and high intertidal zones, respectively. The daily maximum values predicted by the models were compared to *in situ* measurements taken by biomimetic sensors that were designed to replicate the thermal characteristics of living *M. californianus*. These loggers are TidBit (Onset Computer Corporation) temperature sensors that were embedded in a polyester resin that mimics the size, shape and color of a 0.075 m mussel (see Fitzhenry et al. 2004; Helmuth et al. 2006a, 2006b for more details). These loggers were deployed in natural growth positions in mussel beds and data were collected at 10 min intervals. Additionally, loggers were placed on horizontal, unshaded microsites to provide standardization for the effects of topography since very large differences in temperature can occur between microsites due to the highly variable rocky intertidal topography (Helmuth and Hofmann 2001). Previous findings suggest that these loggers record temperatures to within ~2°C of living mussels (Fitzhenry et al. 2004). The number of loggers used for the accuracy assessment depended on the study site and the ASL (Table 2.3).

Logger data were downloaded from a research database maintained by the Helmuth lab at Northeastern University (Boston, MA). This searchable database, with data accessed via a map-based interface, separates aerial temperatures from submerged temperatures based on tidal stage (Research Database 2013). Logger data from this site were downloaded in one hour intervals that were then used to calculate the daily aerial average maximum temperatures. Each parameter was calculated daily as the spatial average of all loggers (i.e. average of the daily maximum for all loggers). Due to this method of calculation, the daily maximum temperatures are not identified by the spatial average and tend to underestimate the extreme temperatures experienced by the loggers.

For each day in the time series, the average difference between the model output and loggers, the absolute value of the difference between the model output and the loggers, and the root mean square error (RMSE) were calculated for the daily maximum temperatures. To assess the accuracy of the model, the average across all study days was taken. To visually compare the overall accuracy of the model, daily maximum logger temperatures were plotted as a function of daily maximum model temperatures for each intertidal zone for each site. Included on each graph is a 1:1 line which are used to illustrate how closely a model is able to predict actual body temperatures. The closer the points are to the 1:1 line, the more accurate are the model predictions. Frequency distributions of the daily maximum temperatures were used to visually display the ability of the model to predict temperatures within different thermal physiological categories defined in *Section 2.7* (*Section 3.2*).

Comparisons of the temperatures predicted by the model(s) versus those recorded by the loggers for the hottest months were conducted to determine if the model is able to accurately predict extreme temperatures during the most extreme months of the year. The months with the highest recorded daily maximum temperatures were considered to be the hottest months (Helmuth et al. 2011). Only days where all data were available for each model were graphed (i.e. Bodega Bay: Logger, LWS and CFSR all had to have a temperature present for the day in order for it to be used) (Table 2.4).

2.6. Changing Wave Climates

The effects of changing wave climates were examined by changing the significant wave height, an oceanographic input obtained from NOAA NDBC (2013; Table 2.1), within the general model (Table 2.2). The significant wave heights were changed at 5%

increments to a maximum increase (climate change scenario) and decrease (wave energy farm scenario) of ±50%. These changes were made for each intertidal zone at all sites using CFSR data as inputs instead of LWS weather data.

These data were not being compared to the logger observational data; therefore, the amount of missing data was different from the amount of data missing for the accuracy assessments (Table 2.5). For this analysis, the daily aerial maximum values predicted by the model were examined to determine the relationship between changing wave climates and mussel body temperature.

Table 2.4 Data available for accuracy assessments. The total number of days within the time frame, total number of days available for the accuracy assessments and the percentage of days in the time span where the data are available to use for the accuracy assessments is shown. The available days column provides the total sample count (N) for all accuracy assessments unless otherwise noted. Each site has these data separated by intertidal zone. The bolded intertidal zones have more missing data than data available in the time frame.

Study Site	Intertidal Zone	Total Days	Available Days	Percent Available
Bodega Bay	**Low**	1,637	512	31%
	Mid	1,637	1,324	81%
	High	1,637	1,182	72%
Hopkins	**Low**	1,826	640	35%
	Mid	1,826	1,555	85%
	High	1,826	1,443	79%
Alegria	**Low**	3,287	588	18%
	Mid	3,287	1,986	60%
	High	3,287	1,670	51%
Coal Oil Point	**Low**	2,192	500	23%
	Mid	2,192	766	35%
	High	2,192	608	28%

Table 2.5 Data available for wave climate simulations. The total number of days within the time frame, total number of days available for the wave climate simulations and the percentage of days in the time span where the data are available to use for the wave climate simulations is shown. The available days column provides the total sample count (N) for all changing wave climate simulations unless otherwise noted. Each site has this

data separated by intertidal zone. The bolded intertidal zones have more missing data than data available in the time frame.

Study Site	Intertidal Zone	Total Days	Available Days	Percent Available
Bodega Bay	**Low**	1,637	572	35%
	Mid	1,637	1,364	83%
	High	1,637	1,435	88%
Hopkins	**Low**	1,826	602	33%
	Mid	1,826	1,732	95%
	High	1,826	1,813	99%
Alegria	Low	3,287	2,598	79%
	Mid	3,287	3,208	98%
	High	3,287	3,225	98%
Coal Oil Point	Low	2,192	1,422	65%
	Mid	2,192	2,099	96%
	High	2,192	2,099	96%

2.7. TYPES OF ERROR

A variety of measures can be used to understand the degree of error (skill) of a model. To understand the sensitivity of the model to changing physiological and environmental parameters, six types of errors were calculated: average difference, absolute average difference, RMSE, the number of stressful days, the number of false positives and the number of false negatives. Each of these measures of error provides insight into a different aspect of accuracy for the model predictions. The type of error relied upon depends on the use of the model.

The daily logger temperatures were subtracted from the daily model temperature predictions to obtain the daily difference. These difference values were averaged over the entire time series to calculate the average difference between model temperatures and logger temperatures. If the model generally overestimated mussel body temperatures, the average difference was positive, while if it generally underestimated temperatures, the average difference was negative. The absolute average difference provided an average value used to describe how close the model predictions are to the actual temperatures

reported by the loggers in the field. A lower absolute average difference indicated that the model was more accurate at predicting mussel body temperatures compared to a higher absolute average difference. By measuring the average error between the model predictions and logger temperatures, the RMSE can be used to evaluate the performance of ecological models. A lower RMSE indicated a more accurate model. For all analyses, unless otherwise indicated "error" or "accuracy" refers to the absolute average difference value of daily maximum temperatures.

For several of these analyses mussel body temperatures were categorized into the following physiological framework: cold suboptimal/sublethal (<17°C), optimal (17 – 22°C) (Bayne et al. 1976), high suboptimal (22 – 30°C), high sublethal (30 – 38°C), and high lethal (≥38°C) (Denny et al. 2011; Kish 2013). When mussel body temperatures reach and/or exceed 30°C cellular damage occurs and heat shock proteins are produced (Halpin et al. 2004), which is how the category of high suboptimal and high sublethal were separated. For the sensitivity analyses, accuracy assessments and changing wave climate analyses, "cold temperatures" were those within the cold suboptimal/sublethal category (<17°C) and "stressful temperatures" are those within the high sublethal and high lethal categories (≥30°C). Days when the daily maximum body temperature reached or exceeded 30°C were considered to be stressful, and this threshold was also used for the calculation of false positives and false negatives. False positives occurred when a logger's temperature was less than 30°C but the model predicted a temperature greater than 30°C, while false negatives occurred when the logger temperature was greater than 30°C but the model predicted a temperature less than 30°C. These values provide insight into how well the model can accurately predict extreme high temperatures.

CHAPTER 3

RESULTS

3.1. SENSITIVITY ANALYSES (BODEGA BAY ONLY)

For all intertidal zones, the sensitivity of the model using local weather station (LWS) data to changes in absolute shore level (ASL; Table A.4 & Fig. 3.4), effective shore level (ESL) slope (Table A.5 & Fig. 3.5), and a combination of changes in ASL and ESL slope (Table A.6 & Fig 3.1.6) were evaluated. In addition to these parameter changes, the model for the mid intertidal zone was evaluated for sensitivity to changes in mussel absorptivity (Table A.1 & Fig. 3.1), mussel size (Table A.2 & Fig. 3.2) and Bodega Bay cloud cover (Table A.3 & Fig. 3.3). Bodega Bay was chosen because that is the location for which the original model was developed and the accuracy of the model using LWS data had already been verified (Helmuth et al. 2011). This section is divided by each of these parameters where the primary results for changes within that parameter are presented. Additional, more detailed, results for each parameter can be found in Appendix A.

3.1.1. Mussel Absorptivity

Overall, model accuracy was fairly insensitive to changes in mussel absorptivity between 0.80 (3.11°C) and 0.90 (2.99°C). The number of predicted stressful days, and number of false positives and false negatives did not change with mussel absorptivity (Table A.1). For all mussel absorptivity values, the model predicted colder temperatures than what were actually experienced by the loggers in the field (Fig. 3.1). The model

overestimated the number of cold temperatures from 101 to 169 days as mussel absorptivity values were decreased. The model underestimated the number of stressful temperatures by 19 days for all absorptivity values (Fig. 3.1B).

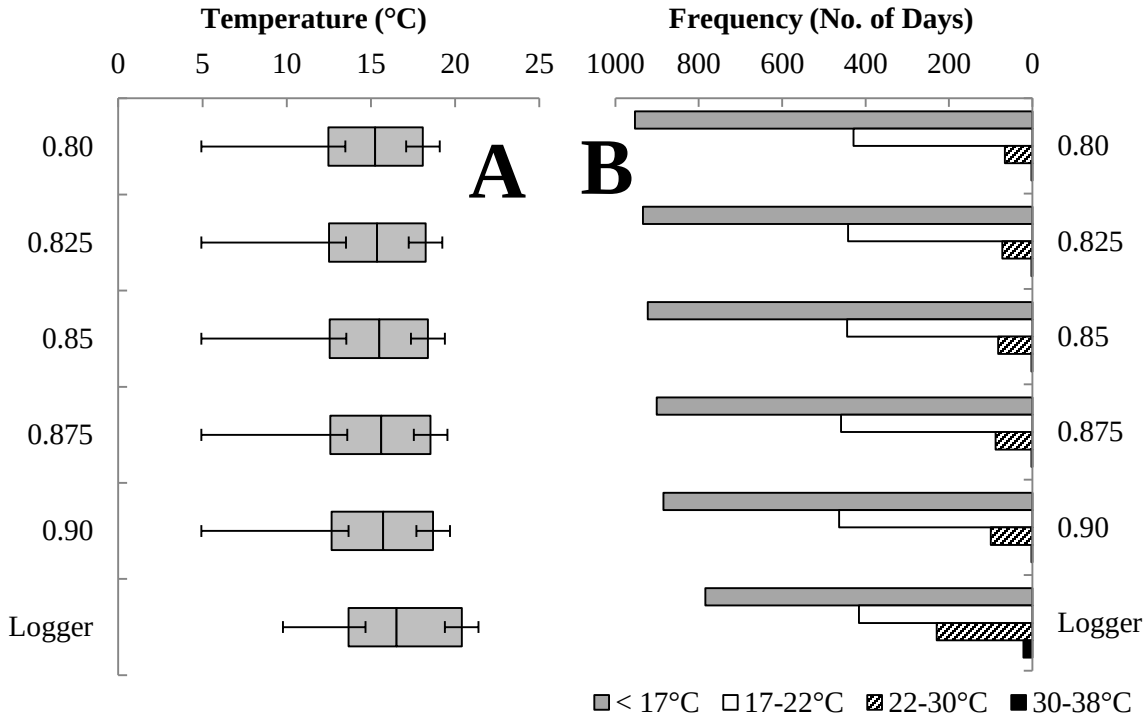

Figure 3.1 Distributions of daily maximum mussel body temperatures predicted by the general model with changing mussel absorptivity values (y-axes). **(A)** The box is the IQR, the line within the box is the median, the left side of the box is the 25th percentile, the right side of the box is the 75th percentile, the left line ends at the minimum value and the right line ends at the maximum value. **(B)** The histogram shows the frequency of the daily maximum temperatures within the four categories cold suboptimal/sublethal (< 17°C), optimal (17-22°C), high suboptimal (22-30°C) and high sublethal (30-38°C).

3.1.2. Mussel Size

The temperature predictions made by the model became more accurate as mussel size decreased, and in particular, overestimations of the number of cold temperature days were fewer at smaller mussel sizes. Using a mussel size of 0.05 m the model predicted daily maximum temperatures to within 2.88°C of the temperatures recorded by the

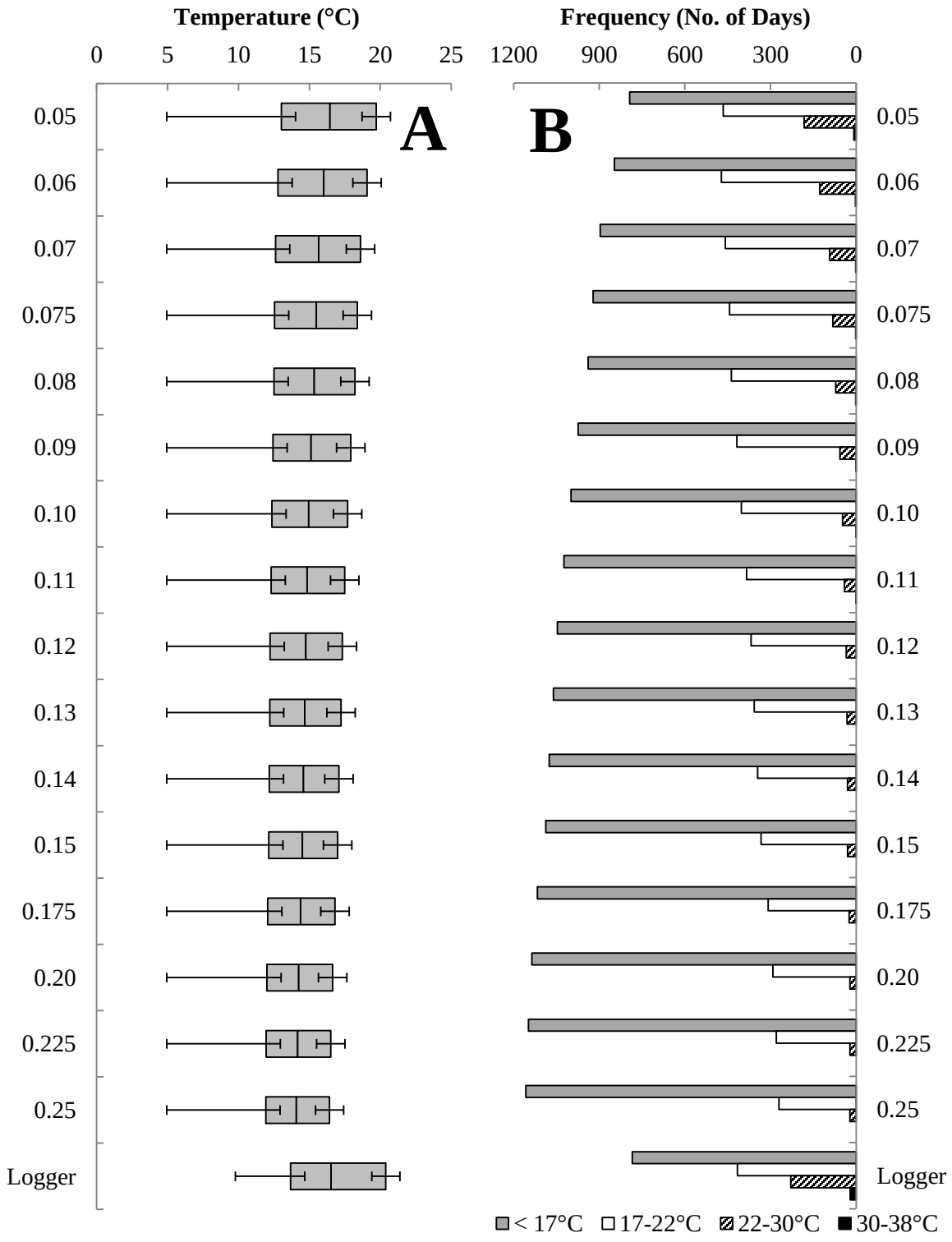

Figure 3.2 Distributions of daily maximum mussel body temperatures predicted by the general model with changing mussel size values (y-axes: meters). **(A)** The box is the IQR, the line within the box is the median, the left side of the box is the 25th percentile, the right side of the box is the 75th percentile, the left line ends at the minimum value and

the right line ends at the maximum value. **(B)** The histogram shows the frequency of the daily maximum temperatures within the four categories cold suboptimal/sublethal (< 17°C), optimal (17-22°C), high suboptimal (22-30°C) and high sublethal (30-38°C).

loggers (Table A.2). At the largest mussel size tested (0.25m), error increased to 3.68°C. At a mussel size matching those of the loggers (~0.075m), the error was 3.05°C (Fig. 3.2). The model overestimated the number of cold temperatures from 10 to 373 days as the mussel size increased from 0.05m to 0.25m. The model underestimated the number of stressful days from 13 to 21 days as the mussel size increased (Fig. 3.2B).

3.1.3. Cloud Cover

Using a generic cloud cover value of 0.60 led to more accurate body temperature predictions than using the normalized cloud cover data (3.98°C vs 4.30°C; Table A.3 & Fig. 3.3). Although both types of cloud cover caused the model to overestimate the number of cold temperature days, the use of a generic value of 0.60 led to the fewest overestimations. The model overestimated the number of cold temperatures by 137 and

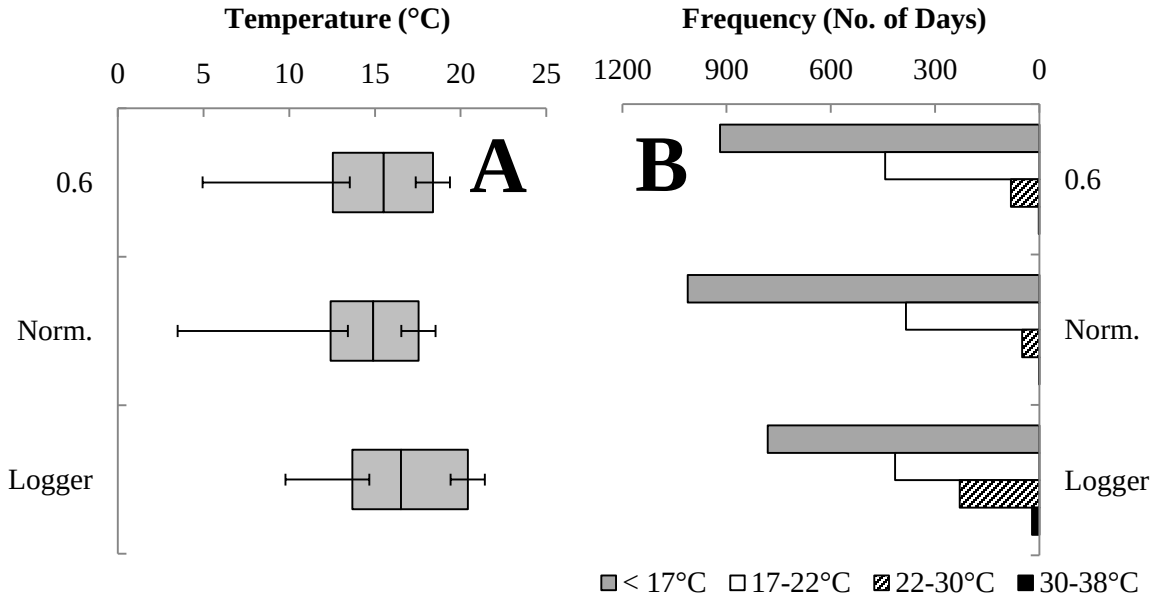

Figure 3.3 Distributions of daily maximum mussel body temperatures predicted by the general model with changing cloud cover values (y-axes). **(A)** The box is the IQR, the

line within the box is the median, the left side of the box is the 25th percentile, the right side of the box is the 75th percentile, the left line ends at the minimum value and the right line ends at the maximum value. **(B)** The histogram shows the frequency of the daily maximum temperatures within the four categories cold suboptimal/sublethal (< 17°C), optimal (17-22°C), high suboptimal (22-30°C) and high sublethal (30-38°C).

230 days and underestimated the number of stressful temperatures by 19 and 20 days using the generic cloud cover value and the normalized cloud cover data, respectively (Fig. 3.3B).

3.1.4. Absolute Shore Level (ASL)

Overall, the model temperature predictions were most accurate for the low intertidal zone and least accurate for the high intertidal zone. Generally, for each intertidal zone (low, mid, high), as the estimate of ASL increased (i.e. the logger was assumed to be higher in the zone), the accuracy of the model increased as did the number of optimal, high suboptimal and high sublethal temperatures predicted (Fig. 3.4). This result is consistent with the general tendency of the model to "run cold" as described in previous sections. The model predicted daily maximum temperatures to within 2.29°C using the "logger" ASL for the low intertidal zone, 3.07°C using the "general" ASL for the mid intertidal zone, and 5.65°C using the "general" ASL for the high intertidal zone (Table A.4).

The number of over- and underestimations in the mid and high intertidal zones increased with decreasing ASL. In contrast, over- and underestimations increased with increasing ASL in the low intertidal zone (Fig. 3.4B). For the low intertidal zone the model underestimated the number of cold temperatures by 4, 17 and 28 days using an ASL value of MLLW + 0.43m, MLLW + 0.5m and MLLW + 0.69m, respectively, and all ASLs caused the model to underestimate the number of stressful temperatures by 1

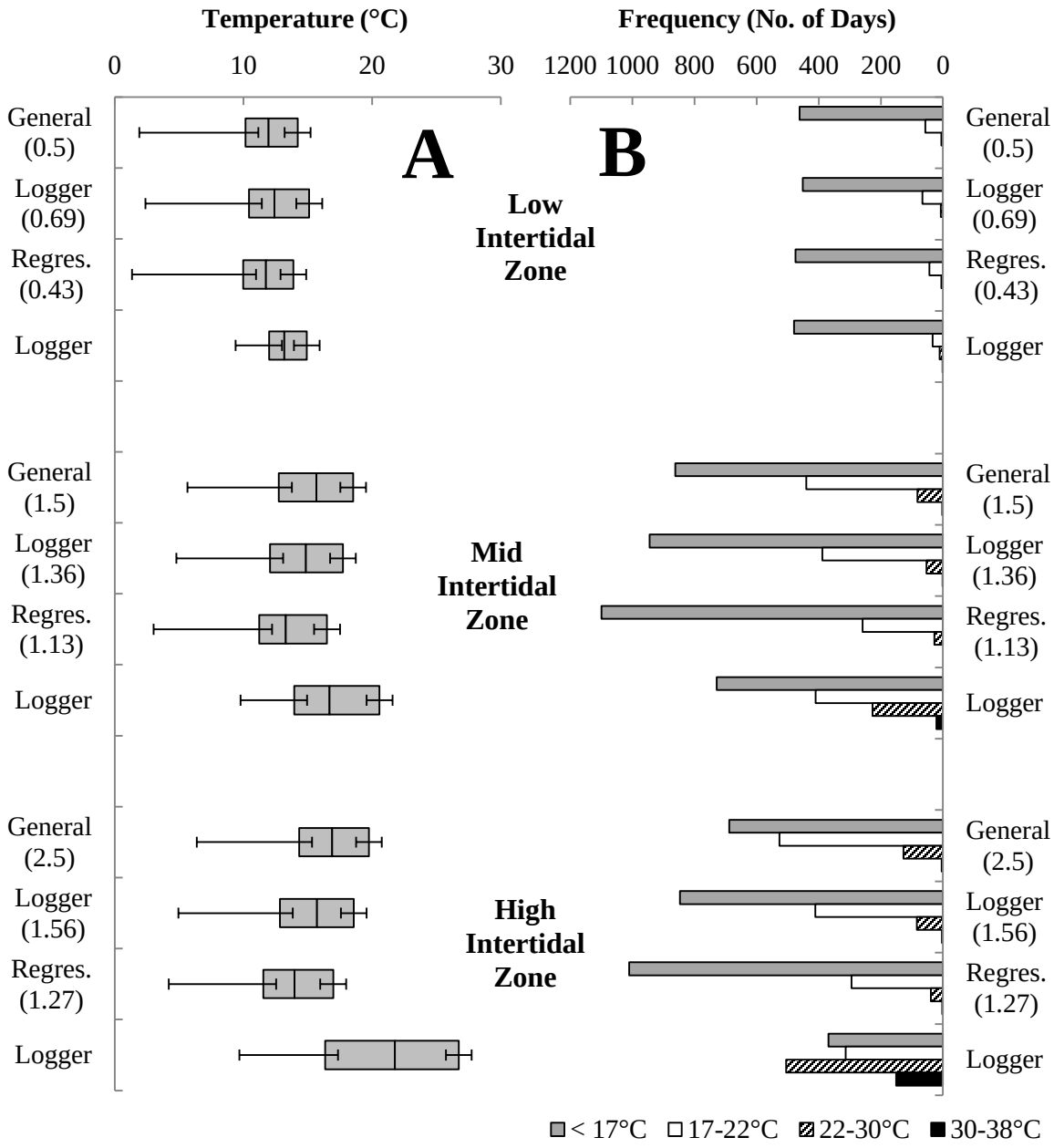

Figure 3.4 Distributions of daily maximum mussel body temperatures predicted by the general model with changing ASL values (y-axes: meters). The second "Logger" in each group is the data collected by the loggers in the field (not model estimations). **(A)** The box is the IQR, the line within the box is the median, the left side of the box is the 25th percentile, the right side of the box is the 75th percentile, the left line ends at the minimum value and the right line ends at the maximum value. **(B)** The histogram shows the frequency of the daily maximum temperatures within the four categories cold suboptimal/sublethal (< 17°C), optimal (17-22°C), high suboptimal (22-30°C) and high sublethal (30-38°C).

day. The model overestimated the number of cold temperatures by 134, 216 and 371 days using ASL values of MLLW + 1.5m, MLLW + 1.36m and MLLW + 1.13m, respectively, for the mid intertidal zone, and 319, 478 and 641 days for the high intertidal zone using ASL values of MLLW + 2.5m, MLLW + 1.56m and MLLW + 1.27m, respectively. The model underestimated the number of stressful temperatures by 19, 20 and 21 days and 147, 148 and 149 days as the ASL decreased for the mid and high intertidal zones, respectively (Fig. 3.4B).

3.1.5. Effective Shore Level (ESL slope)

Model predictions were generally most accurate for the low intertidal zone (2.4°C) and least accurate for the high intertidal zone (5.6°C). "Tailored" ESL slopes calculated using only temperatures recorded during the period of observation in this study were considerably lower than the generic prediction of 0.25m (Table A.5), but had very little effect on model error (Fig. 3.5B). For all three intertidal zones, the model tended to predict colder temperatures than the actual recorded logger temperatures using both of the ESL slope values (Fig. 3.5A). For the low intertidal zone the model underestimated the number of cold temperatures by 24 and 50 days using an ESL value of 0.25m and 0.06m, respectively, and ESLs caused the model to underestimate the number of stressful temperatures by 1 day. The model overestimated the number of cold temperatures by 56 and 138 days using ESL values of 0.16m and 0.25m, respectively, for the mid intertidal zone, and by 321 and 325 days for the high intertidal zone using ESL values of 0.12m and 0.25m, respectively. The model underestimated the number of stressful temperatures by 19 days using either ESL value for the mid intertidal zone and by 152 days using either ESL value for the high intertidal zone (Fig. 3.5B).

3.1.6. Absolute and Effective Shore Level (ASL & ESL slope)

As above, model temperature predictions were most accurate for the low intertidal zone and least accurate for the high intertidal zone. Generally, the model for all intertidal zones predicted colder temperatures than those experienced by the loggers in the field with the mid intertidal zone predicting the highest number of cold temperatures, followed

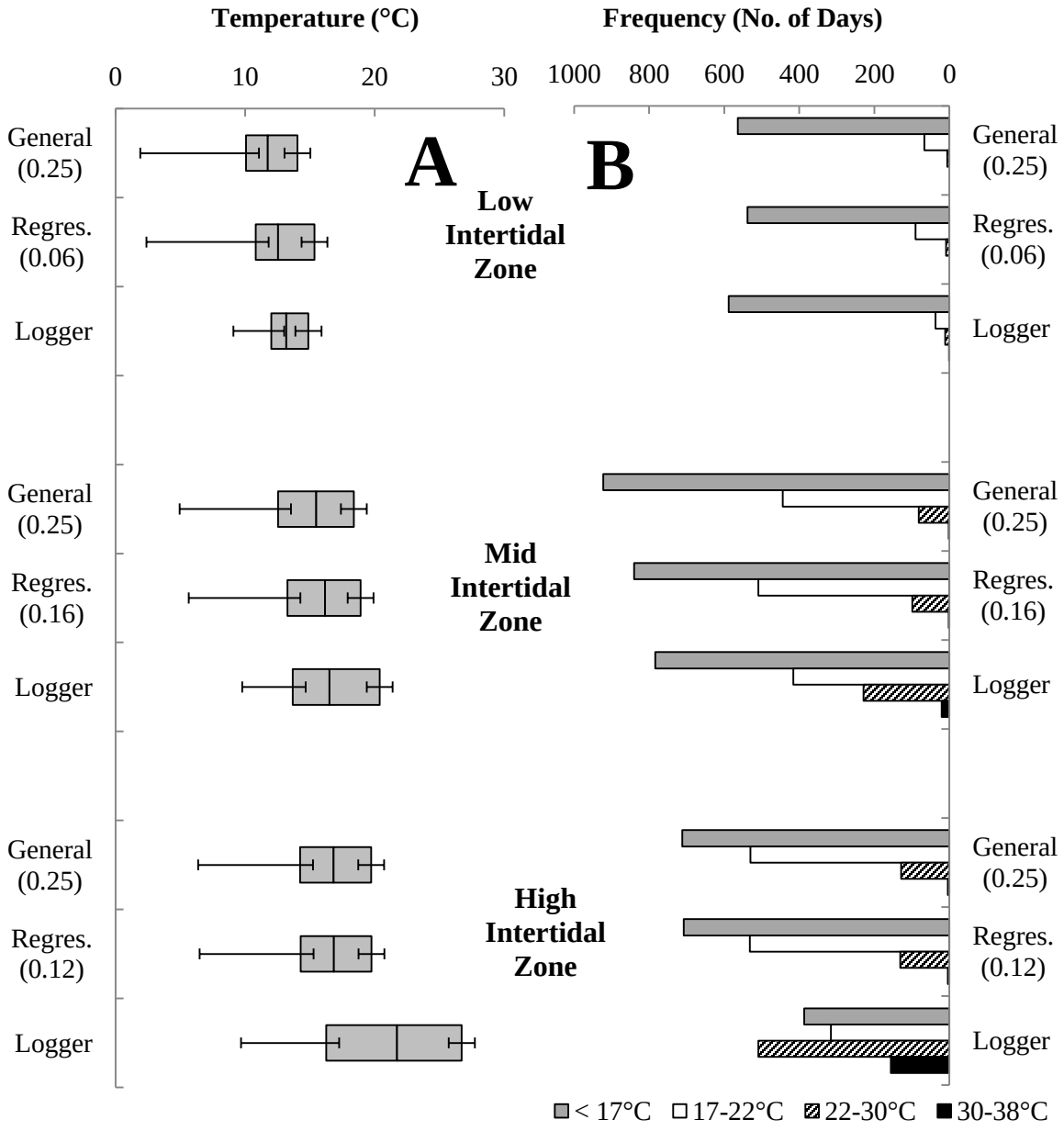

Figure 3.5 Distributions of daily maximum mussel body temperatures predicted by the general model with changing ESL slope values (y-axes: meters). **(A)** The box is the IQR,

the line within the box is the median, the left side of the box is the 25th percentile, the right side of the box is the 75th percentile, the left line ends at the minimum value and the right line ends at the maximum value. **(B)** The histogram shows the frequency of the daily maximum temperatures within the four categories cold suboptimal/sublethal (< 17°C), optimal (17-22°C), high suboptimal (22-30°C) and high sublethal (30-38°C).

by the high then the low intertidal zone. The number of optimal, high suboptimal and stressful temperatures predicted by the model increased from the low to high intertidal zone (Fig. 3.6B). Similar to the ESL slope analysis, there was not one ASL & ESL slope combination that was the most accurate however, considering all measures of error for all intertidal zones, the model using the generic ASL & ESL slope tended to provide more accurate temperature predictions than either of the other two ASL & ESL slope combinations and using the regression ASL & ESL slope provided the least accurate predictions most often (Fig. 3.6A). The model predicted daily maximum temperatures to within 2.35°C using the regression ASL & ESL slope for the low intertidal zone, 3.02°C using the logger ASL & regression ESL slope for the mid intertidal zone, and 5.62°C using the general ASL & ESL slope for the high intertidal zone (Table A.6).

The model was better at not under- or overestimating temperatures using the general ASL & ESL slope combination for all three intertidal zones (Fig. 3.6B). For the low intertidal zone the model underestimated the number of cold temperatures by 24, 43 and 73 days using the general ASL and ESL slope, regression ASL and ESL slope, and the logger ASL and regression ESL slope, respectively. The model underestimated the number of stressful temperatures by 1 day using any of the ASL and ESL slope combinations. The model overestimated the number of cold temperatures by 113, 136, and 267 days using the logger ASL and regression ESL slope, general ASL and ESL slope, and regression ASL and ESL slope, respectively, and underestimated the number of stressful temperatures by 19 days using the general ASL and ESL slope, and the logger

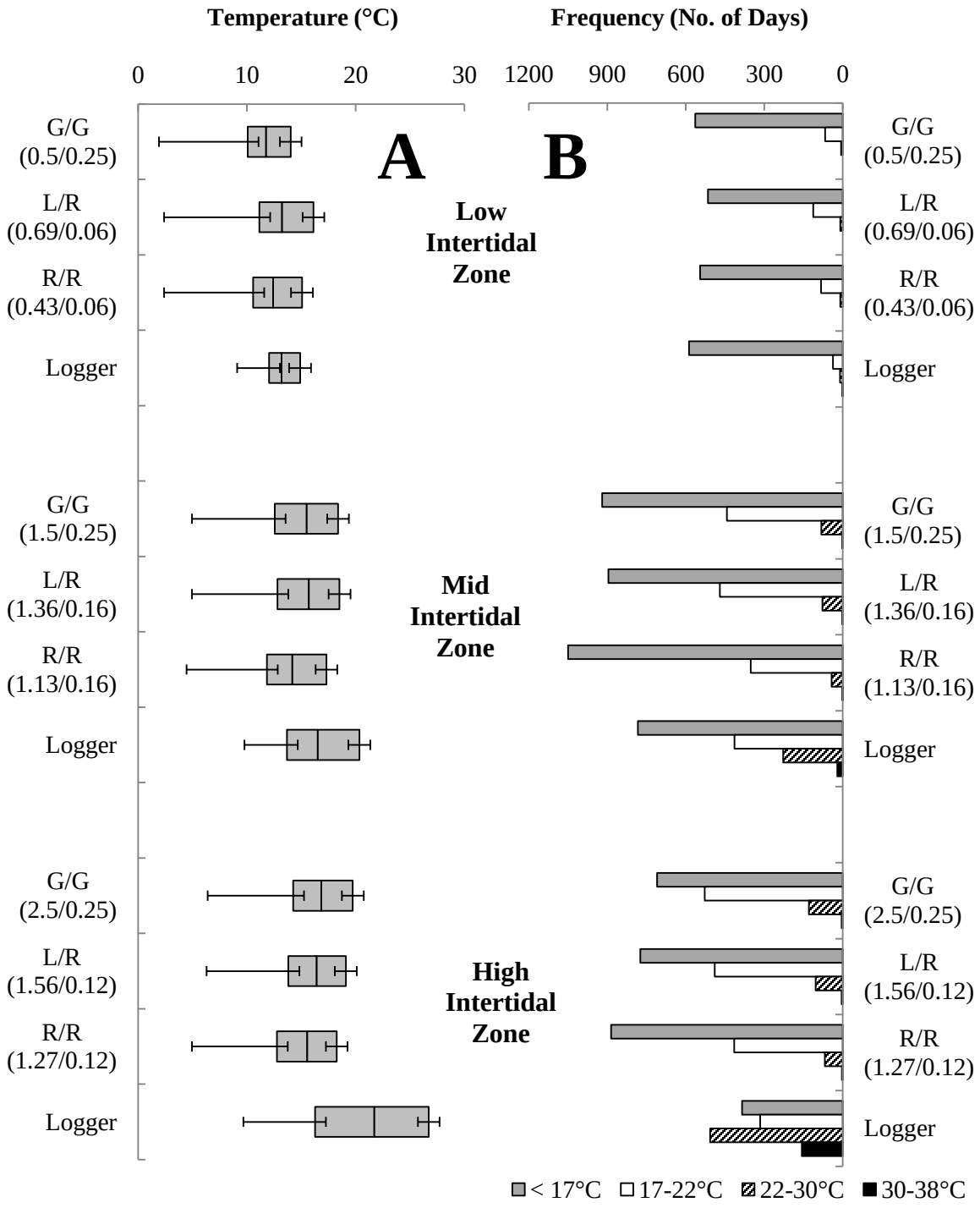

Figure 3.6 Distributions of daily maximum mussel body temperatures predicted by the general model with the ASL and ESL slope values changing (y-axes: meters). In each graph: G = general; L = logger; R = regression. The second "Logger" in each group is the data collected by the loggers in the field (not model estimations). **(A)** The box is the IQR, the line within the box is the median, the left side of the box is the 25th percentile, the right side of the box is the 75th percentile, the left line ends at the minimum value and the

right line ends at the maximum value. **(B)** The histogram shows the frequency of the daily maximum temperatures within the four categories cold suboptimal/sublethal (< 17°C), optimal (17-22°C), high suboptimal (22-30°C) and high sublethal (30-38°C).

ASL and regression ESL slope, and by 20 days using the regression ASL and ESL slope, for the mid intertidal zone. For the high intertidal zone, the model overestimated the number of cold temperatures by 325, 389, and 500 days using the general ASL and ESL slope, logger ASL and regression ESL slope, and regression ASL and ESL slope, respectively, and underestimated the number of stressful temperatures by 152 days using the general ASL and ESL slope, and the logger ASL and regression ESL slope, and by 153 days using the regression ASL and ESL slope (Fig. 3.6B).

3.2. Accuracy Assessment

The accuracy of the biophysical heat budget model using either LWS data or CFSR data was evaluated. The goal was to understand if a coarser, but more widely-available type of weather data (CFSR) could be used in place of a more accurate, yet spatially limited type of weather data (LWS). Comparisons of the model using LWS or CFSR data were made against *in situ* logger data for each intertidal zone at Bodega Bay (*Section 3.2.1*) and Hopkins Marine Lab (*Section 3.2.2*). Comparisons between model outputs using CFSR data and logger data were also completed for the two sites where LWS data were not available, Alegria (*Section 3.2.3*) and Coal Oil Point (*Section 3.2.4*). More detailed accuracy assessment results can be found in Appendix B.

3.2.1. Bodega Bay

Altogether, the model using CFSR data provided results with an error comparable to those using LWS data (Tables 3.1, B.1). Considering absolute average differences between model predictions and logger data, the model using CFSR data showed slightly smaller errors for the high (5.5 vs 6.1°C) and low (2.2 vs 2.4°C) intertidal zones than did

predictions using LWS data but slightly larger errors for the mid (3.3 vs 3.2°C) intertidal zone. In all cases, results were most accurate for the low intertidal zone and least accurate for the high intertidal zone (Table 3.1, Fig. 3.7 & B.1-B.3).

Both types of weather data caused the model to run cold, i.e. predict temperatures colder than the logger measurements (Table 3.1). Generally, the model using CFSR data predicted warmer temperatures than those predicted by the model using LWS data (Table B.1, Fig. 3.7, 3.8, B.1-B.3). On average the model using CFSR data predicted daily maximum temperatures that were 1.19°C, 1.55°C and 1.49°C warmer than those predicted by the LWS model for the low, mid and high intertidal zones, respectively.

Table 3.1 Comparison of the general models' predicted temperatures using LWS data and CFSR data to the logger field measurements for Bodega Bay. A negative average difference indicates that the model tended to underestimate the daily maximum temperatures.

Type of Weather Data	Intertidal Zone	Average Difference (°C)	Absolute Average Difference (°C)	RMS Error (°C)	False Pos.	False Neg.
LWS	Low	-1.44	2.43	3.02	0	1
	Mid	-1.91	3.16	4.12	2	20
	High	-5.33	6.13	7.32	2	161
CFSR	Low	-0.25	2.22	2.98	1	1
	Mid	-0.35	3.34	4.30	2	18
	High	-3.84	5.51	6.74	7	159

The percentage of predicted stressful temperatures increased with intertidal elevation. The model for the low intertidal zone predicted the greatest percentage of cold temperatures and the model for the high intertidal zone predicted the greatest percentage of stressful temperatures. For the low intertidal zone the use of LWS data led to fewer under- or overestimations but for the mid and high intertidal zones CFSR data were more accurate. For the low intertidal zone model predictions using either type of weather data

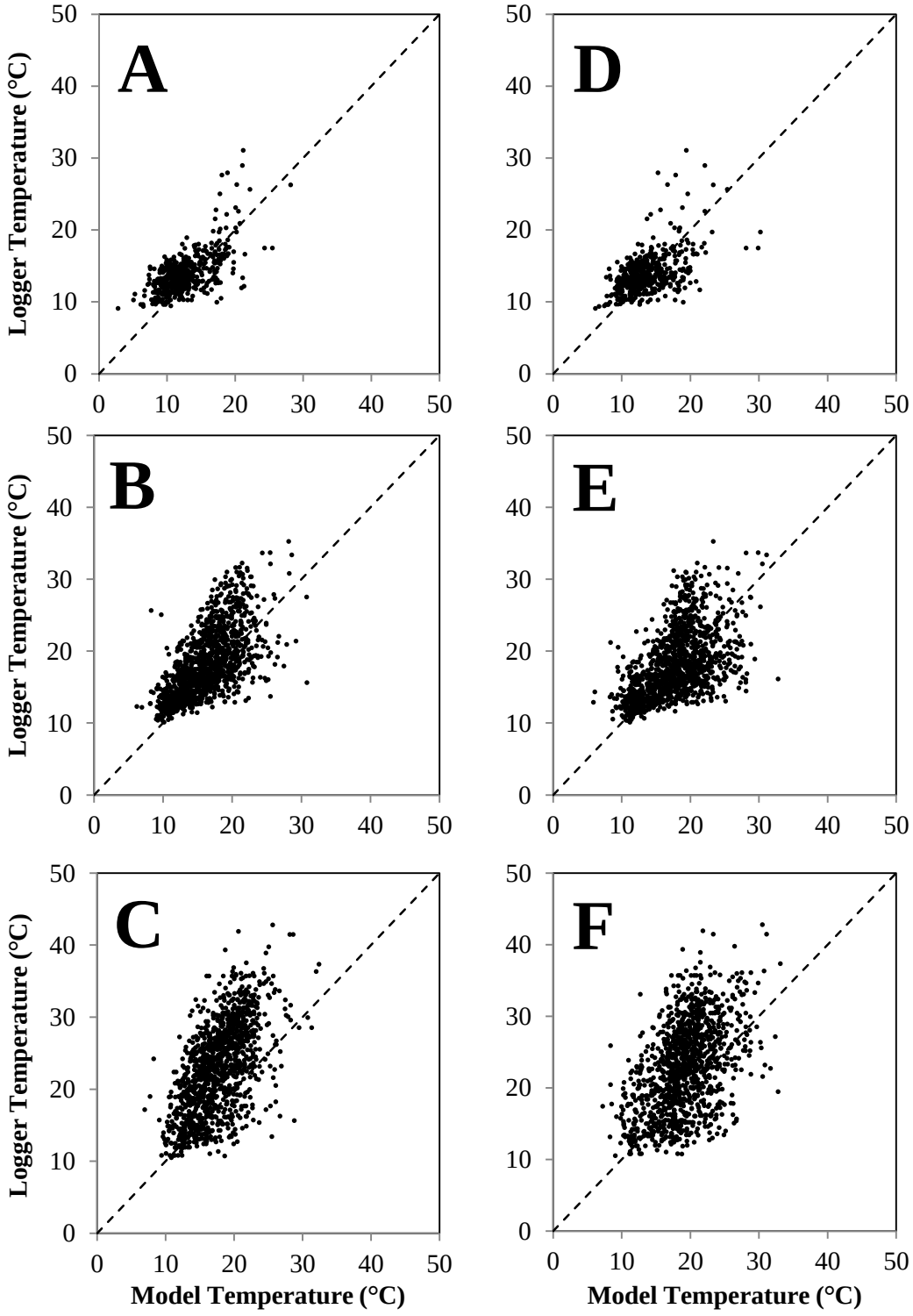

Figure 3.7 Relationship between model predictions and logger temperatures for all three intertidal zones at Bodega Bay. The results for the model using LWS data for the (**A**) low, (**B**) mid, and (**C**) high intertidal zones are shown. The results for the model using CFSR data for the (**D**) low, (**E**) mid and (**F**) high intertidal zones are shown as well. Daily maximum temperatures recorded by loggers in mussel beds at MLLW + 0.5 m

(low), MLLW + 1.5 m (mid) and MLLW + 2.5 m (high) are plotted as a function of model predictions. Dots are individual observations and dotted lines are 1:1 lines.

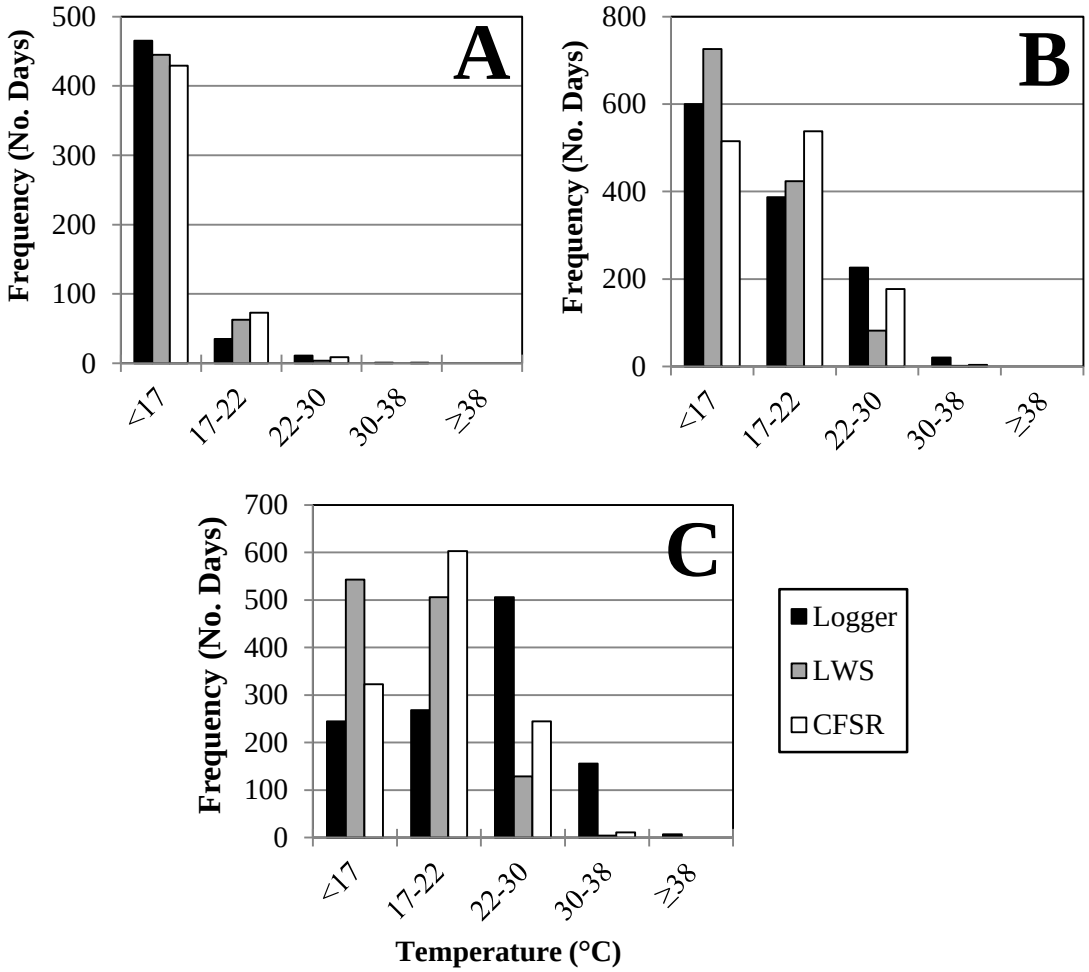

Figure 3.8 Frequency distribution of daily maximum temperatures predicted by the LWS general model, CFSR general model and recorded by the loggers in the field at Bodega Bay. The results for the **(A)** low, **(B)** mid and **(C)** high intertidal zones are reported.

underestimated the number of cold temperatures by at least 20 days; comparable results were observed for the mid intertidal zone using CFSR data. Using either source of weather data for the high intertidal zone caused the model to overestimate the number of cold temperatures by at least 78 days and for the mid intertidal zone using LWS data by 126 days. The model underestimated the number of stressful temperatures by at least 1,

17 and 152 days for the low, mid and high intertidal zones, respectively (Table B.1 & Fig. 3.8).

3.2.2. Hopkins

Model results using either type of weather data were less accurate as a whole compared to the model used for Bodega Bay (Table 3.2). In contrast to Bodega Bay, the use of LWS data led to substantially more accurate temperature predictions than did the use of CFSR data (Table 3.2). Model errors were lowest for the mid intertidal zone (LWS: 3.1°C; CFSR: 6.8°C) and highest for the low intertidal zone (LWS: 6.3°C; CFSR: 7.9°C; Table 3.2, Fig. 3.9 & B.4-B.6).

Table 3.2 Comparison of the general models' predicted temperatures using LWS data and CFSR data to the logger field measurements for Hopkins. A positive average difference value indicates that the model overestimated logger (mussel) temperature.

Type of Weather Data	Intertidal Zone	Average Difference (°C)	Absolute Average Difference (°C)	RMS Error (°C)	False Pos.	False Neg.
LWS	Low	-5.86	6.30	7.73	0	54
	Mid	0.86	3.09	4.04	16	25
	High	-1.86	5.13	6.39	12	269
CFSR	Low	-5.09	7.87	9.65	31	47
	Mid	3.17	6.78	8.30	259	20
	High	1.04	6.90	8.58	240	182

The percentage of predicted stressful temperatures increased with increasing intertidal elevation. The model for the low intertidal zone predicted the greatest percentage of cold temperatures and the model for the high intertidal zone predicted the greatest percentage of stressful temperatures. For the low and high intertidal zones the model was better at not under- or overestimating temperatures while using CFSR data and for the mid intertidal zone it was better using LWS data (Table B.2 & Fig. 3.10).

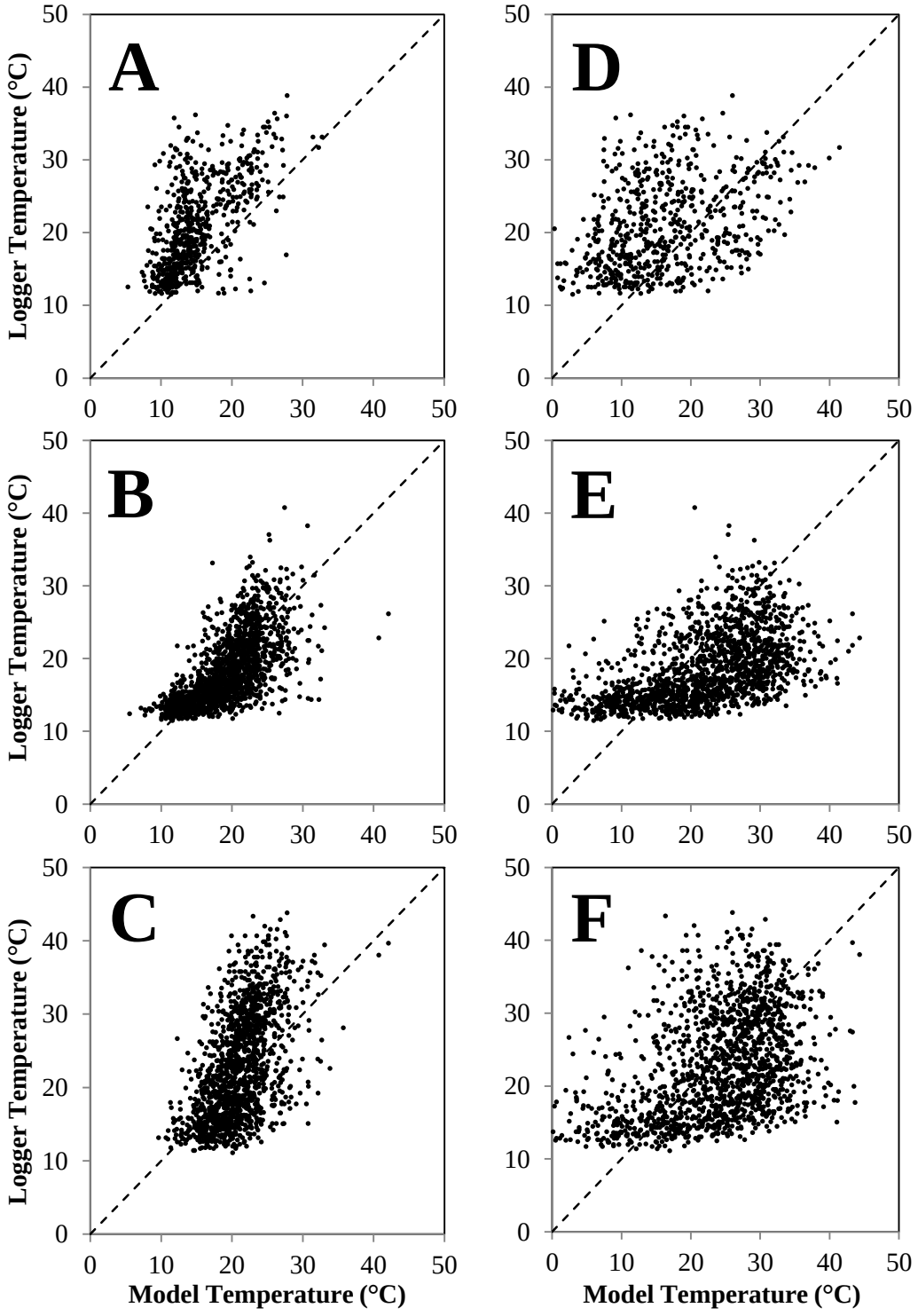

Figure 3.9 Relationship between model predictions and logger temperatures for all three intertidal zones at Hopkins. The results for the model using LWS data for the (**A**) low, (**B**) mid, and (**C**) high intertidal zones are shown. The results for the model using CFSR data for the (**D**) low, (**E**) mid and (**F**) high intertidal zones are also shown. Daily maximum temperatures recorded by data loggers in mussel beds at MLLW + 0.5 m (low),

MLLW + 1.5 m (mid) and MLLW + 2.5 m (high) are plotted as a function of model predictions. Dots are individual observations and dotted lines are 1:1 lines.

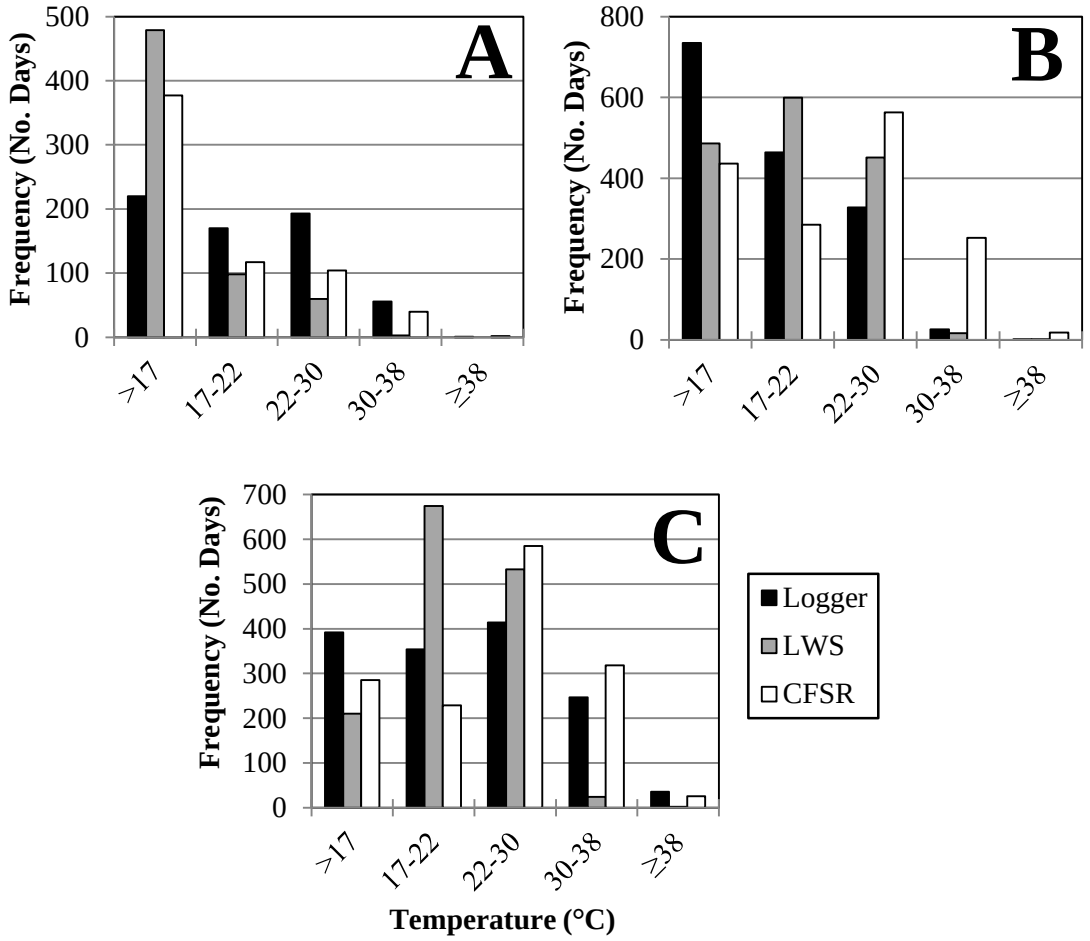

Figure 3.10 Frequency distribution of daily maximum temperatures predicted by the general model using LWS data and CFSR data and recorded by the loggers in the field at Hopkins. Results for the **(A)** low, **(B)** mid and **(C)** high intertidal zones are shown.

Using both types of weather data, the model overestimated cold temperatures for the low intertidal zone by no less than 157 days and underestimated the number of stressful temperatures by at least 17 days. The model for the mid and high intertidal zones using both types of weather data underestimated the number of cold temperatures by at least 249 days and 107 days, respectively. The model using LWS data underestimated the number of stressful temperatures by 9 and 257 days while the model using CFSR data

overestimated the number of temperatures in this category by 243 and 61 days for the mid and high intertidal zones, respectively (Table B.2 & Fig. 3.10).

3.2.3. Alegria

Comparisons of model outputs using CFSR data and logger data indicated high levels of error at this site (Table 3.3), comparable to those predicted using CFSR data at Hopkins Marine Station. The temperatures predicted for this location were the hottest out of all four locations examined. The model was most accurate at predicting daily maximum temperatures for the high intertidal zone (6.41°C) and least accurate for the low intertidal zone (6.72°C; Table 3.3 & Fig. 3.11).

The model results for the mid intertidal zone at Alegria showed the fewest number of over- or underestimations compared to the model outputs for the low and high intertidal zones (Table B.3 & Fig. 3.12). The model tended to predict warmer temperatures than those recorded by the loggers for the mid and high intertidal zones but colder temperatures for the low intertidal zone. The percentage of predicted stressful temperatures increased with increasing intertidal elevation. The model for the low intertidal zone predicted the greatest percentage of cold temperatures and the model for the high intertidal zone predicted the greatest percentage of stressful temperatures (Table B.3, Fig. 3.11, 3.12 & B.7-B.9).

For the low intertidal zone the model overestimated the number of cold temperatures by 162 days and underestimated the number of stressful temperatures by 21 days. The model for the mid and high intertidal zones underestimated the number of cold temperatures by at least 70 days and overestimated the number of stressful temperatures by more than 226 days (Table B.3 & Fig. 3.12).

Table 3.3 Comparison of the temperatures predicted by the CFSR general model to the logger field measurements for Alegria. A positive average difference value indicates that the model overestimated logger (mussel) temperature.

Intertidal Zone	Average Difference (°C)	Absolute Average Difference (°C)	RMS Error (°C)	False Pos.	False Neg.
Low	-1.85	6.72	8.50	69	48
Mid	2.69	6.49	8.09	432	170
High	3.20	6.41	7.96	397	172

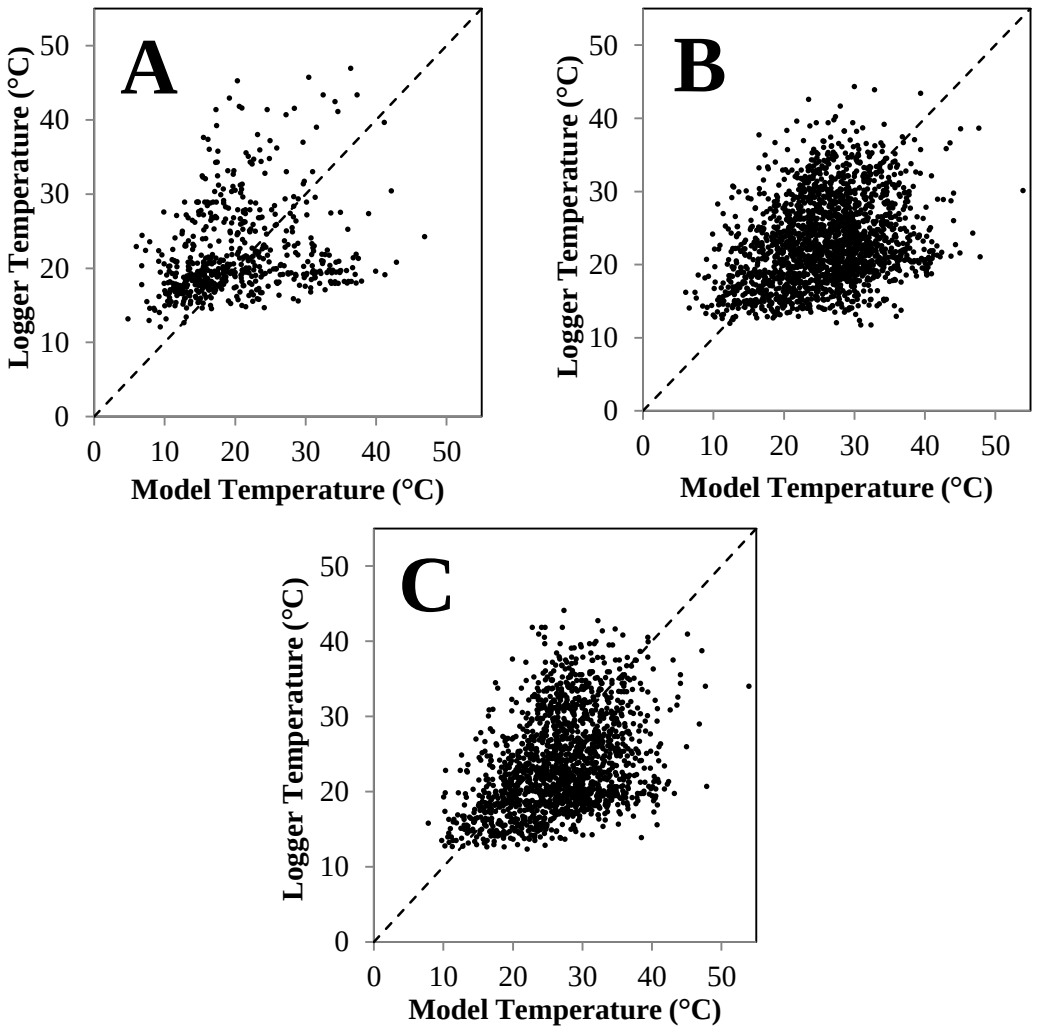

Figure 3.11 Relationship between model predictions and logger temperatures for all three intertidal zones at Alegria. Results are shown for the **(A)** low, **(B)** mid and **(C)** high intertidal zones using the general CFSR model**.** Daily maximum temperatures recorded by data loggers in mussel beds at MLLW + 0.5 m (low), MLLW + 1.5 m

(mid) and MLLW + 2.5 m (high) are plotted as a function of model predictions. Dots are individual observations and dotted lines are 1:1 lines.

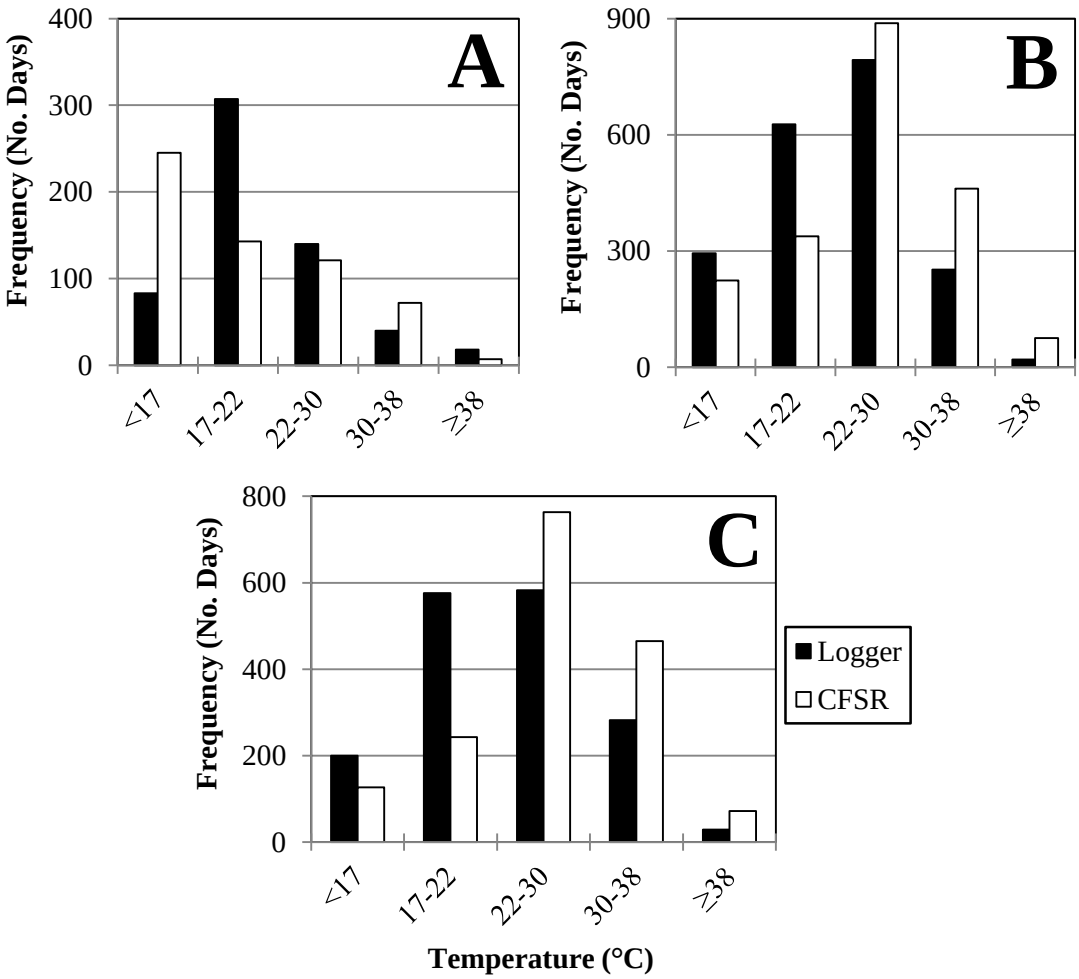

Figure 3.12 Frequency distribution of daily maximum temperatures predicted by the CFSR general model and recorded by the loggers in the field for Alegria. Displayed are the results for the **(A)** low, **(B)** mid and **(C)** high intertidal zones.

3.2.4. Coal Oil Point

Model results for Coal Oil Point showed the lowest accuracy of all of the locations, with errors for the low intertidal zone (6.0°C) comparable to those at Alegria and Hopkins (CFSR) but even greater in the mid (8.5°C) and high (9.4°C) intertidal zones (Table 3.4 & Fig. 3.13). In all cases the model ran hot, tending to overestimate temperatures (Table B.4, Fig. 3.13, 3.14 & B.10-B.12).

Table 3.4 Comparison of the temperatures predicted by the CFSR general model to the logger field measurements for Coal Oil Point. A positive value in average difference indicates that the model overestimated logger (mussel) temperature.

Intertidal Zone	Average Difference (°C)	Absolute Average Difference (°C)	RMS Error (°C)	False Pos.	False Neg.
Low	1.21	6.00	7.56	62	1
Mid	7.14	8.48	10.41	273	7
High	8.21	9.43	11.31	264	8

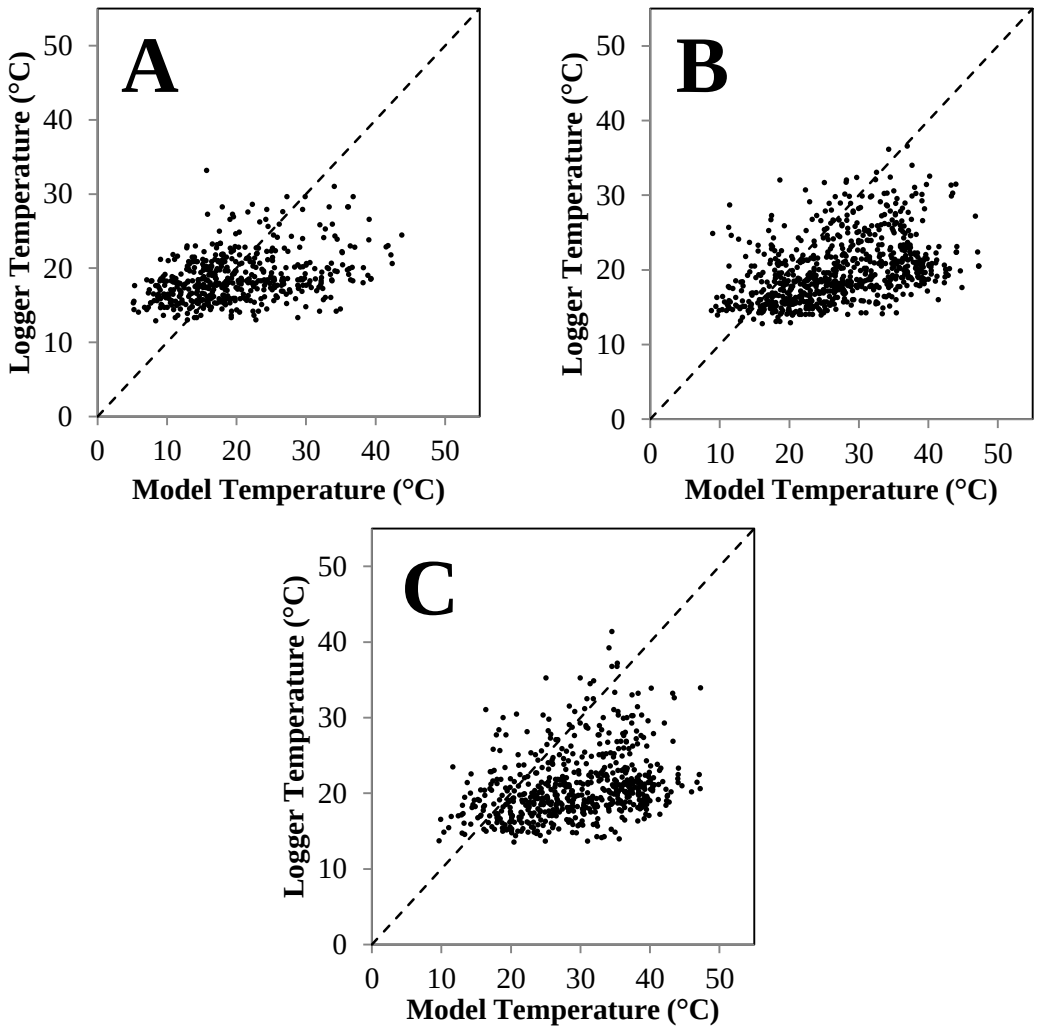

Figure 3.13 Relationship between model predictions and logger temperatures for all three intertidal zones at Coal Oil Point. The results for general CFSR model for the **(A)** low, **(B)** mid and **(C)** high intertidal zones are displayed. Daily maximum temperatures recorded by data loggers in mussel beds at MLLW + 0.5 m (low),

MLLW + 1.5 m (mid) and MLLW + 2.5 m (high) are plotted as a function of model predictions. Dots are individual observations and dotted lines are 1:1 lines.

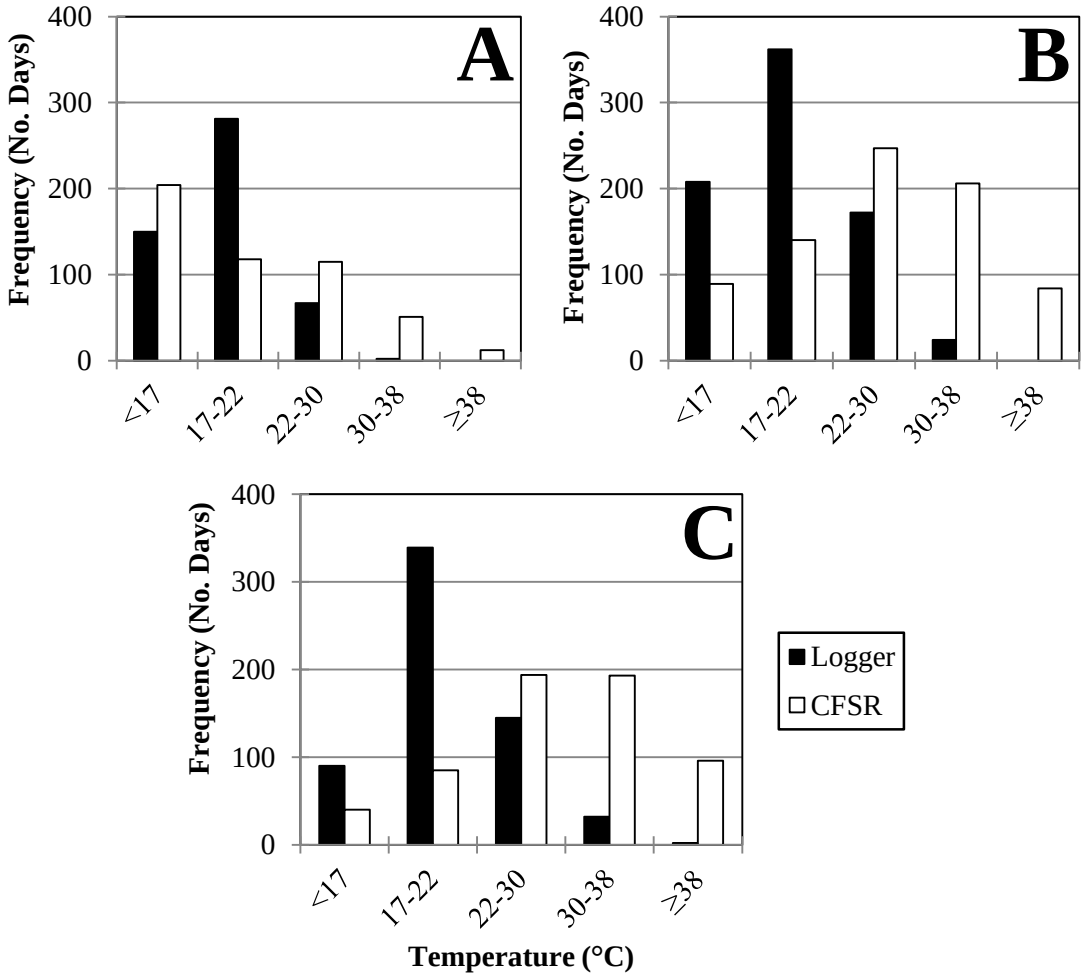

Figure 3.14 Frequency distribution of daily maximum and daily minimum temperatures predicted by the CFSR general model and recorded by the loggers in the field for Coal Oil Point. The results for the **(A)** low, **(B)** mid and **(C)** high intertidal zones are displayed.

The percentage of predicted stressful temperatures increased with increasing intertidal zone. The model for the low intertidal zone predicted the greatest percentage of cold temperatures and the model for the high intertidal zone predicted the greatest percentage of stressful temperatures. For the low intertidal zone the model overestimated the number of cold temperatures by 54 days and underestimated the number of stressful temperatures by 61 days. The model for the mid and high intertidal zones underestimated

the number of cold temperatures by at least 50 days and overestimated the number of stressful temperatures by more than 255 days (Table B.4 & Fig. 3.14).

3.3. Changing Wave Climates

To understand how mussel body temperatures would be affected by changes in wave climates at each location the daily maximum body temperatures predicted by the model using CFSR data with different significant wave heights were calculated. The goal was to understand how changes in wave height would impact certain physiological thresholds, such as optimal to high stressful and high stressful to high lethal or the reverse. Therefore after analyzing the entire time series and categorizing the temperatures into the thermal framework previously designated, the hottest months (May, June, July and August) were examined to determine how changes in wave climate could affect mussel body temperature during these thermally stressful months. The daily maximum body temperatures were averaged for the entire month so that there was one average maximum temperature for each of the hottest months for each year within the time series. The number of months is provided in the captions for Figs. 3.15 – 3.18 and is denoted by N. All comparisons made below are relative to the daily maximum temperatures predicted by the model using recorded significant wave height. More detailed results are available in Appendix C.

3.3.1. Bodega Bay

Generally, as the significant wave height decreased beyond present day conditions, predicted body temperatures increased (the number of cold temperatures decreased, and the number of stressful temperatures increased) in all intertidal zones. Conversely, as the significant wave height increased, the predicted body temperatures

decreased (the number of cold temperatures increased while the number of stressful temperatures decreased) for all intertidal zones. Overall, the mid intertidal zone had the greatest number of cold temperatures while the high intertidal zone had the greatest number of stressful temperatures. When considering the time series as a whole, the mid intertidal zone was most affected and the high intertidal zone was least affected by changing wave heights, and changing the significant wave height did not have an impact on the number of high lethal temperatures for any of the intertidal zones (Table C.1 & Fig. C.1).

The results were slightly different when examining only the hottest months, but the same patterns described above still apply. There were only two times when the distributions of body temperatures were affected by changing wave heights. When the wave height was increased for the low intertidal zone, the number of cold temperatures increased and the number of optimal and high suboptimal temperatures decreased. For the mid and high intertidal zones, the distribution of body temperatures was unaffected by changing wave heights (Fig. 3.15).

For the low intertidal zone there was a significant change when the wave height was decreased. The temperature increased 0.95°C from the optimal range to the high suboptimal range. Although this is not a very large change, it does mark the transition point from an optimal temperature to a semi-stressful temperature which is an important physiological shift. This change occurred when the significant wave height was decreased in the model from 15% to 16% which caused a temperature increase from 21.82°C to 22.08°C. There were not any important physiological shifts for the mid or high intertidal zones (Fig. 3.15).

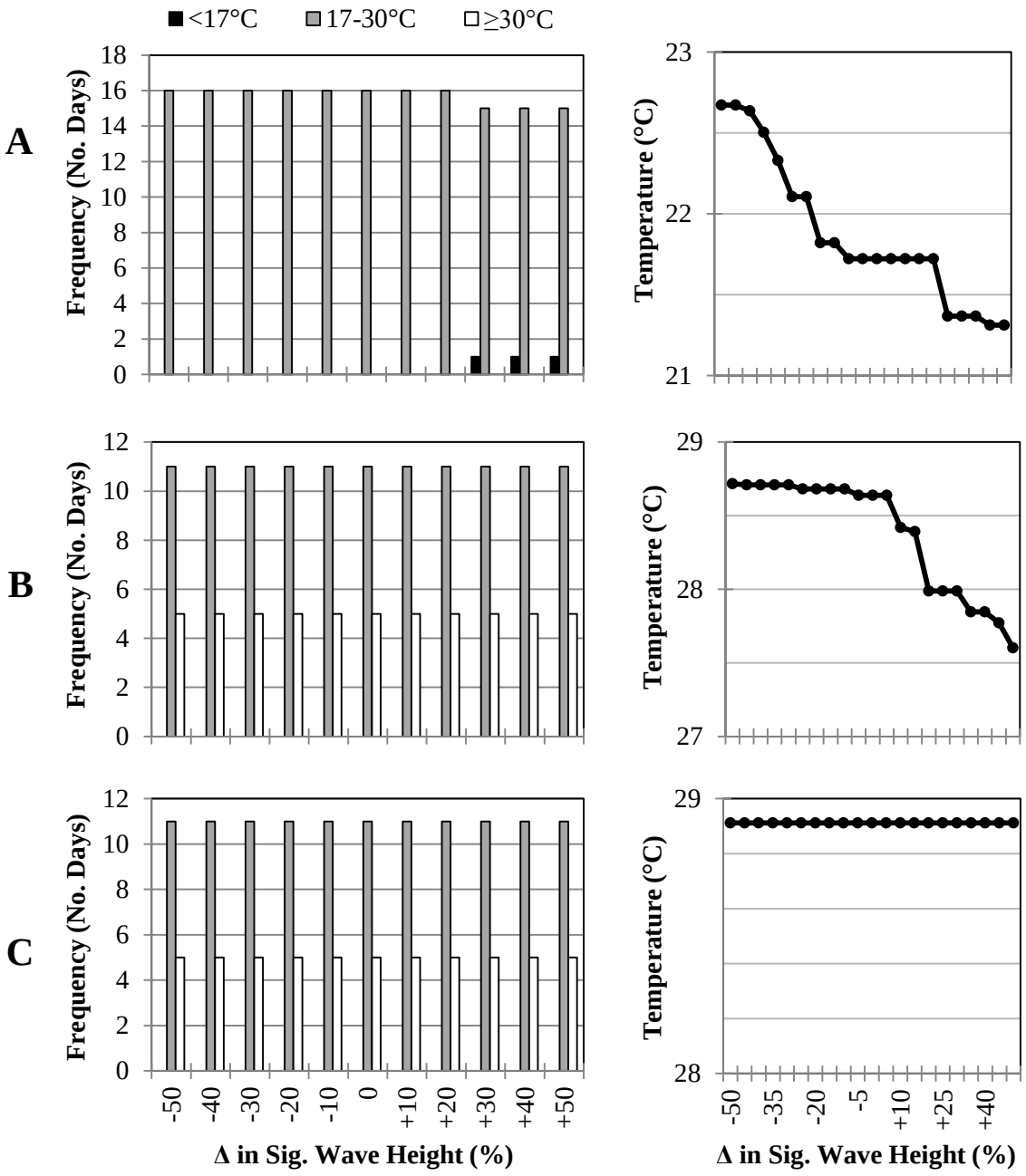

Figure 3.15 Maximum average daily maximum body temperatures predicted by the general model with increasing and decreasing significant wave heights for Bodega Bay. The results are shown for the **(A)** low, **(B)** mid and **(C)** high intertidal zones during the hottest months (N = 16 months).

3.3.2. Hopkins

The distributions of temperatures for Hopkins were similar to that of Bodega Bay. For all three intertidal zones, as wave height decreased the body temperature predictions

increased and as wave height increased the body temperature predictions decreased. The mid intertidal zone had the greatest number of cold temperatures and the high intertidal zone had the greatest number of stressful temperatures. The temperatures predicted by the model for the mid intertidal zone were most impacted by changing wave heights and those predicted for the high intertidal zone were least affected by changing wave heights (Table C.2 & Fig. C.2).

Analysis of the time series as a whole revealed that as the wave height was increased, the number of high lethal temperatures decreased for the low and mid intertidal zones but the high lethal temperatures for the high intertidal zone were unaffected. As the wave height was decreased the number of predicted high lethal temperatures increased for the low intertidal zone but the mid and high intertidal zone predictions were not affected (Table C.2).

When analyzing the hottest months alone the patterns mentioned above still apply but can only truly be seen for the low intertidal zone. For the most part, the distributions of predicted temperatures examined were not affected by changing wave height – the mid and high intertidal zones were not affected at all. For the low intertidal zone as the wave height increased the number of cold, optimal and high suboptimal temperatures increased and the number of stressful temperatures decreased. As the wave height was decreased the number of optimal and high suboptimal temperatures decreased and the number of stressful temperatures increased (Fig. 3.16).

There were no important physiological shifts for the low or high intertidal zones. However, for the mid intertidal zone, as the wave height was increased the temperature decreased 0.94°C from the high lethal range to the high sublethal range. Again, this is not

a large change in temperature but it is an important physiological shift. Body temperature predictions crossed the critical threshold of 38°C as wave heights were increased by ~27% (Fig. 3.16).

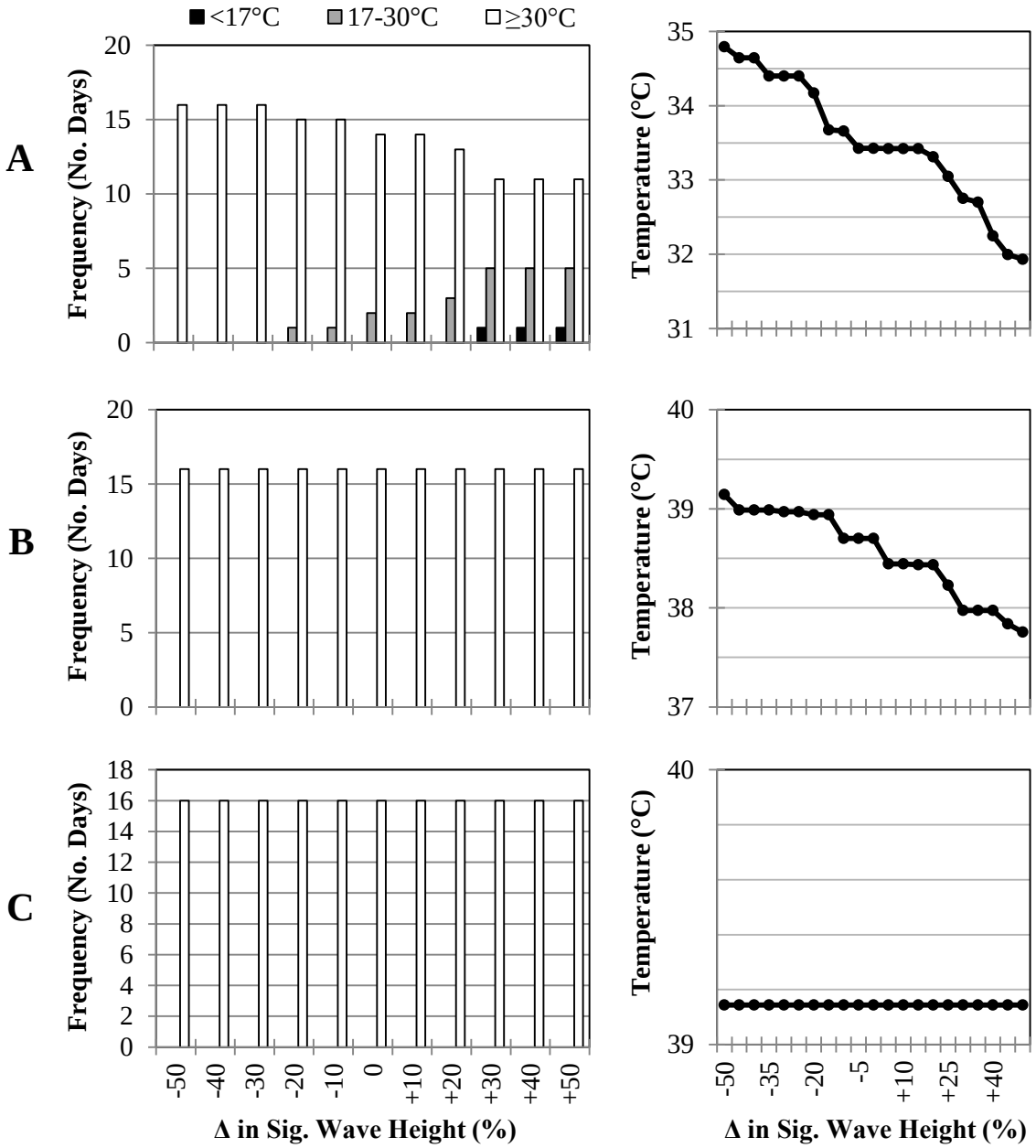

Figure 3.16 Average daily maximum body temperatures predicted by the general model with increasing and decreasing significant wave heights for Hopkins. The results for the **(A)** low, **(B)** mid and **(C)** high intertidal zones during the hottest months are shown (N = 16 months).

3.3.3. Alegria

The patterns for this location follow the two previous locations. The predicted body temperatures become warmer as wave height was decreased and temperatures become colder as wave height was increased. A difference from the previous two locations is that the low intertidal zone had the greatest number of cold temperatures, rather than the mid intertidal zone, while the high intertidal zone had the greatest number of high temperatures. As before, the mid intertidal zone was most affected and the high intertidal zone was least affected by changing wave heights. For the time series as a whole, for the low and mid intertidal zones, as the wave height was increased the number of high lethal temperatures decreased and as the wave height was decreased the number of high lethal temperatures increased. For the high intertidal zone, changing the significant wave height did not have an impact on the number of high lethal temperatures at all (Table C.3 & Fig. C.3).

The analysis for the hottest months produced similar results to Hopkins. The above patterns generally apply and are again most evident for the low intertidal zone. The majority of the distribution of temperatures was unaffected by changing wave heights. In fact, the distributions of predicted temperatures for the mid and high intertidal zones were completely unchanged. For the low intertidal zone the number of cold, optimal and high suboptimal temperatures increased with increasing wave height and the number of stressful temperatures decreased with increasing wave height. As the wave height was decreased the number of cold, optimal and high suboptimal temperatures decreased and the number of stressful temperatures increased (Fig. 3.17).

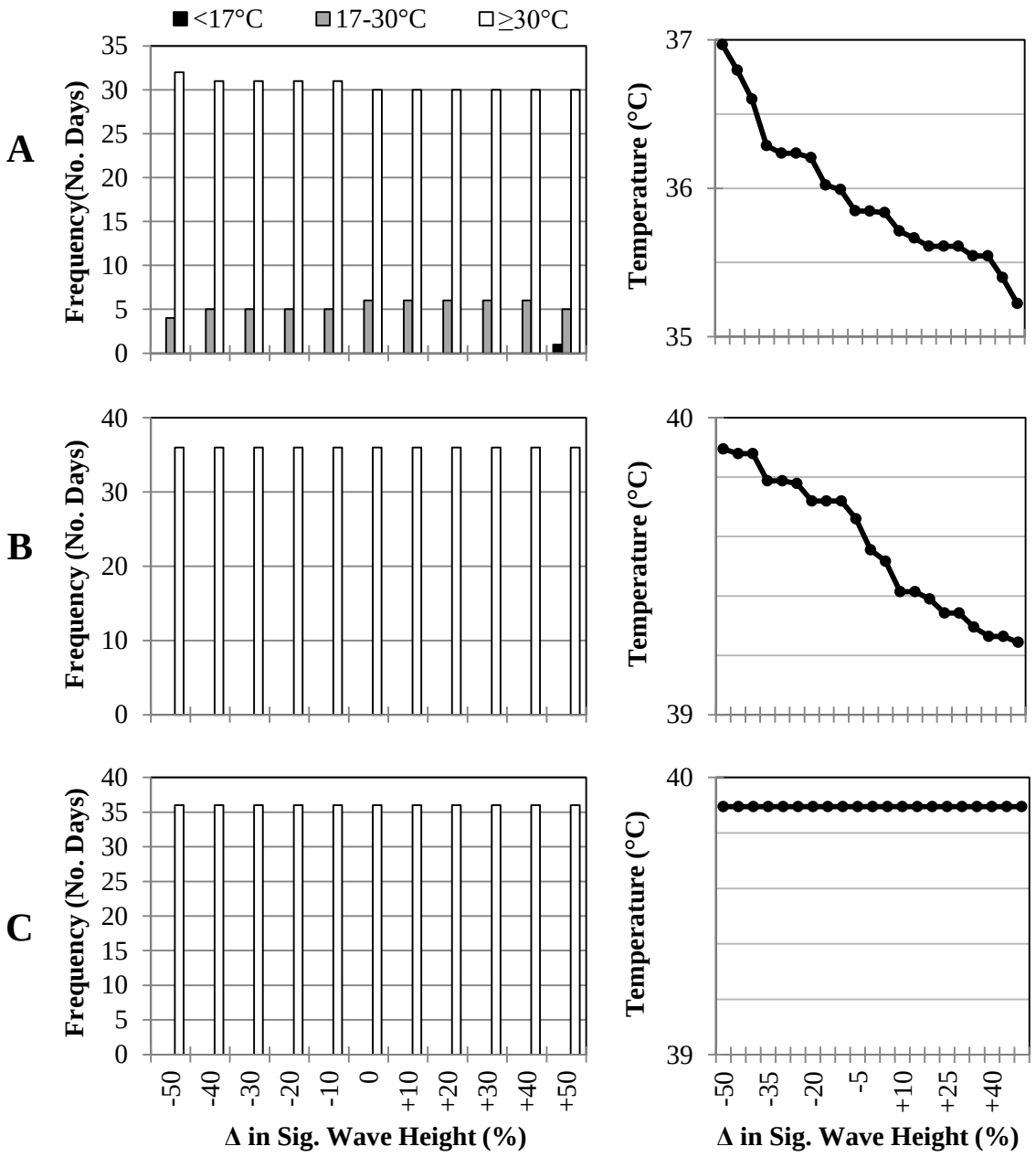

Figure 3.17 Average daily maximum body temperatures predicted by the general model with increasing and decreasing significant wave heights for Alegria. The results for the **(A)** low, **(B)** mid and **(C)** high intertidal zones during the hottest months are shown (N = 36 months).

3.3.4. Coal Oil Point

The distribution of temperatures for Coal Oil Point follows a very similar pattern to Alegria and the general trends seen thus far for all locations apply to this site as well.

The predicted body temperatures become warmer as wave height was decreased and temperatures become colder as wave height was increased. Similar to Alegria, and different from Hopkins and Bodega Bay, the low intertidal zone had the greatest number

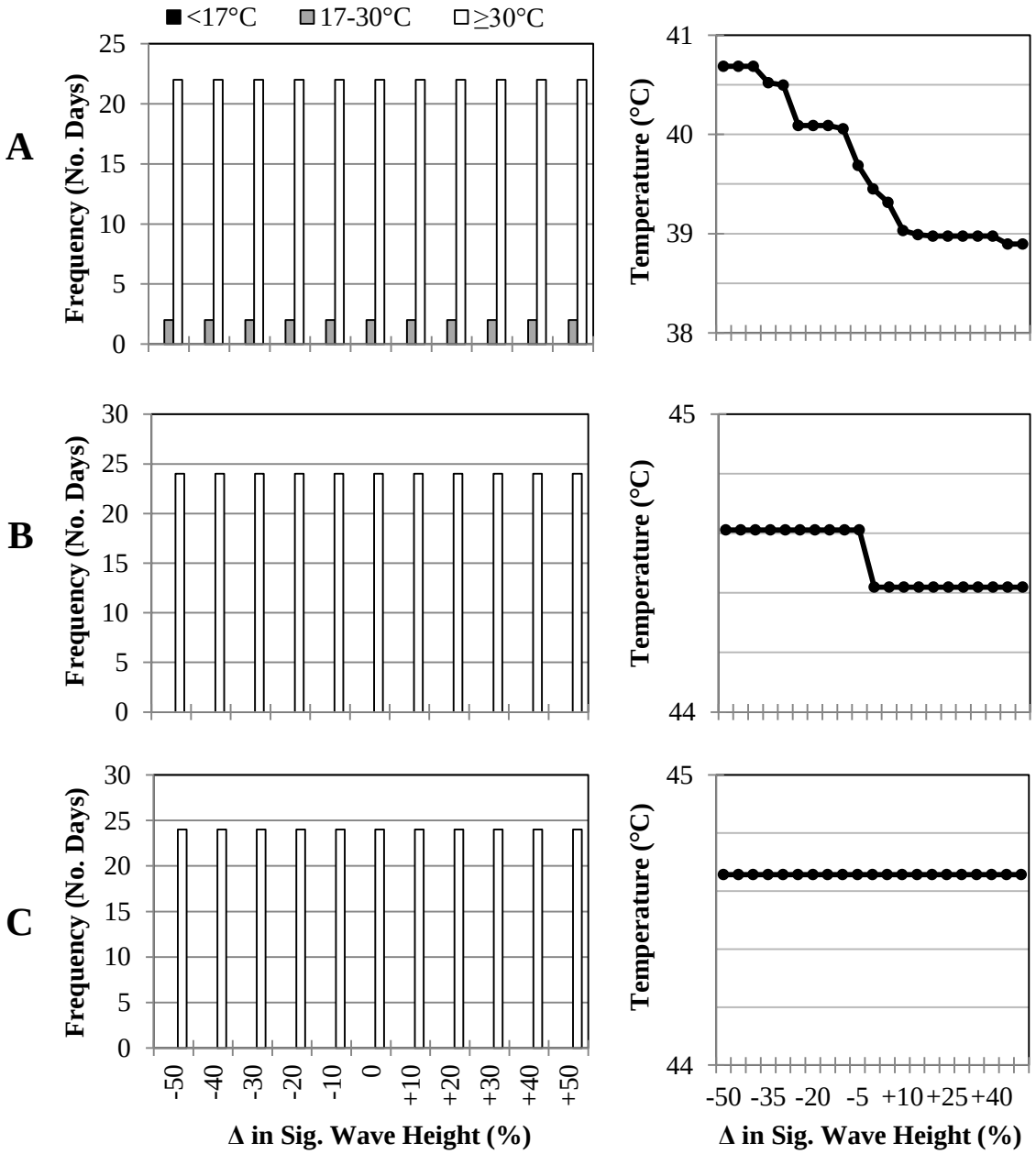

Figure 3.18 Average daily maximum body temperatures predicted by the general model with increasing and decreasing significant wave heights for the three intertidal zones at Coal Oil Point. The results are shown for the **(A)** low, **(B)** mid and **(C)** high intertidal zones during the hottest months (N = 24 months).

of cold temperatures while the high intertidal zone had the greatest number of high temperatures. The high intertidal zone was least affected by changing wave heights but the low intertidal zone is most affected by changing wave heights (Table C.4 & Fig. C.4).

Examining the entire time series, the number of high lethal temperatures was only impacted for the low intertidal zone when the wave height was decreased. This caused an increase in the number of lethal temperatures. Changing the significant wave height for the mid and high intertidal zone did not have an impact on the number of high lethal temperatures (Table C.4). For Coal Oil Point, like all of the other locations, the mid and high intertidal zones were completely unaffected by changing wave heights. A difference between this location and the other locations is that the low intertidal zone is also not impacted by changing wave heights. The analysis for the hottest months revealed that the distribution of temperatures was unaffected by changing wave climates for all three intertidal zones (Fig. 3.18).

CHAPTER 4

DISCUSSION & CONCLUSION

The body temperatures of intertidal organisms are driven by the interaction of oceanographic and atmospheric conditions, the individual's thermal properties and the characteristics of the surrounding microhabitat (Helmuth 1998; Kearney 2006; Porter and Gates 1969). There has been a growing need to model the diverse effects that these conditions and characteristics have on organismal body temperature to better understand species interactions, biogeographic ranges, and the likely impacts of climate change (Broitman et al. 2009; Finke et al. 2009; Fuller et al. 2010; Gilman et al. 2006b; Helmuth et al. 2006a; Jones et al. 2009; Mislan et al. 2014; Wethey 2002; Wethey and Woodin 2008). Specifically, there are several complex models that can be used to predict intertidal organism body temperature (i.e. Gilman et al. 2006b; Sará et al. 2011; Wethey et al. 2011a), but a simple, versatile, user-friendly model is needed that can be used by decision makers, who may not have a background in mathematical modeling, to inform policy.

This research was conducted to evaluate the sensitivity of a simple biophysical heat budget model (adapted from Helmuth et al. 2011) to changes in morphological, oceanographic and atmospheric parameters and to determine the accuracy of that model using coarse gridded weather data in place of local weather station data. Additionally, since local weather stations are not always available (Mislan and Wethey 2011), the use of coarse gridded weather data, from a source such as CFSR, would allow for predictions

to be made for a larger sampling of locations. Furthermore, this model was used to evaluate how the survival of the California ribbed mussel (*Mytilus californianus*) is affected by changes in wave height and to use this information to determine which of the examined sites in California are most sensitive to changing wave climates. This information can be used to influence the placement of wave energy farms and will also be informative of the likely impacts that climate change can have on the zonation and survival of intertidal organisms.

The initial goal of this project was to determine if an existing, Microsoft Excel-based model (Helmuth et al. 2011) could serve this function, and whether detailed information on microhabitat characteristics provided any real advantage in model accuracy. My results suggest that the accuracy of mussel body temperature predictions are insensitive to the parameters describing the organism and its microhabitat. It also suggested that model accuracy was fairly insensitive to changes in cloud cover. This is likely due to the location of the NOAA National Climatic Data Center (NCDC) buoy (Station Name: Environm. Buoy 46013) from which the cloud cover data were obtained. In all cases, changes in the relative accuracy of model outputs, when compared to *in situ* logger data, were on par with errors in the loggers themselves, ~2°C (Fitzhenry et al. 2004). This suggests that, at least at the Bodega Bay site, the use of generic parameter values does not accrue any appreciable decrease in model accuracy.

A second goal of this project was to determine if using local weather station (LWS) data in place of CFSR data significantly improved the accuracy of the model temperature predictions. While the model using LWS data at the Hopkins site yielded lower error rates (between 1.6 – 3.7°C lower) than the model using CFSR data (Table

4.1), model results using the two data sources had very comparable errors at the Bodega site. These errors are comparable to those of the loggers, ~2°C, indicating that the use of CFSR data in place of LWS data at other sites was acceptable. Additionally, the model using LWS data tended to run cold at both locations (Table 4.2) while the model using CFSR data ran hot at all four locations (Table 4.3).

Table 4.1 Indication of which type of weather data (LWS or CFSR) led to more accurate body temperature predictions for each intertidal zone. This designation is based on the absolute average difference between the model predictions and the temperatures recorded by the loggers in the field.

	Intertidal Zone		
Study Location	Low	Mid	High
Bodega Bay	CFSR	LWS	CFSR
Hopkins	LWS	LWS	LWS
Alegria	NA	NA	NA
Coal Oil Point	NA	NA	NA

Table 4.2 Percent difference between body temperatures predicted by model using LWS data and body temperatures measured by loggers. A positive value indicates that the model overestimated the number of body temperatures in the category (running hot) and a negative value means that the model underestimated the number of temperatures (running cold). Data are shown for the five divisions of the physiological framework: cold suboptimal/sublethal (<17°C), optimal (17-22°C), high suboptimal (22-30°C), high sublethal (30-38°C) and high lethal (≥38°C).

		Temperature (%)				
Intertidal Zone	Study Location	<17°C	17-22°C	22-30°C	30-38°C	≥38°C
Low	Bodega Bay	-4.4	57.1	-93.3	-200.0	0.0
	Hopkins	74.1	-53.7	-105.1	-179.7	-200.0
Mid	Bodega Bay	19.0	9.1	-93.5	-165.2	0.0
	Hopkins	-40.8	25.4	31.6	-41.9	0.0
High	Bodega Bay	75.6	61.5	-118.7	-190.0	-200.0
	Hopkins	-60.5	62.3	25.1	-164.6	-178.9

Table 4.3 Percent difference between body temperatures predicted by model using CFSR data and body temperatures measured by loggers. A positive value indicates that the model overestimated the number of body temperatures in the category (running hot) and a negative value means that the model underestimated the number of temperatures (running cold). Data are shown for the five divisions of the physiological framework:

cold suboptimal/sublethal (<17°C), optimal (17-22°C), high suboptimal (22-30°C), high sublethal (30-38°C) and high lethal (≥38°C).

Intertidal Zone	Study Location	Temperature (%)				
		<17°C	17-22°C	22-30°C	30-38°C	≥38°C
Low	Bodega Bay	-8.1	70.4	-20.0	0.0	0.0
	Hopkins	52.6	-36.9	-59.9	-33.3	66.7
	Alegria	98.8	-72.9	-14.6	57.1	-88.0
	Coal Oil Point	30.5	-81.7	52.7	184.9	200.0
Mid	Bodega Bay	-15.2	32.6	-24.3	-136.0	0.0
	Hopkins	-51.1	-47.8	52.7	162.7	160.0
	Alegria	-27.0	-59.9	11.3	58.6	115.8
	Coal Oil Point	-80.1	-88.4	35.8	158.3	200.0
High	Bodega Bay	27.5	76.9	-69.5	-173.7	-200.0
	Hopkins	-31.6	-42.9	34.2	25.1	-32.3
	Alegria	-44.6	-81.3	26.7	49.0	85.1
	Coal Oil Point	-76.9	-119.8	28.9	143.1	191.8

These results are similar to those reported by Mislan and Wethey (2011) who used a more complex model to determine if different types of large scale gridded weather data, including CFSR, could be used in place of local weather station data to predict monthly daily maximum temperatures. They compared model output using different data inputs against in *in situ* logger data for sites in Oregon and California, including Bodega Bay and Hopkins. Their model using CFSR data predicted temperatures that were most similar to those recorded by the loggers in the field compared to the other types of gridded data examined, including NARR, GCIP, and NASA MERRA. Similar to the results presented here, the model using CFSR data was more accurate at Bodega Bay than it was at Hopkins and predicted temperatures that were higher than those predicted by the model using LWS data. One notable difference between their study and this one is that the temperatures predicted by their model were warmer for Bodega Bay than they were for Hopkins, whereas for this study the reverse was true. This was likely due their use of

the monthly average daily maximum temperatures as a measure of error (Mislan and Wethey, 2011) versus the use of average daily maximum used here.

The range of error associated with different models is complex, as are differences among some of the heat budget models themselves, but comparisons are difficult given the different error measures used. Gilman et al. (2006b) reported errors that were similar to those of the loggers, but this was comparing monthly average daily maxima, rather than all daily maxima as reported here. The original model that was adapted for this research predicted mussel daily maximum body temperatures within 2.8°C at Bodega Bay (Helmuth et al. 2011). The model used for this research, at its most accurate point (for the mid intertidal zone), was able to predict temperatures to within a very comparable 3.1°C using LWS data at Hopkins.

Much of the variation in temperatures within sites has been attributed to differences in wave exposure (Gilman et al. 2006b; Helmuth et al. 2002). For example, Helmuth et al. (2006a) and this study found that the mussels located at wave protected sites experienced warmer temperatures than those at wave exposed locations. Also, the model used in this study and the model used by Finke et al. (2009) ran hot. Finke et al. (2009) explained their model's overestimation of temperature as a result of the difference in the actual tide height and the predicted tide height (i.e. difference in wave exposure). Their model did not account for the swash that was cooling the organism during aerial exposure. Advances have been made in an attempt to quantify and incorporate wave exposure into models (Gilman et al. 2006a; Helmuth et al. 2006a; Mislan et al. 2011), but it is an ongoing complication within model predictions that will require additional research (Helmuth et al. 2011).

There is more than one measure of error or uncertainty. The selection of the specific measure of error/uncertainty depends on the model's functionality. Here, several measures of error have been provided for determining whether or not this model was able to accurately predict mussel body temperatures, specifically, the calculated difference between the loggers observations and model predictions, and uncertainty, the range of temperatures in which the loggers' measurements may actually be located. I provided more measurements of error (average difference, absolute average difference, RMSE, number of stressful days, false positives/negatives) than uncertainty (ability to accurately distribute temperatures in a physiological framework that matches the distribution of logger temperatures). Providing all these measures of error and uncertainty is a way of ensuring that the end-user has a useful measure of error to examine in order to determine if the model is 'good enough' to be used for their needs.

A model's usefulness to one person could depend on a metric of error, such as the absolute average difference as I have focused on here, while to another person the uncertainty of the model is important, and they may be focused on statistical p-values, which I have not discussed. A model that is right for one application may not be right for another. Therefore, the successful application of a model depends on the questions that it is being used to address, and the end-users tolerance for false positives and false negatives. For example, an end user who errs on the side of precaution and needs a model that overestimates the number of stressful temperatures experienced by mussels could use this model for Bodega Bay or Hopkins. On the other hand, someone who needs this model to underestimate the number of stressful temperatures could use this model for Alegria or Coal Oil Point. In the end, some measures of error/uncertainty associated with

this model are better for some sites and worse for others and it all depends on which type of error is most important to the person that uses the model. For the purposes of understanding the effects of changing wave climates on intertidal organisms, I used a measure of uncertainty (the physiological framework) to determine what study locations are most and least impacted.

Despite wave exposure difficulties with the model predictions, which potentially led to a higher number of false stressful and lethal temperature predictions, the final goal of this project was to determine how body temperatures would be impacted by changes in significant wave heights. For all four locations, the predicted body temperatures increased with decreasing wave heights, which also led to an increased number of stressful and lethal temperature predictions (Table 4.4). As wave height increased, body temperatures and the number of stressful and lethal temperature days decreased (Table 4.5). As wave heights decrease or increase, the amount of surge and splash also decreases or increases, thereby reducing or increasing the amount of time organisms are cooled during aerial exposure, respectively (Mislan et al. 2011).

Table 4.4 Effect of decreasing significant wave height on model predicted body temperatures. Data are shown for the five divisions of the physiological framework: cold suboptimal/sublethal (<17°C), optimal (17-22°C), high suboptimal (22-30°C), high sublethal (30-38°C) and high lethal (≥38°C). Values shown are the percent change from the number of temperatures within each category predicted by the model with the actual wave height (no change) to the number of temperatures predicted by the model using the maximum decrease (-50%) in wave height. A positive value is an increase in the number of temperatures and a negative value is a decrease in the number of temperatures.

Intertidal Zone	Study Location	Temperature (%)				
		<17°C	17-22°C	22-30°C	30-38°C	≥38°C
Low	Bodega Bay	-5.7	13.6	37.5	0.0	0.0
	Hopkins	-13.1	4.0	14.5	14.4	200.0
	Alegria	-28.7	6.3	9.1	9.9	13.0
	Coal Oil Point	-17.3	4.3	6.4	8.3	5.4

Mid	Bodega Bay	-28.5	10.5	23.0	31.6	0.0
	Hopkins	-23.8	-4.0	6.6	11.6	25.5
	Alegria	-21.1	-5.5	-0.9	7.2	11.1
	Coal Oil Point	87.6	13.0	-40.4	-85.4	-104.2
High	Bodega Bay	-0.3	-0.3	0.9	0.0	0.0
	Hopkins	-0.9	1.0	0.0	0.0	0.0
	Alegria	-1.7	0.5	0.0	0.1	0.0
	Coal Oil Point	0.0	0.0	0.0	0.0	0.0

Table 4.5 Effect of increasing significant wave height on model predicted body temperatures. Data are shown for the five divisions of the physiological framework: cold suboptimal/sublethal (<17°C), optimal (17-22°C), high suboptimal (22-30°C), high sublethal (30-38°C) and high lethal (≥38°C). Values shown are the percent change from the number of temperatures within each category predicted by the model with the actual wave height (no change) to the number of temperatures predicted by the model using the maximum increase (+50%) in wave height. A positive value is an increase in the number of temperatures and a negative value is a decrease in the number of temperatures.

Intertidal Zone	Study Location	Temperature (%)				
		<17°C	17-22°C	22-30°C	30-38°C	≥38°C
Low	Bodega Bay	4.5	-15.8	-16.7	0.0	0.0
	Hopkins	14.6	-22.4	-8.1	-25.0	0.0
	Alegria	13.6	-6.3	-3.8	-7.9	-2.4
	Coal Oil Point	15.0	-6.2	-7.1	-9.1	-1.9
Mid	Bodega Bay	28.0	-18.2	-33.1	-13.3	0.0
	Hopkins	32.0	0.0	-10.2	-24.9	-40.0
	Alegria	37.5	7.0	-1.5	-11.8	-15.9
	Coal Oil Point	16.2	2.6	1.6	-1.5	-7.7
High	Bodega Bay	4.3	-1.8	-1.0	0.0	0.0
	Hopkins	3.9	-0.7	-0.9	-1.0	0.0
	Alegria	6.1	1.1	-0.8	-0.3	-1.2
	Coal Oil Point	0.8	0.0	-0.2	0.0	0.0

The two wave exposed locations, Bodega Bay and Hopkins, were more sensitive to changing wave heights compared to the two wave protected locations, Alegria and Coal Oil Point. This could be due to the timing of the low tide being different in northern locations versus southern locations. At northern locations, low tide tends to occur midday during the hottest months of the year, while in southern locations low tides seldom occur midday during these thermally stressful months (Helmuth et al. 2006a). Decreasing or

increasing wave heights would impact the height of low tides and therefore the amount of swash available to cool organisms during low tide. If low tide occurs during the hottest time of the day during the hottest time of the year, and wave heights are decreased, there may be a higher occurrence of stressful and lethal temperatures among mussels in the high intertidal zone. This could lead to a decrease in the upper zonation limit of these organisms. Likewise, if the low tide height is increased, then mussels would be able to live higher on the shore and still be within their physiological limits.

Due to the oceanographic conditions that characterize the southern coast of California (low waves and weak seasonal upwelling), installing wave energy devices off of the coast of Coal Oil Point of Alegria would be fruitless. Therefore, Hopkins or Bodega Bay would be the most likely locations of wave energy development where there are high waves and strong upwelling, therefore leading to a greater renewable energy resource. Wave energy farms off the coast of Hopkins would lead to more stressful temperatures in the low and mid intertidal zones and potentially more lethal temperatures within the mid and high intertidal zones. For Bodega Bay, although the installation of wave energy farms would lead to temperatures rising above the optimal threshold, they would not reach into the stressful category above 30°C, even in the high intertidal zone. Conclusively, although one of the more wave energy sensitive locations, wave energy installments off the coast of Bodega Bay would provide the greatest amount of energy, as the northernmost study location, with the lowest impact on the intertidal community, with the lowest overall temperatures.

Researchers have documented that rising sea level and increases in temperature due to climate change will have effects on biogeographic shifts of organisms (Berke et al.

2010; Jones et al. 2009; Jones et al. 2010; Wethey et al. 2011b). These changes can also lead to shifts in vertical zonation (Thompson et al. 2002). While wave heights are expected to increase with climate change, wave energy conversion devices can decrease wave height and swash. Understanding the impacts that these changes will have on aerial and submerged body temperatures of organisms in the intertidal zone are important considerations for predicting the likely impacts of climate change and wave energy farms on intertidal communities.

In conclusion, although the model was able to accurately predict mussel daily maximum temperatures at Bodega Bay using both LWS (3.16°C) and CFSR (3.34°C) data for the mid intertidal zone, its ability to accurately predict temperatures of mussels for other locations was not reliable. Due to the inaccuracy of this model, its use by decision-makers to inform policy decisions should be approached with caution. My work provides a general foundation for understanding the impacts that changing wave climates will have on mussels in the rocky intertidal zone along the coast of California; however, more analyses need to be completed using a model that is more site specific in order to determine which sites along the west coast will be least impacted by changing significant wave heights.

REFERENCES

Bayne BL, Bayne CJ, Carefoot TC, Thompson RJ. 1976. The physiological ecology of *Mytilus californianus* Conrad. 1. Metabolism and Energy Balance. Oecologia. 22(3):211-228.

Berke SK, Mahon AR, Lima FP, Halanych KM, Wethey DS, Woodin SA. 2010. Range shifts and species diversity in marine ecosystem engineers: patterns and predictions for European sedimentary habitats. Global Ecol Biogeogr. 19:223-232.

Berlow EL. 1999. Strong effects of weak interactions in ecological communities. Nature. 398:330-334.

Bernhardt JR, Leslie HM. 2013. Resilience to climate change in coastal marine ecosystems. Ann Rev Mar Sci. 5:371-392.

Blanchette CA. 1997. Size and survival of intertidal plants in response to wave action: A case study with *Fucus gardneri*. Ecology. 78(5):1563-1578.

Blanchette CA, Helmuth B, Gaines SD. 2007. Spatial patterns of growth in the mussel, *Mytilus californianus*, across a major oceanographic and biogeographic boundary at Point Conception, California, USA. J Exp Mar Biol Ecol. 340(2):126-148.

Boehlert GW, Gill AB. 2010. Environmental and ecological effects of ocean renewable energy development: A current synthesis. Oceanography. 23(2):68-81.

Boulding EG. 1990. Are the opposing selection pressures on exposed and protected shores sufficient to maintain genetic differentiation between gastropod populations with high intermigration rates? Hydrobiologia. 193(1):41-52.

Boulding EG, VanAlstyne KL. 1993. Mechanisms of differential survival and growth of two species of *Littorina* on wave-exposed and on protected shores. J Exp Mar Biol Ecol. 169(2):139-166.

Brown KM, Quinn JF. 1988. The effect of wave action on growth in three species of intertidal gastropods. Oecologia. 75(3):420-425.

Broitman BR, Szathmary PL, Mislan KAS, Blanchette CA, Helmuth B. 2009. Predator-prey interactions under climate change: The importance of habitat vs body temperature. Oikos. 118:219-224.

Burrows EM, Conway E, Lodge SM, Powell HT. 1954. The raising of intertidal algal zones on Fair Isle. J Ecol. 42(2):283-288.

Burrows MT, Harvey R, Robb L. 2008. Wave exposure indices from digital coastlines and the prediction of rocky shore community structure. Mar Ecol Prog Ser. 353:1-12.

Cimberg RL. 1975. Zonation, species diversity, and redevelopment in the rocky intertidal near Trinidad, northern California [dissertation]. [Arcata, (CA)]: Humboldt State University. 236 p.

Colman J. 1933. The nature of the intertidal zonation of plants and animals. J Mar Biol Assoc UK (New Series). 18(2):435-476.

Connell JH. 1972. Community interactions on marine rocky intertidal shores. Annu Rev Ecol Syst. 3:169-192.

Davenport J, Davenport JL. 2005. Effects of shore height, wave exposure and geographical distance on thermal niche width of intertidal fauna. Mar Ecol Prog Ser. 292:41-50.

Dayton PK. 1971. Competition, disturbance and community organization: The provision and subsequent utilization of space in a rocky intertidal community. Ecol Monogr. 41(4):351-389.

Denny M. 1995. Predicting physical disturbance: Mechanistic approaches to the study of survivorship on wave-swept shores. Ecol Monogr. 65(4):371-418.

Denny MW. 2006. Ocean waves, nearshore ecology, and natural selection. Aquat Ecol. 40(4):439-461.

Denny MW, Miller LP, Harley CDG. 2006. Thermal stress on intertidal limpets: Long-term hindcasts and lethal limits. J Exp Biol. 209(13):2420-2431.

Denny MW, Dowd WW, Bilir L, Mach KJ. 2011. Spreading the risk: Small-scale body temperature variation among intertidal organisms and its implications for species persistence. J Exp Mar Biol Ecol. 400(1-2):175-190.

Doty MS. 1946. Critical tide factors that are correlated with the vertical distribution of marine algae and other organisms along the Pacific Coast. Ecology. 27(4):315-328.

Doty MS, Archer JG. 1950. An experimental test of the tide factor hypothesis. Am J Bot. 37(6):458-464.

Etter RJ. 1989. Life history variation in the intertidal snail *Nucella lapillus* across a wave-exposure gradient. Ecology. 70(6):1857-1876.

Finke GR, Bozinovic F, Navarrete SA. 2009. A mechanistic model to study the thermal ecology of a Southeastern Pacific dominant intertidal mussel and implications for climate change. Physiol Biochem Zool. 82(4):303-313.

Fitzhenry T, Halpin PM, Helmuth B. 2004. Testing the effects of wave exposure, site, and behavior on intertidal mussel body temperatures: Applications and limits of temperature logger design. Mar Biol. 145(2):339-349.

Flater D. XTide: Harmonic tide clock and tide predictor [Internet]. [cited 2013 May 8]. Available from: http://www.flaterco.com/xtide/.

Foster BA. 1969. Tolerance of high temperatures by some intertidal barnacles. Mar Biol. 4:326-332.

Fuller A, Dawson T, Helmuth B, Hetem RS, Mitchell D, Maloney SK. 2010. Physiological mechanisms in coping with climate change. Physiol Biochem Zool. 83(5):713-720.

Gaylord B. 1999. Detailing agents of physical disturbance: wave-induced velocities and accelerations on a rocky shore. J Exp Mar Biol Ecol. 239(1):85-124.

Gilman SE, Harley CDG, Strickland DC, Vanderstraeten O, O'Donnell MJ, Helmuth B. 2006a. Evaluation of effective shore level as a method of characterizing intertidal wave exposure regimes. Limnol Oceanogr Methods. 4:448-457.

Gilman SE, Wethey DS, Helmuth B. 2006b. Variation in the sensitivity of organismal body temperature to climate change over local and geographic scales. Proc Natl Acad Sci USA. 103(25):9560-9565.

Halpin PM, Menge BA, Hofmann GE. 2004. Experimental demonstration of plasticity in the heat shock response of the intertidal mussel *Mytilus californianus*. Mar Ecol Prog Ser. 276:137-145.

Harger JRE. 1970. The effect of wave impact on some aspects of the biology of sea mussels. Veliger. 12(4):401-414.

Harley C. 2007. Zonation. In: Encyclopedia of the Natural World: Encyclopedia of Tidepools & Rocky Shores. 1st Ed. Berkeley and Los Angeles, CA: University of California Press. p. 641-647.

Harley CDG. 2008. Tidal dynamics, topographic orientation, and temperature-mediated mass mortalities on rocky shores. Mar Ecol Prog Ser. 371:37-46.

Harley CDG, Helmuth BST. 2003. Local- and regional-scale effects of wave exposure, thermal stress, and absolute vs. effective shore level on patterns of intertidal zonation. Limnol Oceanogr. 48(4):1498-1508.

Harley CDG, Denny MW, Mach KJ, Miller LP. 2009. Thermal stress and morphological adaptations in limpets. Funct Ecol. 23(2):292-301.

Helmuth BST. 1998. Intertidal mussel microclimates: Predicting the body temperature of a sessile invertebrate. Ecol Monogr. 68(1):29-52.

Helmuth B. 1999. Thermal biology of rocky intertidal mussels: Quantifying body temperatures using climatological data. Ecology. 80(1):15-34.

Helmuth B. 2002. How do we measure the environment? Linking intertidal thermal physiology and ecology through biophysics. Integr Comp Biol. 42(4):837-845.

Helmuth BST, Hofmann GE. 2001. Microhabitats, thermal heterogeneity, and patterns of physiological stress in the rocky intertidal zone. Biol Bull. 201(3):374-384.

Helmuth B, Harley CD, Halpin P, O'Donnell M, Hofmann GE, Blanchette C. 2002. Climate change and latitudinal patterns of intertidal thermal stress. Science. 298:1015-1017.

Helmuth B, Broitman BR, Blanchette CA, Gilman S, Halpin P, Harley CDG, O'Donnell MJ, Hofmann GE, Menge B, Strickland D. 2006a. Mosaic patterns of thermal stress in the rocky intertidal zone: Implications for climate change. Ecol Monogr. 76(4):461-479.

Helmuth B, Mieszkowska N, Moore P, Hawkins SJ. 2006b. Living on the edge of two changing worlds: Forecasting the responses of rocky intertidal ecosystems to climate change. Annu Rev Ecol Evol Syst. 37:373-404.

Helmuth B, Yamane L, Lalwani S, Matzelle A, Tockstein A, Gao N. 2011. Hidden signals of climate change in intertidal ecosystems: What (not) to expect when you are expecting. J Exp Mar Biol Ecol. 400(1-2):191-199.

Huey RB, Stevenson RD. 1979. Integrating thermal physiology and ecology of ectotherms: A discussion of approaches. Am Zool. 19(1):357-366.

Jones SJ, Mieszkowska N, Wethey DS. 2009. Linking thermal tolerances and biogeography: *Mytilus edulis* (L.) at its southern limit on the east coast of the United States. Biol Bull. 217(1):73-85.

Jones SJ, Lima FP, Wethey DS. 2010. Rising environmental temperatures and biogeography: Poleward range contraction of the blue mussel, *Mytilus edulis* L., in the western Atlantic. J Biogeogr. 37(12):2243-2259.

Jost J, Helmuth B. 2007. Morphological and ecological determinants of body temperature of *Geukensia demissa*, the Atlantic Ribbed Mussel, and their effects on mussel mortality. Biol Bull. 213(2):141-151.

Jubb CA, Hughes RN, Rheinallt T. 1983. Behavioral mechanisms of size-selection by crabs, *Carcinus maenas* (L.) feeding on mussels, *Mytilus edulis* L. J Exp Mar Biol Ecol. 66(1):81-87.

Kanter RG. 1977. Structure and diversity in *Mytilus californianus* (*Mollusca*: *Bivalvia*) communities [dissertation]. [Los Angeles, (CA)]: University of Southern California. 114 p.

Kanter RG. 1980. Biogeographic patterns in mussel community distribution from the Southern California Bight. In: The California Islands: Proceedings of a

Multidisciplinary Symposium. Santa Barbara, CA: Santa Barbara Museum of Natural History. p. 341-355

Kearney M. 2006. Habitat, environment and niche: What are we modelling? Oikos. 115:186-191.

Kearney M, Simpson SJ, Raubenheimer D, Helmuth B. 2010. Modelling the ecological niche from functional traits. Philos T Roy Soc B. 365(1557):3469-3483.

Kish N. 2013. Modeling approaches, physiological responses, and climate change: How good is 'good enough?' [Thesis]. [Columbia, (SC)]: University of South Carolina. 47 p.

Lawson GW. 1957. Seasonal variation of intertidal zonation on the coast of Ghana in relation to tidal factors. J Ecol. 45(3):831-860.

Leigh EG, Paine RT, Quinn JF, Suchanek TH. 1987. Wave energy and intertidal productivity. Proc Natl Acad Sci USA. 84(5):1314-1318.

Lively CM, Raimondi PT, Delph LF. 1993. Intertidal zommunity structure: Space-time interactions in the northern Gulf of California. Ecology. 74(1):162-173.

McNeill, M. 2010. Vertical zonation: Studying ecological patterns in the rocky intertidal zone. Sci Act: Classroom Projects and Curriculum Ideas. 47(1):8-14.

Menge BA. 1976. Organization of the New England Rocky intertidal community: Role of predation, competition, and environmental heterogeneity. Ecol Monogr. 46(4):355-393.

Menge BA, Berlow EL, Blanchette CA, Navarrete SA, Yamada SB. 1994. The keystone species concept: Variation in interaction strength in a rocky intertidal habitat. Ecol Monogr. 64(3):249-286.

Millar DL, Smith HCM, Reeve DE. 2007. Modelling analysis of the sensitivity of shoreline change to a wave farm. Ocean Eng. 34(5-6):884-901.

Minerals Management Service [MMS] (US). Technology White Paper on Wave Energy Potential on the U.S. Outer Continental Shelf [Internet]. Renewable Energy and Alternate Use Program. U.S. Department of the Interior; 2006 May [cited 2011 Sept 11]. Available from: http://www.boem.gov/Renewable-Energy-Program/Renewable-Energy-Guide/Ocean-Current-Energy.aspx.

Mislan KAS, Wethey DS. 2011. Gridded meteorological data as resource for mechanistic ecology in coastal environments. Ecol Appl. 21(7):2678-2690.

Mislan KAS, Blanchette CA, Broitman BR, Washburn L. 2011. Spatial variability of emergence, splash, surge, and submergence in wave-exposed rocky-shore ecosystems. Limnol Oceanogr. 56(3):857-866.

Mislan KAS, Helmuth B, Wethey DS. 2014. Geographical variation in climatic sensitivity of intertidal mussel zonation. Glob Ecol Biogeogr. 23(7):744-756.

National Data Buoy Center [NDBC] [Internet]. Standard Meteorological Historical Data. Hancock County (MS): Stennis Space Center. [updated 2013 Dec 11; cited 2013 May 8]. Available from: http://www.ndbc.noaa.gov/.

NOMADS Data Access [Internet]. Dataset: CFSR – Hi-Priority Time Series. Asheville (NC): National Climatic Data Center. [updated 2013 Dec 12; cited 2013 May 9]. Available from: http://nomads.ncdc.noaa.gov/thredds/catalog/cfsr1hr/catalog.html.

Paasch R, Ruehl K, Hovland J, Meicke S. 2012. Wave energy: A Pacific perspective. Philos T Roy Soc A. 370(1959):481-501.

Paine RT. 1966. Food web complexity and species diversity. Am Nat. 100(910):65-75.

Paine RT. 1974. Intertidal community structure: Experimental studies on the relationship between a dominant competitor and its principal predator. Oecologia. 15(2):93-120.

Palha A, Mendes L, Fortes CJ, Brito-Melo A, Sarmento A. 2010. The impact of wave energy farms in the shoreline wave climate: Portuguese pilot zone case study using Pelamis energy wave devices. Renew Energy. 35(1):62-77.

Pincebourde S, Sanford E, Helmuth B. 2008. Interaction between underwater and aerial body temperatures in influencing a top predator feeding rate in the intertidal. Comp Biochem Physiol A Mol Integr Physiol. 150(3)Supplement:S95.

Pincebourde S, Sanford E, Casas J, Helmuth B. 2012. Temporal coincidence of environmental stress events modulates predation rates. Ecol Lett. 15(7):680-688.

Porter WP, Gates DM. 1969. Thermodynamic equilibria of animals with environment. Ecol Monogr. 39(3):227-244.

Raimondi PT. 1988. Settlement cues and determination of the vertical limit of an intertidal barnacle. Ecology. 69(2):400-407.

Research Database [Internet]. Boston (MA): Northeastern University Helmuth Lab. [updated 2013; cited 2013 April 25]. Available from: http://www.northeastern.edu/helmuthlab/database/.

Robles C, Sweetnam D, Eminike J. 1990. Lobster predation on mussels: Shore-level differences in prey vulnerability and predator preference. Ecology. 71(4):1564-1577.

Saha S, Moorthi S, Pan H-L, Wu X, Wang J, Nadiga S, *et al*. 2010. The NCEP Climate Forecast System Reanalysis. B Am Meteorol Soc. 91:1015-1057.

Sanford E. 2002. The feeding, growth, and energetics of two rocky intertidal predators (*Pisaster ochraceus* and *Nucella canaliculata*) under water temperatures simulating episodic upwelling. J Exp Mar Biol Ecol. 273(2):199-218.

Sanford E, Roth MS, Johns GC, Wares JP, Somero GN. 2003. Local selection and latitudinal variation in a marine predator-prey interaction. Science. 300(5622):1135-1137.

Sarà G, Kearney M, Helmuth B. 2011. Combining heat-transfer and energy budget models to predict thermal stress in Mediterranean intertidal mussels. Chem Ecol. 27(2):135-145.

Sarà G, Palmeri V, Rinaldi A, Montalto V, Helmuth B. 2013. Predicting biological invasions in marine habitats through eco-physiological mechanistic models: A case study with the bivalve *Brachidontes pharaonis*. Divers Distrib. 19(10):1235-1247.

Smith HCM, Pearce C, Millar DL. 2012. Further analysis of change in nearshore wave climate due to an offshore wave farm: An enhanced case study for the Wave Hub site. Renew Energy. 40(1):51-64.

Smith JR, Fong P, Ambrose RF. 2006. Dramatic declines in mussel bed community diversity: Response to climate change? Ecology. 87(5):1153-1161.

Smith KA. 2010. Measuring and forecasting environmental conditions from the perspective of rocky intertidal organisms [dissertation]. [Columbia, (SC)]: University of South Carolina. 135 p.

Somero GN. 2002. Thermal physiology and vertical zonation of intertidal animals: Optima, limits, and costs of living. Integr Comp Biol. 42(4):780-789.

Sousa WP. 1979. Disturbance in marine intertidal boulder fields: The nonequilibrium maintenance of species diversity. Ecology. 60(6):1225-1239.

Stephenson TA, Stephenson A. 1949. The universal features of zonation between tide-marks on rocky coasts. J Ecol. 37(2):289-305.

Stillman JH. 2002. Causes and consequences of thermal tolerance limits in rocky intertidal porcelain crabs, genus *Petrolisthes*. Integr Comp Biol. 42(4):790-796.

Stillman JH, Somero GN. 1996. Adaptation to temperature stress and aerial exposure in congeneric species of intertidal porcelain crabs (genus *Petrolisthes*): Correlation of physiology, biochemistry and morphology with vertical distribution. J Exp Biol. 199(8):1845-1855.

Suchanek TH. 1979. The *Mytilus californianus* community: Studies on the composition, structure, organization and dynamics of a mussel bed [dissertation]. [Seattle, (WA)]: University of Washington. 572 p.

Thompson RC, Crowe TP, Hawkins SJ. 2002. Rocky intertidal communities: Past, environmental changes, present status and predictions for the next 25 years. Environmental Conservation. 29(2):168-191.

Tomanek L, Helmuth B. 2002. Physiological ecology of rocky intertidal organisms: A synergy of concepts. Integr Comp Biol. 42(4):771-775.

Tsuchiya M. 1983. Mass mortality in a population of the mussel *Mytilus edulis* L. caused by high temperature on rocky shores. J Exp Mar Biol Ecol. 66(2):101-111.

Underwood AJ. 1972. Tide-model analysis of the zonation of intertidal prosobranchs, I. Four species of *Littorina* (L.). J Exp Mar Biol Ecol. 9(3):239-255.

Underwood AJ. 1978. A refutation of critical tidal levels as determinants of the structure of intertidal communities on British shores. J Exp Mar Biol Ecol. 33(3):261-276.

Underwood AJ. 1981. Structure of a rocky intertidal community in New South Wales: Patterns of vertical distribution and seasonal changes. J Exp Mar Biol Ecol. 51(1):57-85.

Underwood AJ. 2000. Experimental ecology of rocky intertidal habitats: What are we learning? J Exp Mar Biol Ecol. 250(1-2):51-76.

Underwood AJ, Jernakoff P. 1984. The effects of tidal height, wave-exposure, seasonality and rock-pools on grazing and the distribution of intertidal macroalgae in New South Wales. J Exp Mar Biol Ecol. 75(1):71-96.

Wethey DS. 1983. Geographic limits and local zonation: The barnacles *Semibalanus* (*Balanus*) and *Chthamalus* in New England. Biol Bull. 165(1):330-341.

Wethey DS. 2002. Microclimate, competition, and biogeography: The barnacle *Chthamalus fragilis* in New England. Integr Comp Biol. 42:872-880.

Wethey DS, Woodin SA. 2008. Ecological hindcasting of biogeographic responses to climate change in the European intertidal zone. Hydrobiologia. 606:139-151.

Wethey DS, Brin LD, Helmuth B, Mislan KAS. 2011a. Predicting intertidal organism temperatures with modified land surface models. Ecol Modell. 222(19):3568-3576.

Wethey DS, Woodin SA, Hilbish TJ, Jones SJ, Lima FP, Brannock PM. 2011b. Response of intertidal populations to climate: Effects of extreme events versus long term change. J Exp Mar Biol Ecol. 400:132-144.

Wolcott TG. 1973. Physiological ecology and intertidal zonation in limpets (*Acmaea*): A critical look at "limiting factors." Biol Bull. 145(2):389-422.

Wootton JT. 2010. Experimental species removal alters ecological dynamics in a natural ecosystem. Ecology. 91(1):42-48.

WWW Tide and Current Predictor [Internet]. Tidal Height and Current Site Selection. Columbia (SC): University of South Carolina. [cited 2013 May 8]. Available from: http://tbone.biol.sc.edu/tide/.

Zippay ML, Helmuth B. 2012. Effects of temperature change on mussel, *Mytilus*. Integr Zool. 7(3):312-327.

APPENDIX A: DETAILED RESULTS FOR THE SENSITIVITY ANALYSES

On average, all of the **mussel absorptivity** values considered in this study caused the model to underestimate the logger temperatures (negative average difference). The model was able to predict daily maximum mussel body temperatures from within 3.09°C to 2.97°C of the logger temperatures using an absorptivity value of 0.80 and 0.90, respectively, thus model accuracy increased with increasing values of mussel absorptivity. Changing the mussel absorptivity values in the model did not have an impact on the number of predicted stressful days nor the number of false positives or false negatives (Table A.1). The difference in the minimum value between the predicted and actual temperature was the same for all of the mussel absorptivity values (4.84°C).The temperatures predicted using an absorptivity value of 0.90 had the highest mean, highest max, largest range (Fig. 3.1A) and lowest error (Table A.1).

Table A.1 Errors between the mussel body temperatures predicted by the general model with varying values of mussel absorptivity and the logger field measurements in the mid intertidal zone. The errors were determined for each change in parameter using the daily maximum temperature. The value that is used in the general model is 0.85, in bold. The total number of stressful days recorded by the loggers in the field is 20 for the mid intertidal zone.

Mussel Absorptivity	Avg. Diff. (°C)	Abs. Avg. Diff. (°C)	RMSE (°C)	Stressful Days	False Pos.	False Neg.
0.8	-2.07	3.11	4.07	2	2	20
0.825	-1.97	3.08	4.02	2	2	20
0.85	-1.86	3.05	3.98	2	2	20
0.875	-1.76	3.02	3.94	2	2	20
0.9	-1.66	2.99	3.90	2	2	20

As mussel absorptivity decreased the model overestimated more cold temperatures but fewer optimal temperatures and underestimated more high suboptimal temperatures. All mussel absorptivity values caused the model to overestimate the number of temperatures within the cold suboptimal/sublethal category by 92 (absorp. = 0.90) to 160 (absorp. = 0.80) days and the optimal category by 21 (absorp. = 0.80) to 55 (absorp. = 0.90) days. All of the mussel absorptivity values also caused the model to underestimate the number of temperatures within the high suboptimal category by 128 (absorp. = 0.90) to 162 (absorp. = 0.80) days and the high sublethal category by 19 days (all absorp. values) (Fig. 3.1B).

The model underestimated logger temperatures for all **mussel size**s (negative average difference). The model predicted daily maximum mussel body temperatures from within 3.63°C to 2.88°C of the logger temperatures using a mussel size of 0.25 m and 0.05 m, respectively, thus model accuracy increased with decreasing mussel size. The model using a mussel size of 0.05 m predicted the most accurate number of stressful days and was the most accurate when considering false negatives; however this mussel size caused the model to be least accurate when considering false positives (Table A.2).

Table A.2 Errors between the mussel body temperatures predicted by the general model with varying values of mussel size and the logger field measurements in the mid intertidal zone. The errors were determined for each change in parameter using the daily maximum temperature. The value that is used in the general model is 0.075 m, in bold. The loggers in the mid intertidal zone recorded a total number of 20 stressful days.

Mussel Size (m)	Avg. Diff. (°C)	Abs. Avg. Diff. (°C)	RMSE (°C)	Stressful Days	False Pos.	False Neg.
0.05	-0.89	2.88	3.73	8	6	18
0.06	-1.38	2.93	3.81	3	3	20
0.07	-1.72	3.01	3.92	2	2	20
0.075	-1.86	3.05	3.98	2	2	20
0.08	-1.98	3.08	4.03	2	2	20

Mussel Size (m)	Avg. Diff. (°C)	Abs. Avg. Diff. (°C)	RMSE (°C)	Stressful Days	False Pos.	False Neg.
0.09	-2.19	3.15	4.13	1	1	20
0.1	-2.35	3.22	4.22	1	1	20
0.11	-2.48	3.28	4.30	1	1	20
0.12	-2.59	3.33	4.37	0	0	20
0.13	-2.69	3.37	4.43	0	0	20
0.14	-2.76	3.41	4.49	0	0	20
0.15	-2.83	3.45	4.54	0	0	20
0.175	-2.97	3.53	4.64	0	0	20
0.2	-3.07	3.59	4.71	0	0	20
0.225	-3.15	3.64	4.77	0	0	20
0.25	-3.22	3.68	4.82	0	0	20

As the mussel size increased to 0.25 m, the model predictions had a lower minimum, lower mean, lower maximum, smaller range (Fig. 3.2A) and higher error (Table A.2). As mussel size was increased the model overestimated more cold temperatures (up to 363 days) and underestimated more optimal (up to 135 days), high suboptimal (up to 207 days) and high sublethal temperatures (up to 21 days). The only time the model underestimated the number of cold temperatures was when using a mussel size of 0.05 m. The model overestimated the number of optimal temperatures using mussel sizes less than and equal to 0.09 m and underestimated optimal temperatures using sizes greater than 0.09 m. The model using all mussel sizes underestimated the number of high suboptimal and high sublethal temperatures (Fig. 3.2B).

Both values of **cloud cover** data caused the model to underestimate the logger temperatures (negative average difference). The model was able to predict daily maximum mussel body temperatures to within 3.24°C using the normalized cloud cover data but was more accurate using the general cloud cover value. The model using the general cloud cover value was able to better successfully predict the number of stressful days but was less accurate when considering false positives (Table A.3).

Table A.3 Errors between the mussel body temperatures predicted by the general model with varying values of cloud cover and the logger field measurements in the mid intertidal zone. The errors were determined for each change in parameter using the daily maximum temperature. The value that is used in the general model is 0.6, in bold. Twenty stressful days were recorded by the loggers in the mid intertidal zone.

Cloud Cover	Avg. Diff. (°C)	Abs. Avg. Diff. (°C)	RMSE (°C)	Stressful Days	False Pos.	False Neg.
0.6	-1.86	3.05	3.98	2	2	20
Norm.	-2.41	3.28	4.30	1	1	20

The temperatures predicted by the model using the normalized cloud cover data had a lower mean, minimum, and maximum, larger range (Fig. 3.3A) and higher error (Table A.3). Both cloud cover types caused the model to overestimate cold temperatures (129 days using 0.60 and 219 days using normalized data) and underestimate the number of temperatures within the high suboptimal (0.60 = 146 days; normalized = 175 days) and high sublethal (0.60 = 19 days; normalized = 20 days) categories. The model using 0.60 overestimated the number of optimal temperatures by 36 days and the model using the normalized cloud cover data underestimated the number of optimal temperatures by 26 days (Fig. 3.3B).

For the different changes in **ASL**, the model predictions of daily maximum temperature were less accurate for the high intertidal zone. The high intertidal zone also had the greatest number of false negatives but was able to more accurately predict the number of stressful days. The model predictions for the low intertidal zone were most accurate and while it was the best when considering false positives and false negatives, it was least successful at predicting the number of stressful days. All of the ASLs for all intertidal zones caused the model to underestimate the mussel body temperatures (negative average difference) (Table A.4).

For all three intertidal zones, changing the ASL did not have an effect on the maximum predicted temperature and the model predictions using the regression ASLs had the lowest mean, lowest minimum, largest range (Fig. 3.4A), and highest error (Table A.4). The mid and high intertidal zones' general ASLs provided the highest mean, highest minimum, smallest range (Fig. 3.4A), and lowest error (Table A.4). The logger ASL for the low intertidal zone caused the predictions to have the highest mean, highest minimum, smallest range (Fig. 3.4A) and lowest error (Table A.4).

Table A.4 Errors between the mussel body temperatures predicted by the general model with varying values of ASL and the logger field measurements in the low, mid and high intertidal zones. The errors were determined for each change in parameter using the daily maximum temperature. The values that are used in the general model for each intertidal zone are bolded. The second ASL value for each intertidal zone is the logger ASL value and the third value is the regression ASL value. The total number of stressful days recorded by the loggers in the field is 1, 20 and 158 for the low, mid and high intertidal zones, respectively.

Intertidal Zone	ASL (m)	Avg. Diff. (°C)	Abs. Avg. Diff. (°C)	RMSE (°C)	Stressful Days	False Pos.	False Neg.
Low	**0.5**	-1.28	2.36	2.98	0	0	1
	0.69	-0.71	2.29	2.95	0	0	1
	0.43	-1.58	2.41	3.04	0	0	1
Mid	**1.5**	-1.88	3.07	4.00	2	2	20
	1.36	-2.56	3.27	4.22	1	1	20
	1.13	-3.76	4.08	5.21	0	0	20
High	**2.5**	-4.80	5.65	6.88	4	2	156
	1.56	-6.03	6.26	7.42	3	1	156
	1.27	-7.47	7.54	8.93	2	1	157

For the low intertidal zone the three ASLs used caused the model to underestimate the number of cold, high suboptimal and high sublethal temperatures and overestimate the number of optimal temperatures. As the ASL increased the model underestimated more cold temperatures (60 days) and overestimated more optimal temperatures (62 days) (Fig. 3.4B). For the mid intertidal zone, as the ASL decreased the model overestimated more cold (356 days) temperatures and underestimated more high

suboptimal (197 days) and high sublethal (21 days) temperatures. The model using the logger and regression ASLs, the two lower ASLs, caused the model to underestimate the number of optimal temperatures by 14 and 138 days, respectively, while the model using the general ASL caused the model to overestimate the number of optimal temperatures by 35 days (Fig. 3.4B). There is a similar pattern for the high intertidal zone. As the ASL decreased the model overestimated more cold (629 days) temperatures and underestimated more high suboptimal (464 days) and high sublethal (152 days) temperatures. The regression ASL, which is the lowest ASL, underestimated the number of optimal temperatures (6 days) while the logger and general ASLs overestimated the number of optimal temperatures by 109 and 217 days, respectively (Fig. 3.4B).

The change in **ESL slope** for the low, mid and high intertidal zones did not affect the number of stressful days, false positives or false negatives. The high intertidal zone had the greatest number of false negatives and the low intertidal zone had the least. Based on the absolute average difference, the model predictions of daily maximum temperature were less accurate for the high intertidal zone. The model underestimated temperatures for all of the ESL slopes for all of the zones (negative average difference) except the regression low ESL slope (positive average difference). The regression ESL slope produced more accurate results for the low intertidal zone and less accurate results for the mid intertidal zone. The change in ESL slope did not affect the accuracy of the model for the high intertidal zone as indicated by the absolute average difference (Table A.5).

Changes in ESL slope did not have an effect on the predicted maximum temperature for all intertidal zones. The model predictions with the regression ESL slope had the highest mean for all of the intertidal zones. For the low and mid intertidal zone,

the general ESL slope caused the model predictions to have the largest range and the regression ESL slope caused the model predictions to have the highest minimum temperatures (Fig. 3.5A). The regression ESL slope for the low intertidal zone and the general ESL for the mid intertidal zone produced model results with the lowest error (Table A.5). The ESL slope did not affect the minimum, range (Fig. 3.5A), or error (Table A.5) of the model predictions for the high intertidal zone.

Table A.5 Errors between the mussel body temperatures predicted by the general model with varying values of ESL slope and the logger field measurements in the low, mid and high intertidal zones. The errors were determined for each change in parameter using the daily maximum temperature. The values that are used in the general model for each intertidal zone are bolded and the second value for each intertidal zone is the regression ESL slope. The total number of stressful days recorded by the loggers in the field is 1, 20 and 163 for the low, mid and high intertidal zones, respectively.

Intertidal Zone	ESL slope (m)	Avg. Diff. (°C)	Abs. Avg. Diff. (°C)	RMSE (°C)	Stressful Days	False Pos.	False Neg.
Low	**0.25**	-1.39	2.44	3.04	0	0	1
	0.06	-0.43	2.32	2.99	0	0	1
Mid	**0.25**	-1.86	3.05	3.98	2	2	20
	0.16	-1.21	3.07	4.03	2	2	20
High	**0.25**	-4.77	5.63	6.89	4	2	161
	0.12	-4.74	5.63	6.89	4	2	161

The model for the low intertidal zone underestimated the number of cold and high sublethal temperatures and overestimated the number of optimal temperatures using both ESL slopes. However, the model using the regression ESL slope underestimated more cold days (90) and overestimated more optimal days (89) than the model using the general ESL slope. The regression ESL slope caused the model for the low zone to overestimate high suboptimal temperatures while the general ESL slope caused the model to underestimate high suboptimal temperatures. The model using both ESL slopes caused the model to underestimate the number of high sublethal temperatures by one day (Fig. 3.5B).

Both ESL slopes used in the model for the mid intertidal zone overestimated the number of temperatures within the cold and optimal categories and underestimated the number of temperatures within the high suboptimal and high sublethal categories. The model using the general ESL slope overestimated more cold days (129) and underestimated more high suboptimal days (146) than the model using the regression ESL slope, while the model using the regression ESL slope overestimated more optimal days (98) than the model using the general ESL slope. Both ESL slopes caused the model to underestimate the number of high sublethal temperatures by 19 days (Fig. 3.5B).

Similarly, for the high intertidal zone, the model using both ESL slopes overestimated the number of cold and optimal temperatures and underestimated the number of high suboptimal and high sublethal temperatures. The general ESL slope caused the model to overestimate more cold days (321) and more high suboptimal days (380), while the regression ESL slope caused the model to overestimate more optimal days (220). Both ESL slopes caused the model to underestimate the number of high sublethal temperatures by 152 days (Fig. 3.5B).

Model predictions were less accurate for the high intertidal zone and all of the **ASL & ESL slope combinations** caused the model to underestimate temperatures (negative average difference), except for the low logger ASL & regression ESL slope (positive average difference). The change in ASL & ESL slope combination for the low intertidal zone did not affect the number of stressful days, false positives or false negatives. The high intertidal zone had the greatest number of false negatives and the low intertidal zone had the least. For the low intertidal zone, the general ASL (MLLW + 0.5 m) & ESL slope (0.25 m) produced the least accurate temperatures. For the mid intertidal

zone the regression ASL (MLLW + 1.13 m) & ESL slope (0.16 m) was the least accurate. The regression ASL (MLLW + 1.27 m) & ESL slope (0.12 m) for the high intertidal zone provided the least accurate model predictions (Table A.6).

Table A.6 Errors between the mussel body temperatures predicted by the general model with varying values of ASL and ESL slope in combination and the logger field measurements in the low, mid and high intertidal zones. The errors were determined for each change in parameter using the daily maximum temperature. The ASL and ESL slope values that are used in the general model for each intertidal zone are bolded. For each intertidal zone the second set of values is the logger ASL and regression ESL slope and the third set of values is the regression ASL and regression ESL slope. The total number of stressful days recorded by the loggers in the field is 1, 20 and 163 for the low, mid and high intertidal zones, respectively.

Intertidal Zone	ASL (m) ESL slope (m)	Avg. Diff. (°C)	Abs. Avg. Diff. (°C)	RMSE (°C)	Stressful Days	False Pos.	False Neg.
Low	**0.5 0.25**	-1.39	2.44	3.04	0	0	1
	0.69 0.06	0.13	2.37	3.08	0	0	1
	0.43 0.06	-0.62	2.35	3.01	0	0	1
Mid	**1.5 0.25**	-1.85	3.04	3.97	1	1	20
	1.36 0.16	-1.67	3.02	3.96	2	2	20
	1.13 0.16	-2.83	3.42	4.42	1	1	20
High	**2.5 0.25**	-4.77	5.62	6.88	4	2	161
	1.56 0.12	-5.23	5.79	7.02	4	2	161
	1.27 0.12	-6.12	6.37	7.62	3	1	161

The maximum temperature predicted was not altered by changes in the ASL & ESL slope combinations for the mid or high intertidal zones but for the low intertidal zone the model using the logger ASL & regression ESL slope combination produced the highest maximum temperature. For the low intertidal zone, the model using the general

ASL & ESL slope combination had the lowest mean, lowest minimum, largest range (Fig. 3.6A), and highest error (Table A.6), while the model using the logger ASL & regression ESL slope combination had the highest mean (Fig. 3.6A) and smallest error (Table A.6). For the mid intertidal zone the logger ASL & regression ESL slope model predictions had the highest mean and smallest range (Fig. 3.6A). The model predictions using the regression ASL & ESL slope had the lowest mean and minimum, largest range (Fig. 3.6A) and highest error (Table A.6). The model predictions using the general ASL & ESL slope had the highest mean and minimum, smallest range (Fig. 3.6A) and lowest error (Table A.6). The model predictions using regression ASL & ESL slope had the lowest mean and minimum, largest range (Figure 3.6A) and the largest error (Table A.6).

For the low intertidal zone, all three ASL and ESL slope combinations caused the model to underestimate the number of cold and high sublethal temperatures and overestimate the number of optimal temperatures. The model using the general ASL & ESL slope caused the model to underestimate the number of high suboptimal temperatures while the other two combinations caused the model to overestimate temperatures in this category. All combinations led to the model underestimating the number of high sublethal temperatures by one day. The model using the logger ASL and regression ESL slope caused the model to underestimate the highest number of days in the cold suboptimal/sublethal category (117) and overestimate the greatest number of optimal (114) and high suboptimal (4) days (Fig. 3.6B).

The model using all three combinations for the mid intertidal zone overestimated the number of cold temperatures and underestimated the number of high suboptimal and high sublethal temperatures. Using the regression ASL and ESL slope, the model

overestimated the greatest number of days in the cold category (255) and underestimated the greatest number of days in the high suboptimal (184) and high sublethal (20) categories. This combination also led to the model underestimating the number of optimal temperatures whereas the other two combinations led to the model overestimating temperatures in this category (Fig. 3.6B).

All three combinations for the high intertidal zone caused the model to overestimate the number of cold temperatures by more than 300 days and the number of optimal temperatures by more than 100 days. The number of high suboptimal temperatures were underestimated by more than 300 days using all three combinations as were the number of high sublethal temperatures, but these were only underestimated by a little more than 150 days. Similar to the mid intertidal zone, the model using the regression ASL and ESL slope overestimated the highest number of cold temperatures (488) and underestimated the highest number of high suboptimal (438) and high sublethal (153) temperatures. The model using the general ASL and ESL slope caused the model to overestimate the highest number of optimal temperatures (216 days) (Fig. 3.6B).

APPENDIX B: DETAILED RESULTS FOR THE ACCURACY ASSESSMENT

At **Bodega Bay**, for all three intertidal zones, the model using CFSR data predicts temperatures that are closer to the temperatures recorded by the loggers in the field. The model using CFSR data generally predicts temperatures higher than those predicted by the model using LWS data. The model using both types of weather data predicted temperatures lower than those recorded by the loggers in the field and the logger monthly maximum average daily maximum temperature was greater than that predicted by both of the models (Fig. B.1-B.3). The maximum temperature recorded by the logger was 31.09°C, 35.28°C, and 42.83°C for the low, mid and high intertidal zone, respectively. The maximum temperature predicted by the model using LWS data was 28.14°C, 30.78°C, and 32.38°C for the low, mid and high intertidal zone respectively. Finally, the model using CFSR data predicted a maximum temperature of 30.19°C, 32.77°C, and 33.12°C for the low, mid and high intertidal zone, respectively.

The model using LWS data was more accurate when predicting the number of daily maximum temperatures within the optimal range for all three intertidal zones. The model using CFSR data had better accuracy when predicting the number of daily maximum temperatures within the high sublethal ranges for all three intertidal zones. The accuracy of the model using LWS data was better for predicting the number of daily maximum temperatures within the cold suboptimal/sublethal range for the low intertidal zone but the model using CFSR data was more accurate at predicting temperatures within this range for the mid and high intertidal zones. The model using CFSR data was able to

more accurately predict temperatures within the high suboptimal range for the mid and high intertidal zones (Table B.1).

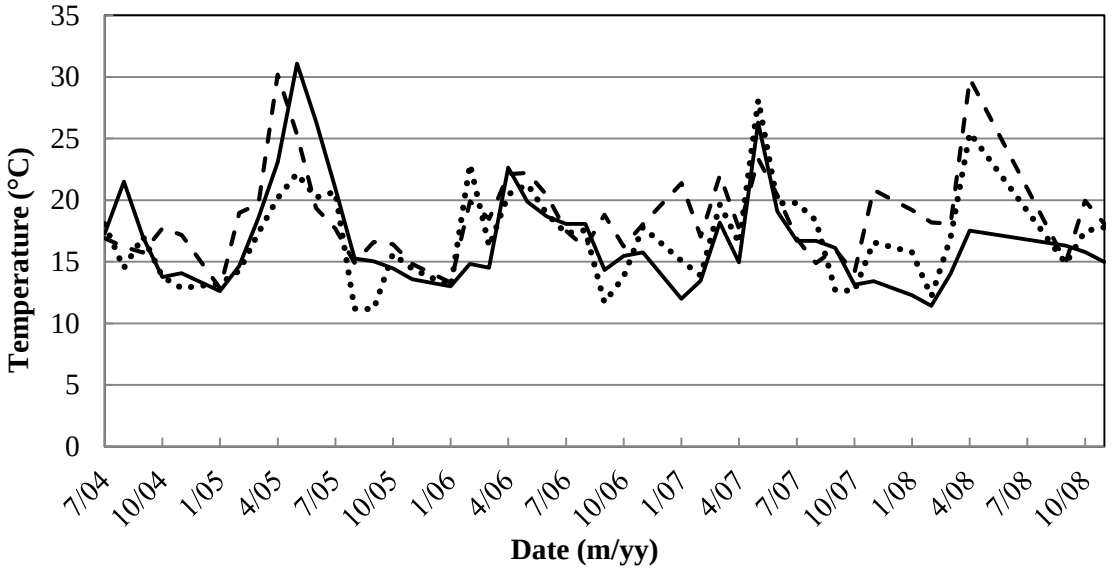

Figure B.1 Monthly maximum temperatures for the model using LWS data, the model using CFSR data and the logger measurements for the low intertidal zone at Bodega Bay. The time frame can be found in Table 2.1 (N = 45 months). The solid line represents the logger temperatures, dotted line are the temperatures predicted by the model using LWS data and the dashed line represents the model using CFSR data.

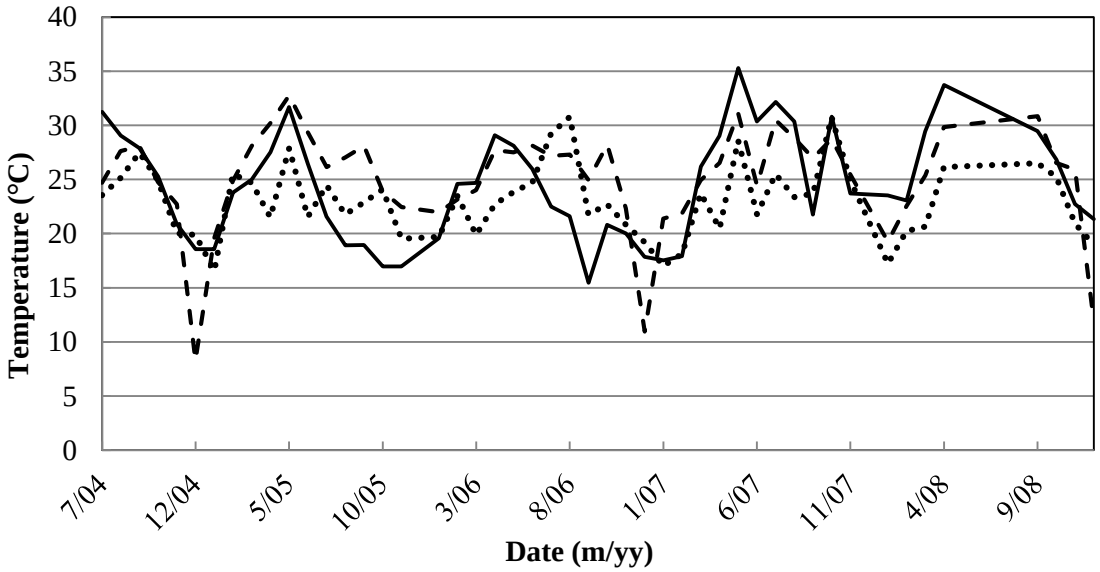

Figure B.2: Monthly maximum temperatures for the model using LWS data, the model using CFSR data and the logger measurements for the mid intertidal zone at Bodega Bay. The time frame can be found in Table 2.1 (N = 48 months). The solid line represents the

logger temperatures, dotted line are the temperatures predicted by the model using LWS data and the dashed line represents the model using CFSR data.

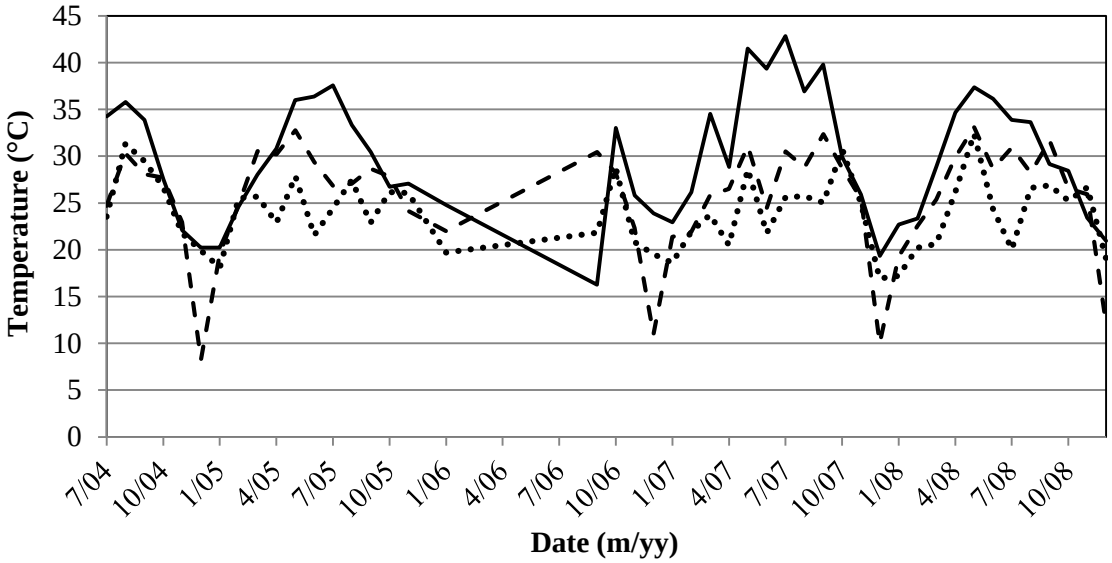

Figure B.3 Monthly maximum temperatures for the model using LWS data, the model using CFSR data and the logger measurements for the high intertidal zone at Bodega Bay. The time frame can be found in Table 2.1 (N = 46 months). The solid line represents the logger temperatures, dotted line are the temperatures predicted by the model using LWS data and the dashed line represents the model using CFSR data.

Table B.1 Distribution of daily maximum temperatures predicted by the general LWS model, general CFSR model and the measured logger temperatures for the low, mid and high intertidal zones at Bodega Bay. The false positives and false negatives were obtained by comparing the model predictions to the logger measurements. The threshold for false positives and false negatives was set to 30°C. The percentage of each was obtained by dividing the number of false positives/negatives by the total number of days in the time series (N) for that intertidal zone.

Intertidal Zone	Data Used	Number of temperatures (°C): < 17	17 – 22	22 – 30	30 – 38	≥ 38	Percentage of: False Pos.	False Neg.
Low	Logger	465	35	11	1	0		
	LWS	445	63	4	0	0	0%	0.20%
	CFSR	429	73	9	1	0	0.20%	0.20%
Mid	Logger	600	387	226	21	0		
	LWS	726	424	82	2	0	0.15%	1.51%
	CFSR	515	538	177	4	0	0.15%	1.36%
High	Logger	245	268	506	156	7		
	LWS	543	506	129	4	0	0.17%	13.6%
	CFSR	323	603	245	11	0	0.59%	13.5%

At **Hopkins**, the model using CFSR data predicted temperatures that are closer to the temperatures recorded by the loggers for the low and mid intertidal zones and for the mid intertidal zone the model using LWS data predicted temperatures closer to those recorded by the loggers in the field. Like Bodega Bay, the model using CFSR data generally predicted temperatures higher than those predicted by the model using LWS data. Overall, the model using CFSR data predicted the highest temperatures, followed by the logger measurements then the temperatures predicted by the model using LWS data (Fig. B.4-B.6).

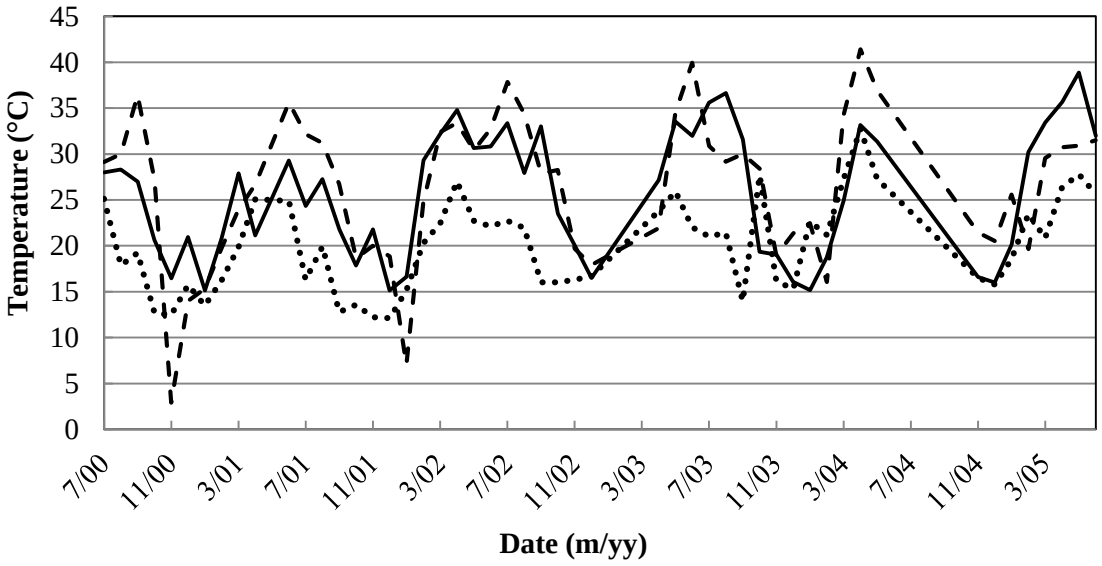

Figure B.4 Monthly maximum temperatures for the model using LWS data, the model using CFSR data and the logger measurements for the low intertidal zone at Hopkins. The time frame can be found in Table 2.1 (N = 51 months). The solid line represents the logger temperatures, dotted line are the temperatures predicted by the model using LWS data and the dashed line represents the model using CFSR data.

The maximum temperature recorded by the logger was 38.87°C, 40.79°C, and 43.83°C for the low, mid and high intertidal zone, respectively. The maximum temperature predicted by the model using LWS data was 32.73°C, 42.08°C, and 42.08°C for the low, mid and high intertidal zone respectively. Finally, the model using CFSR

data predicted a maximum temperature of 41.39°C, 44.31°C, and 44.31°C for the low, mid and high intertidal zone, respectively.

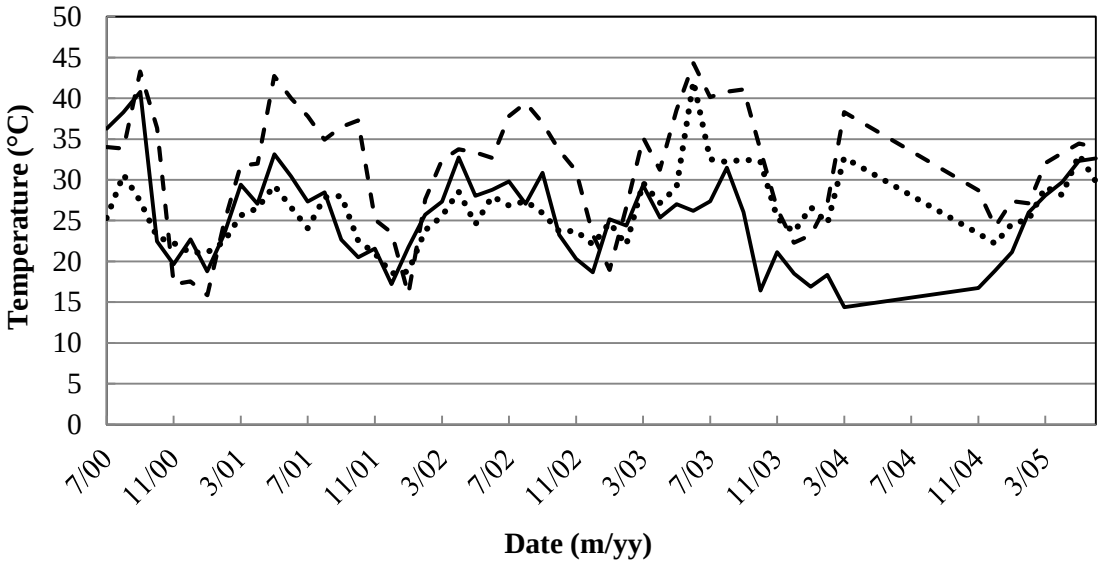

Figure B.5 Monthly maximum temperatures for the model using LWS data, the model using CFSR data and the logger measurements for the mid intertidal zone at Hopkins. The time frame can be found in Table 2.1 (N = 53 months). The solid line represents the logger temperatures, dotted line are the temperatures predicted by the model using LWS data and the dashed line represents the model using CFSR data.

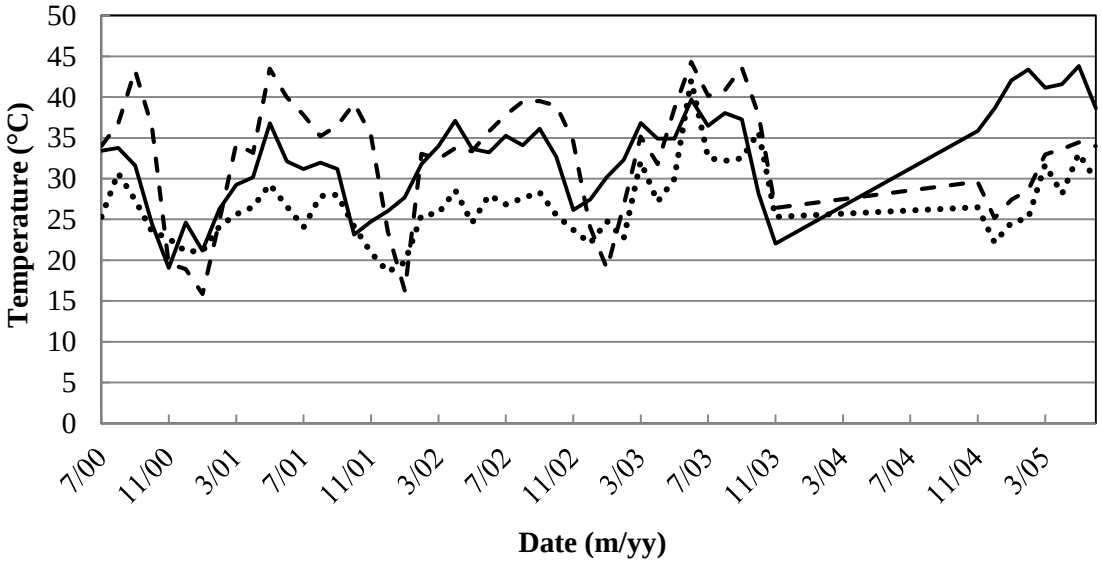

Figure B.6 Monthly maximum temperatures for the model using LWS data, the model using CFSR data and the logger measurements for the high intertidal zone at Hopkins. The time frame can be found in Table 2.1 (N = 49 months). The solid line represents the

logger temperatures, dotted line are the temperatures predicted by the model using LWS data and the dashed line represents the model using CFSR data.

The model using LWS data was able to more accurately predict the number of daily maximum temperatures within cold suboptimal/sublethal, optimal and high sublethal and high lethal range for the mid intertidal zone and the high suboptimal range for the mid and high intertidal zones. The model using CFSR data more accurately predicted daily maximum temperatures for the cold suboptimal/sublethal, optimal, and high sublethal ranges for the low and mid intertidal zones, the number of high suboptimal temperatures for the low zone and the number of high lethal temperatures for the high intertidal zone (Table B.2).

Table B.2 Distribution of daily maximum temperatures predicted by the general LWS model, general CFSR model and the measured logger temperatures for the low, mid and high intertidal zones at Hopkins. The false positives and false negatives were obtained by comparing the model predictions to the logger measurements. The threshold for false positives and false negatives was set to 30°C. The percentage of each was obtained by dividing the number of false positives/negatives by the total number of days in the time series (N) for that intertidal zone.

Intertidal Zone	Data Used	Number of temperatures (°C):					Percentage of:	
		< 17	17 – 22	22 – 30	30 – 38	≥ 38	False Pos.	False Neg.
Low	Logger	220	170	193	56	1		
	LWS	479	98	60	3	0	0%	8.44%
	CFSR	377	117	104	40	2	4.84%	7.34%
Mid	Logger	735	464	328	26	2		
	LWS	486	599	451	17	2	1.03%	1.61%
	CFSR	436	285	563	253	18	16.7%	1.35%
High	Logger	392	354	414	247	36		
	LWS	210	674	533	24	2	0.83%	18.6%
	CFSR	285	229	585	318	26	16.6%	12.6%

At **Alegria**, the model predicted temperatures that are closer to the temperatures recorded by the loggers for the low intertidal zone. The model predicted temperatures higher than those recorded by the loggers in the field for the mid and high intertidal zones

but recorded lower temperatures for the low intertidal zone (Fig. B.7-B.9). The maximum temperature recorded by the logger was 46.97°C, 44.38°C, and 44.14°C for the low, mid and high intertidal zone, respectively. The maximum temperature predicted by the model was 46.85°C, 53.90°C, and 53.90°C for the low, mid and high intertidal zone respectively.

The model for the low intertidal zone predicted a more accurate number of temperatures within the optimal, high suboptimal, high sublethal and high lethal categories. The model for the mid intertidal zone predicted a more accurate number of temperatures within the cold suboptimal/sublethal category. The model for the low intertidal zone was poor at predicting the correct number of cold temperatures, the model for the mid intertidal zone was poor at predicting the correct number of high sublethal and high lethal temperatures and the model for the high intertidal zone was least able to predict the correct number of optimal and high suboptimal temperatures (Table B.4).

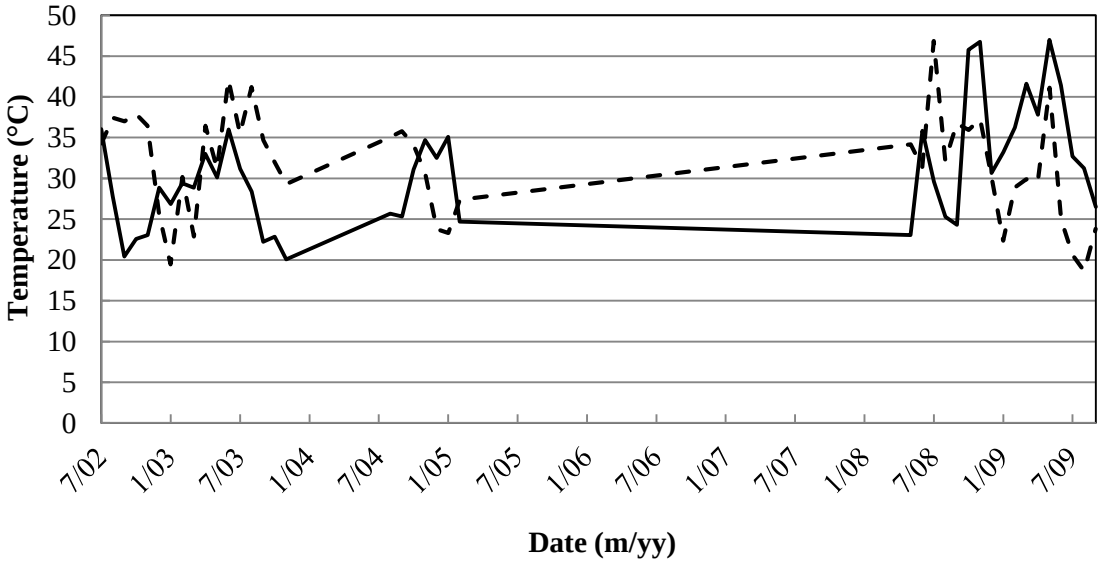

Figure B.7 Monthly maximum temperatures for the model using LWS data, the model using CFSR data and the logger measurements for the low intertidal zone at Alegria. The time frame can be found in Table 2.1 (N = 41 months). The solid line represents the

logger temperatures, dotted line are the temperatures predicted by the model using LWS data and the dashed line represents the model using CFSR data.

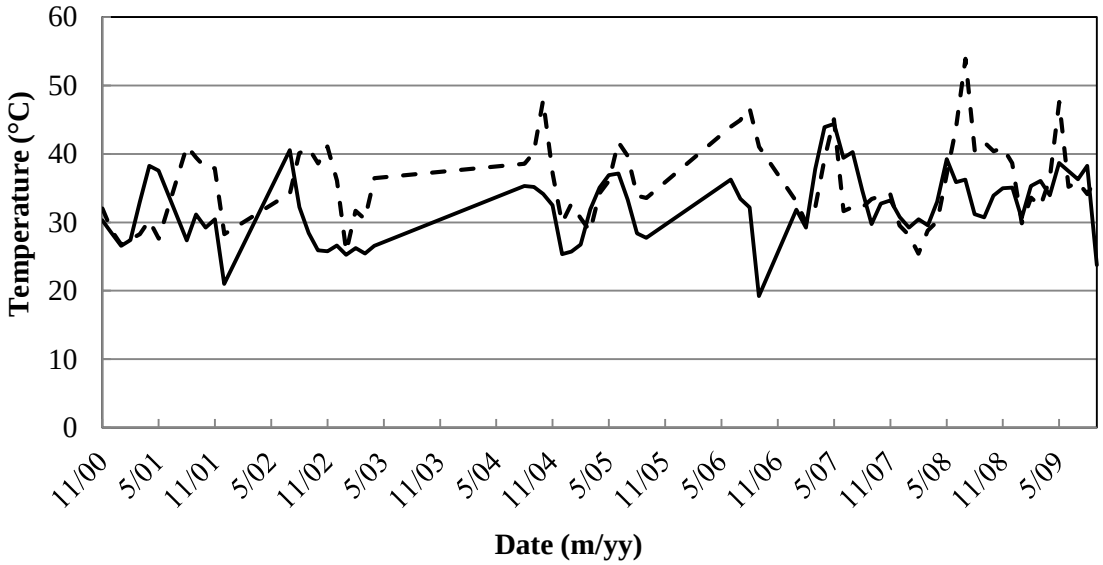

Figure B.8 Monthly maximum temperatures for the model using LWS data, the model using CFSR data and the logger measurements for the mid intertidal zone at Alegria. The time frame can be found in Table 2.1 (N = 73 months). The solid line represents the logger temperatures, dotted line are the temperatures predicted by the model using LWS data and the dashed line represents the model using CFSR data.

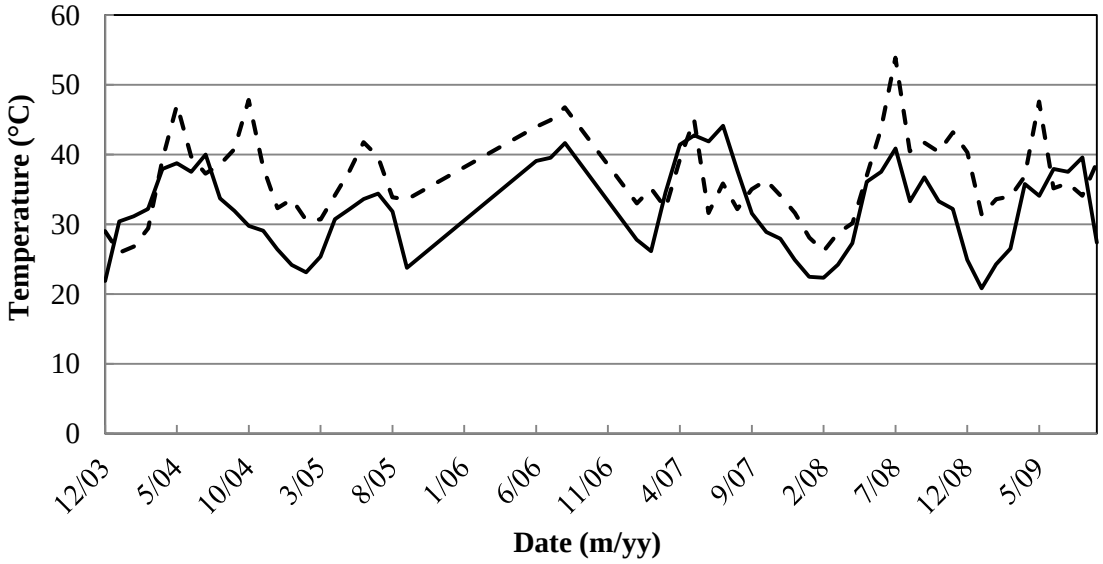

Figure B.9 Monthly maximum temperatures for the model using LWS data, the model using CFSR data and the logger measurements for the high intertidal zone at Alegria. The time frame can be found in Table 2.1 (N = 58 months). The solid line represents the logger temperatures, dotted line are the temperatures predicted by the model using LWS data and the dashed line represents the model using CFSR data.

Table B.3 Distribution of daily maximum temperatures predicted by the general CFSR model and the measured logger temperatures for the low, mid and high intertidal zones at Alegria. The false positives and false negatives were obtained by comparing the model predictions to the logger measurements. The threshold for false positives and false negatives was set to 30°C. The percentage of each was obtained by dividing the number of false positives/negatives by the total number of days in the time series (N) for that intertidal zone.

Intertidal Zone	Data Used	Number of temperatures (°C):					Percentage of:	
		< 17	17–22	22–30	30–38	≥ 38	False Pos.	False Neg.
Low	Logger	83	307	140	40	18		
	CFSR	245	143	121	72	7	11.7%	8.16%
Mid	Logger	294	627	793	252	20		
	CFSR	224	338	888	461	75	21.8%	8.56%
High	Logger	200	576	583	282	29		
	CFSR	127	243	763	465	72	23.8%	10.3%

At **Coal Oil Point**, the model for the low intertidal zone predicted temperatures that are closer to the temperatures recorded by the loggers. The model predicted temperatures higher than those recorded by the loggers in the field for all three intertidal zones (Fig. B.7-B.9). The maximum temperature recorded by the logger was 33.22°C, 36.62°C, and 41.40°C for the low, mid and high intertidal zone, respectively. The maximum temperature predicted by the model was 43.74°C, 47.23°C, and 47.23°C for the low, mid and high intertidal zone respectively.

The model for the low intertidal zone predicted a more accurate number of temperatures within the high suboptimal, high sublethal and high lethal and categories. The model for the high intertidal zone predicted a more accurate number of temperatures within the cold suboptimal/sublethal and optimal categories. The model for the low intertidal zone was poor at predicting the correct number of cold temperatures, the model for the mid intertidal zone was poor at predicting the correct number of optimal, high

suboptimal, and high sublethal temperatures and the model for the high intertidal zone was least able to predict the correct number of high lethal temperatures (Table B.4).

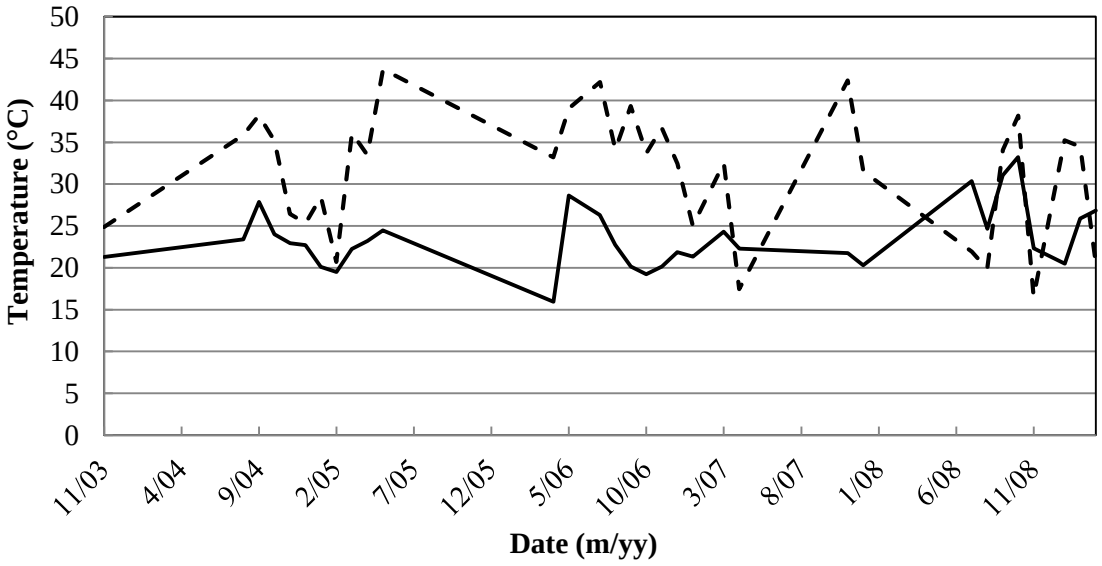

Figure B.10 Monthly maximum temperatures for the model using LWS data, the model using CFSR data and the logger measurements for the low intertidal zone at Coal Oil Point. The time frame can be found in Table 2.1 (N = 32 months). The solid line represents the logger temperatures, dotted line are the temperatures predicted by the model using LWS data and the dashed line represents the model using CFSR data.

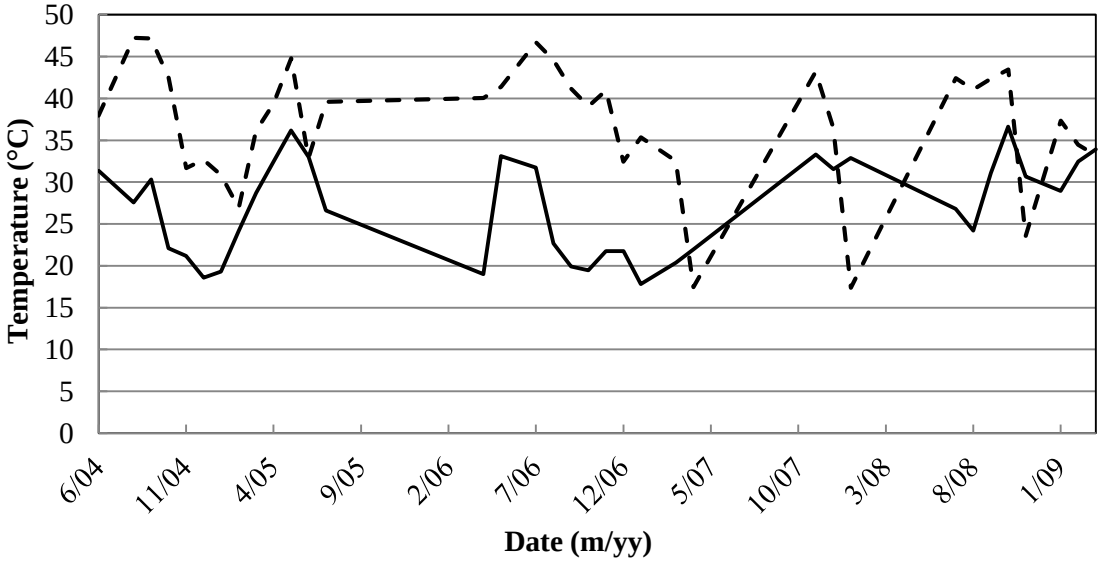

Figure B.11 Monthly maximum temperatures for the model using LWS data, the model using CFSR data and the logger measurements for the mid intertidal zone at Coal Oil Point. The time frame can be found in Table 2.1 (N = 35 months). The solid line

represents the logger temperatures, dotted line are the temperatures predicted by the model using LWS data and the dashed line represents the model using CFSR data.

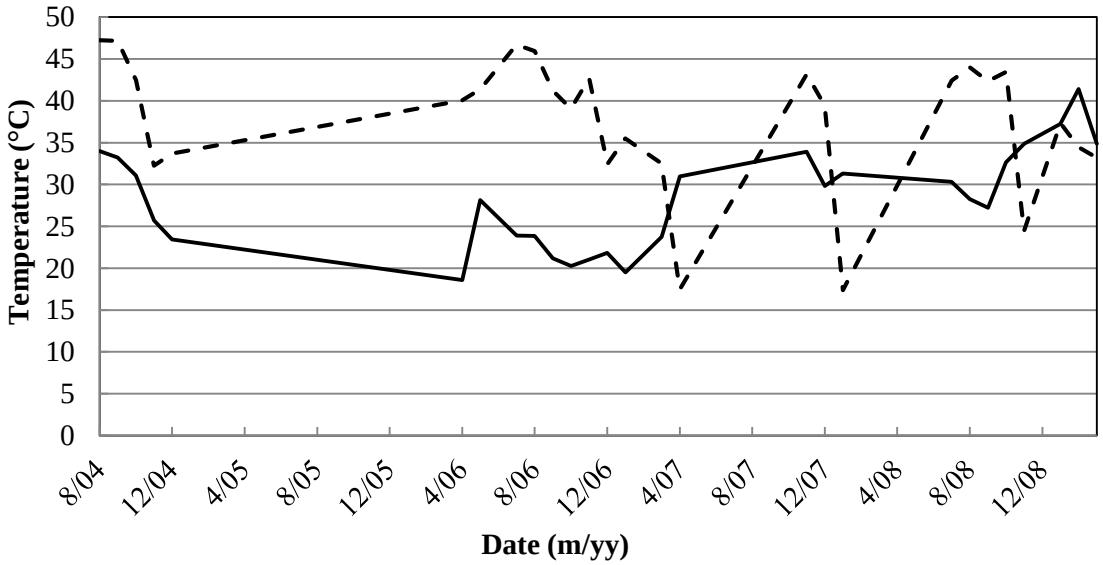

Figure B.12 Monthly maximum temperatures for the model using LWS data, the model using CFSR data and the logger measurements for the high intertidal zone at Coal Oil Point. The time frame can be found in Table 2.1 (N = 27 months). The solid line represents the logger temperatures, dotted line are the temperatures predicted by the model using LWS data and the dashed line represents the model using CFSR data.

Table B.4 Distribution of daily maximum temperatures predicted by the general CFSR model and the measured logger temperatures for the low, mid and high intertidal zones at Coal Oil Point. The false positives and false negatives were obtained by comparing the model predictions to the logger measurements. The threshold for false positives and false negatives was set to 30°C. The percentage of each was obtained by dividing the number of false positives/negatives by the total number of days in the time series (N) for that intertidal zone.

Intertidal Zone	Data Used	Number of temperatures (°C): < 17	17–22	22–30	30–38	≥ 38	Percentage of: False Pos.	False Neg.
Low	Logger	150	281	67	2	0		
	CFSR	204	118	115	51	12	12.4%	0.20%
Mid	Logger	208	362	172	24	0		
	CFSR	89	140	247	206	84	35.6%	0.91%
High	Logger	90	339	145	32	2		
	CFSR	40	85	194	193	96	43.3%	1.32%

APPENDIX C: DETAILED RESULTS FOR CHANGING WAVE CLIMATES

In **Bodega Bay**, as wave height decreased, for the low and mid intertidal zones the number of cold temperatures decreased and the number of optimal and high suboptimal temperatures increased. For the high intertidal zone the number of cold and temperatures decreased and the number of temperatures within the high suboptimal range increased. The only change that occurred for stressful temperatures was for the mid intertidal zone where the number of these temperatures increased as wave height was decreased (Table C.1 & Fig. C.1).

As wave height increased, the number of cold temperatures increased and the number of optimal and high suboptimal temperatures decreased. The only change in the number of stressful temperatures occurred again for the mid intertidal zone where there were fewer temperatures as wave height increased. Decreasing or increasing the significant wave height did not have an impact on the number of temperatures within the high lethal range (Table C.1 & Fig. C.1).

For the low intertidal zone, as the significant wave height was increased in the model, the temperature remained within the optimal range and only decreased 0.41°C. The temperature for the mid intertidal zone remained within the high suboptimal range, decreasing 1.03°C when the wave height was increased and increasing 0.09°C when the wave height was decreased. The temperature for the high intertidal zone remained within the high suboptimal range and did not change at all with any change in significant wave height in the model (Fig. 3.15).

Table C.1 Temperatures predicted by the general model with increasing and decreasing significant wave heights for the low, mid and high intertidal zones at Bodega Bay. Daily maximum body temperatures are thermally categorized.

Intertidal Zone	Sig. Wave Height Δ (%)	Number of Temperatures in Thermal Category: < 17°C	17 – 22°C	22 – 30°C	30 – 38°C	≥ 38°C
Low	–50	411	141	19	1	0
	–40	416	137	18	1	0
	–30	421	133	17	1	0
	–20	424	130	17	1	0
	–10	430	125	16	1	0
	0	435	123	13	1	0
	+10	438	120	13	1	0
	+20	442	116	13	1	0
	+30	449	109	13	1	0
	+40	453	106	12	1	0
	+50	455	105	11	1	0
Mid	–50	382	714	257	11	0
	–40	400	704	250	10	0
	–30	417	696	242	9	0
	–20	444	682	229	9	0
	–10	472	665	218	9	0
	0	509	643	204	8	0
	+10	546	619	191	8	0
	+20	587	591	179	7	0
	+30	618	572	167	7	0
	+40	647	552	158	7	0
	+50	675	536	146	7	0
High	–50	359	745	318	13	0
	–40	359	745	318	13	0
	–30	359	745	318	13	0
	–20	359	745	318	13	0
	–10	359	747	316	13	0
	0	360	747	315	13	0
	+10	365	742	315	13	0
	+20	365	742	315	13	0
	+30	368	741	313	13	0
	+40	373	737	312	13	0
	+50	376	734	312	13	0

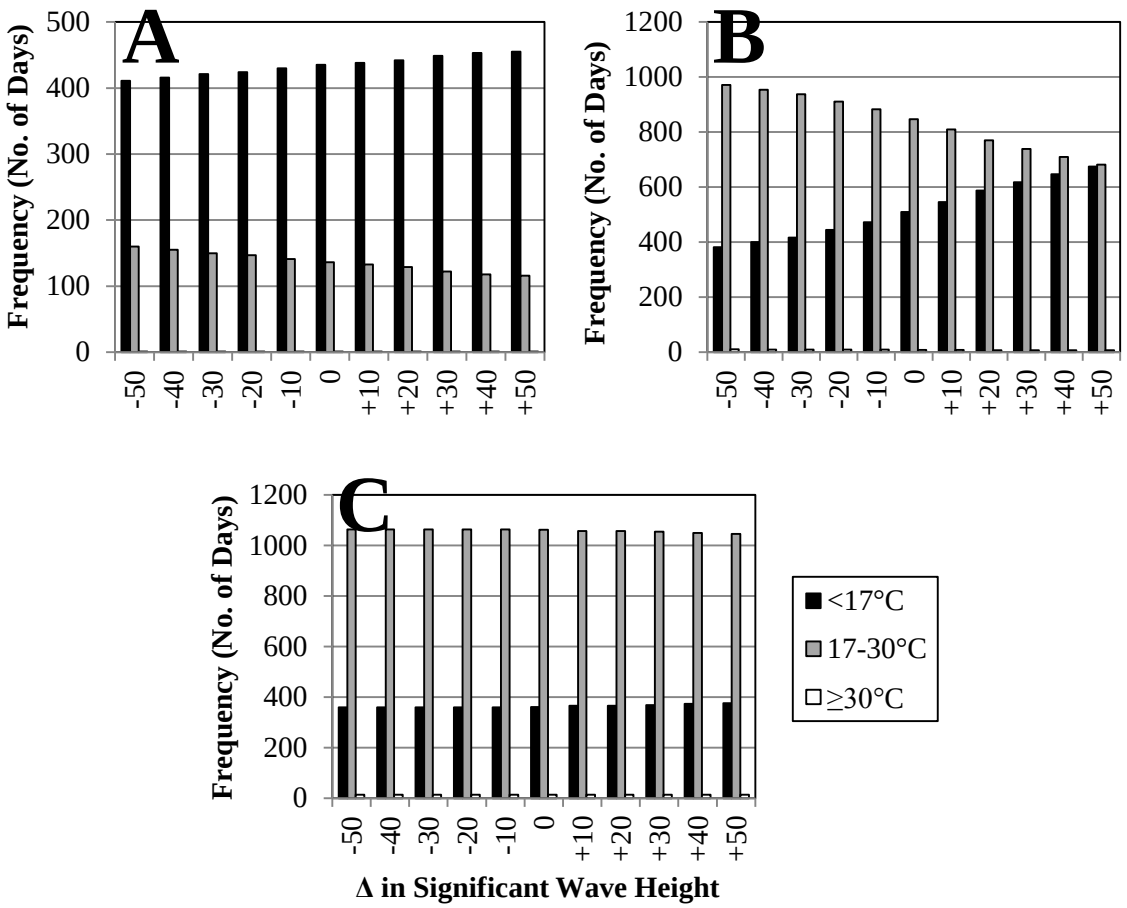

Figure C.1 Average daily maximum temperatures predicted by the general model with increasing and decreasing significant wave heights for Bodega Bay. The results are shown for the **(A)** low, **(B)** mid and **(C)** high intertidal zones.

For **Hopkins**, as wave height decreased, for the low intertidal zone the number of cold temperatures decreased and the number of optimal, high suboptimal, and stressful temperatures increased. For the mid intertidal zone the number of cold and optimal temperatures decreased and the number of high suboptimal and stressful temperatures increased. For the high intertidal zone the number of cold temperatures decreased while the number of optimal temperatures increased. The high suboptimal and stressful temperatures were not affected by decreasing the significant wave height in the model for the high intertidal zone. For all three intertidal zones increasing the significant wave

height caused the number of cold temperatures to increase and the number of optimal, high suboptimal and stressful temperatures to decrease (Table C.2 & Fig. C.2).

Table C.2 Temperatures predicted by the general model with increasing and decreasing significant wave heights for the low, mid and high intertidal zone at Hopkins. Daily maximum body temperatures are thermally categorized.

Intertidal Zone	Sig. Wave Height Δ (%)	Number of Temperatures in Thermal Category: < 17°C	17 – 22°C	22 – 30°C	30 – 38°C	≥ 38°C
Low	–50	256	129	163	52	2
	–40	267	125	157	51	2
	–30	280	119	154	48	1
	–20	281	123	151	46	1
	–10	282	127	147	46	0
	0	292	124	141	45	0
	+10	302	119	137	44	0
	+20	312	115	135	40	0
	+30	321	110	133	38	0
	+40	325	107	134	36	0
	+50	338	99	130	35	0
Mid	–50	304	294	738	365	31
	–40	308	301	735	357	31
	–30	322	301	727	351	31
	–20	337	303	718	347	27
	–10	360	300	712	334	26
	0	386	306	691	325	24
	+10	408	306	687	308	23
	+20	442	299	672	298	21
	+30	464	304	655	289	20
	+40	505	297	641	269	20
	+50	533	306	624	253	16
High	–50	324	304	747	401	37
	–40	324	304	747	401	37
	–30	324	304	747	401	37
	–20	326	302	747	401	37
	–10	327	301	747	401	37
	0	327	301	747	401	37
	+10	329	301	745	401	37
	+20	331	301	743	401	37
	+30	332	303	741	400	37
	+40	336	301	741	398	37
	+50	340	299	740	397	37

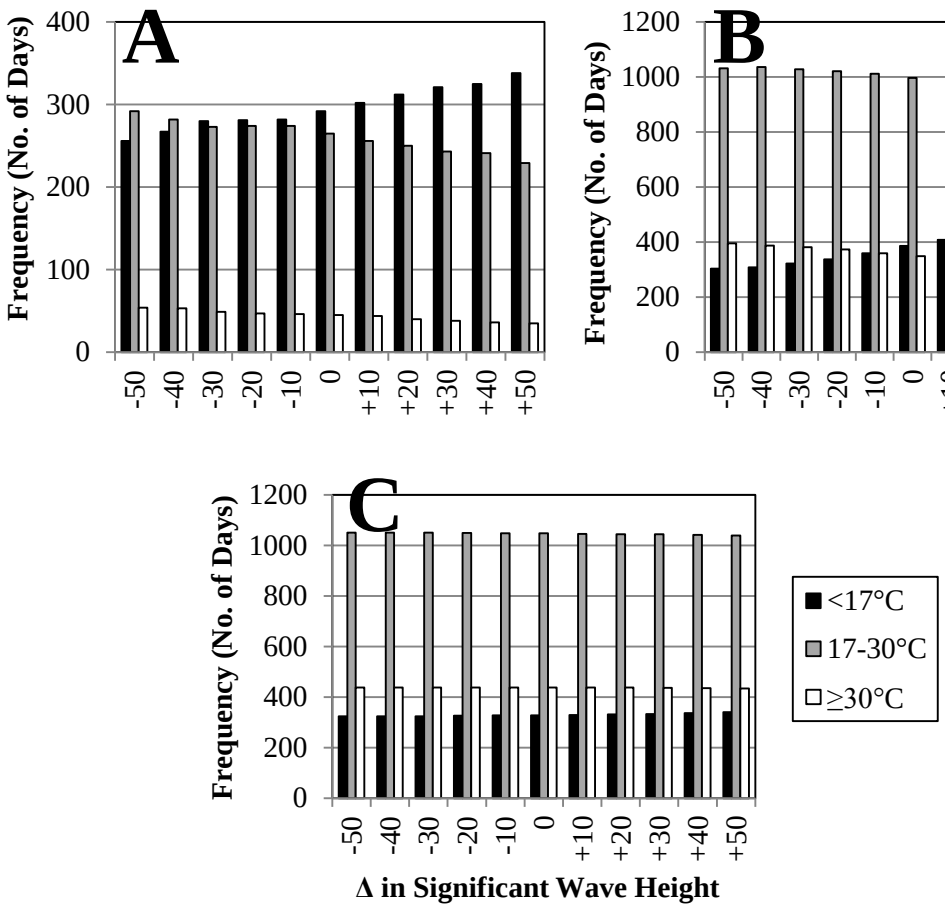

Figure C.2 Average daily maximum temperatures predicted by the general model with increasing and decreasing significant wave heights for Hopkins. The results are shown for the **(A)** low, **(B)** mid and **(C)** high intertidal zones.

For the low intertidal zone, as the significant wave height was increased in the model, the temperature decreased 1.5°C but remained within the sublethal range. When the wave height was decreased the temperature increased 1.36°C but remained within the high sublethal range. For the mid intertidal zone, as the wave height was decreased the temperature increased 0.44°C but remained with the high lethal range. The temperature for the high intertidal zone remained within the high lethal range. It decreased when the significant wave height was decreased in the model and the predicted temperature also decreased when the wave height was increased in the model. It should be noted that the

decrease was extremely small (< 0.0001°C) for decreasing and increasing significant wave height in the model) (Fig. 3.16).

For **Alegria**, as the significant wave height was decreased, for the low intertidal zone the number of cold temperatures decreased and the number of optimal, high suboptimal and stressful temperatures increased. For the mid intertidal zone the number of cold, optimal and high suboptimal temperatures decreased and the number of stressful temperatures increased. For the high intertidal zone the number of cold temperatures decreased and the number of optimal, high suboptimal and stressful temperatures increased (Table C.3 & Fig. C.3).

Table C.3 Temperatures predicted by the general model with increasing and decreasing significant wave heights for the low, mid and high intertidal zone at Alegria. Daily maximum body temperatures are thermally categorized.

Intertidal Zone	Sig. Wave Height Δ (%)	Number of Temperatures in Thermal Category: < 17°C	17 – 22°C	22 – 30°C	30 – 38°C	≥ 38°C
Low	–50	514	558	1000	477	49
	–40	549	546	986	470	47
	–30	584	545	965	459	45
	–20	613	539	952	450	44
	–10	647	530	935	443	43
	0	686	524	913	432	43
	+10	709	514	908	424	43
	+20	725	513	902	415	43
	+30	747	505	893	410	43
	+40	767	496	888	404	43
	+50	786	492	879	399	42
Mid	–50	191	457	1424	984	152
	–40	198	463	1425	972	150
	–30	208	466	1430	958	146
	–20	213	472	1437	943	143
	–10	226	473	1441	926	142
	0	236	483	1437	916	136
	+10	253	487	1438	896	134
	+20	271	491	1439	877	130
	+30	293	501	1442	847	125
	+40	323	505	1429	832	119

Intertidal Zone	Sig. Wave Height Δ (%)	Number of Temperatures in Thermal Category: < 17°C	17 – 22°C	22 – 30°C	30 – 38°C	≥ 38°C
	+50	345	518	1415	814	116
High	–50	173	444	1410	1028	170
	–40	174	443	1410	1028	170
	–30	175	442	1411	1027	170
	–20	176	441	1411	1027	170
	–10	176	441	1411	1027	170
	0	176	442	1410	1027	170
	+10	177	444	1407	1027	170
	+20	178	446	1405	1026	170
	+30	181	443	1407	1025	169
	+40	181	448	1403	1024	169
	+50	187	447	1399	1024	168

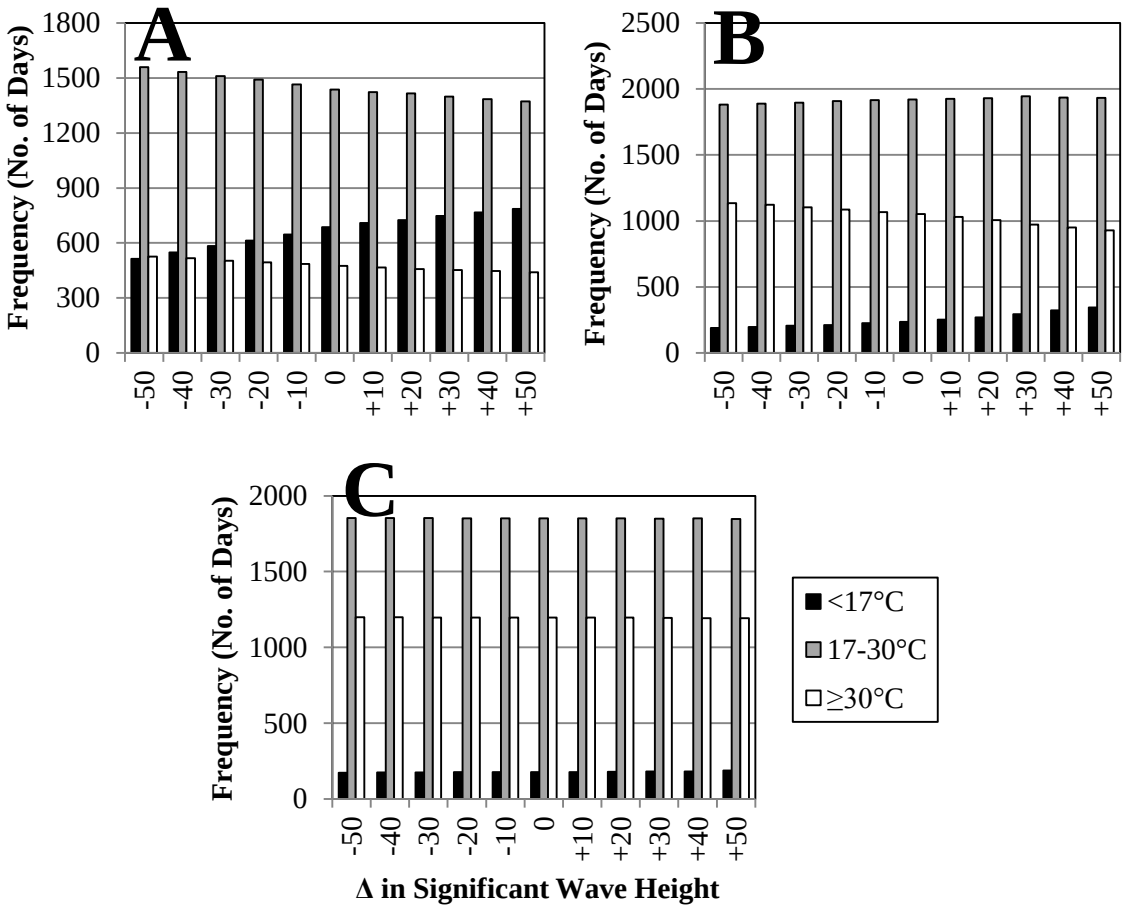

Figure C.3 Average daily maximum temperatures predicted by the general model with increasing and decreasing significant wave heights for Alegria. The results are shown for the **(A)** low, **(B)** mid and **(C)** high intertidal zones.

Increasing the significant wave height for the low intertidal zone caused the number of cold temperatures to increase and the number of optimal, high suboptimal, and stressful temperatures to decrease. For the mid and high intertidal zones the number of cold and optimal temperatures increased and the number of high suboptimal and stressful temperatures decreased (Table C.3 & Fig. C.3).

For the low intertidal zone, as the significant wave height was increased in the model, the temperature decreased 0.63°C but remained within the high sublethal range. When the wave height was decreased the temperature increased 1.12°C but remained within the high sublethal range. As the wave height was increased for the mid intertidal zone, the temperature decreased 0.32°C but remained within the high lethal range. As the wave height was decreased in the model the temperature increased 0.34°C but remained within the high lethal range. The temperature for the high intertidal zone remained within the high lethal range. It increased with decreasing and increasing significant wave heights in the model; however, the increase is extremely small (< 0.0001°C) for decreasing and increasing wave height) (Fig. 3.17).

At **Coal Oil Point**, as the wave height was decreased in the model, for the low intertidal zone the number of cold temperatures decreased and the number of optimal, high suboptimal and stressful temperatures increased. For the mid intertidal zone the number of cold, optimal and high suboptimal temperatures increased and the number of stressful temperatures decreased. For the high intertidal zone the thermal categorization was not affected by decreasing the significant wave height in the model.

Increasing the significant wave height for the low intertidal zone increased the number of cold temperatures predicted and decreased the number of optimal, high

suboptimal and stressful temperatures predicted. For the mid intertidal zone the number of cold, optimal and high suboptimal temperatures increased and the number of stressful temperatures decreased. For the high intertidal zone the number of cold temperatures increased, the number of optimal and high suboptimal temperatures decreased and the number of stressful temperatures were unchanged (Table C.4 & Fig. C.4).

Table C.4 Temperatures predicted by the general model with increasing and decreasing significant wave heights for the low, mid and high intertidal zone at Coal Oil Point. Daily maximum body temperatures are thermally categorized.

Intertidal Zone	Sig. Wave Height Δ (%)	Number of Temperatures in Thermal Category: < 17°C	17 – 22°C	22 – 30°C	30 – 38°C	≥ 38°C
Low	–50	348	262	373	325	114
	–40	357	260	369	324	112
	–30	368	261	361	321	111
	–20	383	260	357	314	108
	–10	396	259	351	308	108
	0	414	251	350	299	108
	+10	428	246	349	292	107
	+20	435	250	344	287	106
	+30	454	243	335	284	106
	+40	467	237	336	276	106
	+50	481	236	326	273	106
Mid	–50	348	262	373	325	114
	–40	125	218	557	818	381
	–30	126	220	557	817	379
	–20	127	230	556	811	375
	–10	133	231	559	807	369
	0	136	230	562	809	362
	+10	138	231	568	806	356
	+20	140	231	571	806	351
	+30	144	235	572	798	350
	+40	153	234	571	795	346
	+50	160	236	571	797	335
High	–50	122	210	534	828	405
	–40	122	210	534	828	405
	–30	122	210	534	828	405
	–20	122	210	534	828	405
	–10	122	210	534	828	405
	0	122	210	534	828	405
	+10	123	209	534	828	405

Intertidal Zone	Sig. Wave Height Δ (%)	Number of Temperatures in Thermal Category: < 17°C	17 – 22°C	22 – 30°C	30 – 38°C	≥ 38°C
	+20	123	209	534	828	405
	+30	123	209	534	828	405
	+40	123	210	533	828	405
	+50	123	210	533	828	405

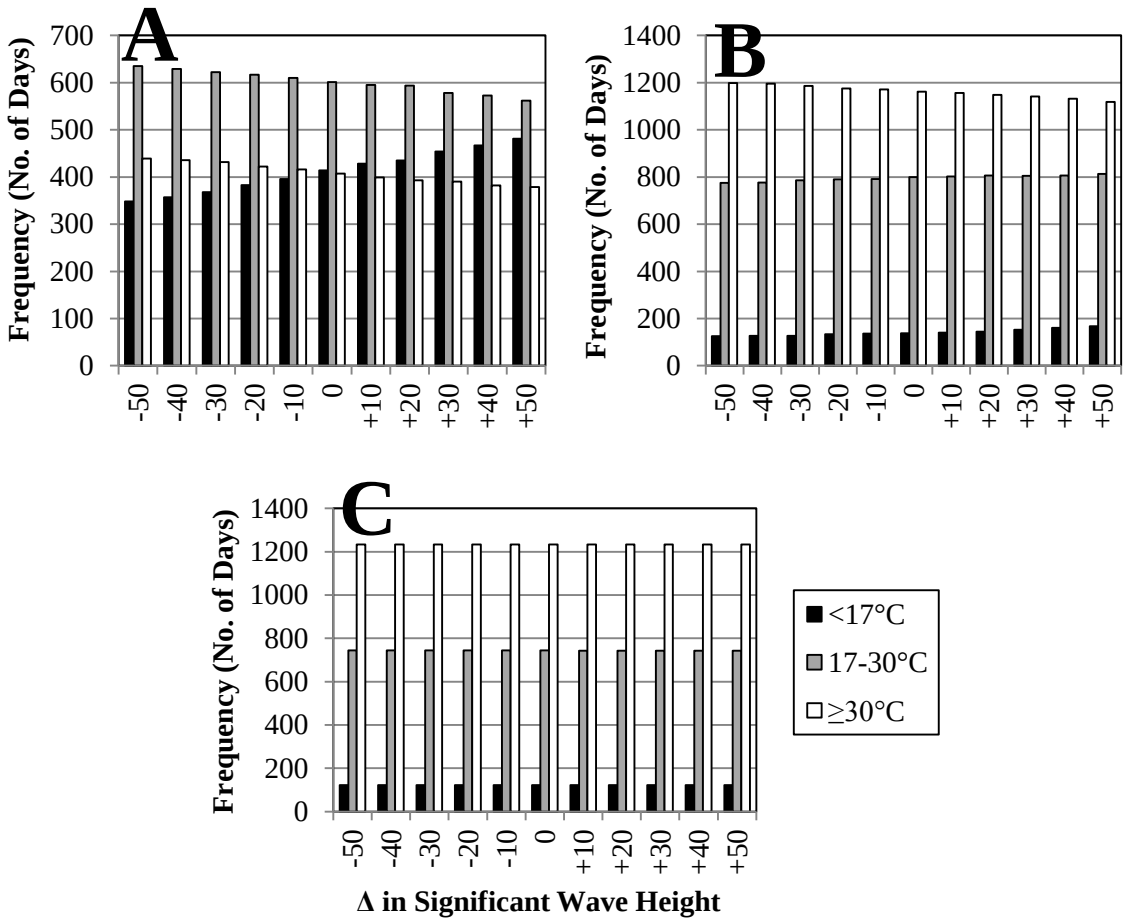

Figure C.4 Average daily maximum temperatures predicted by the general model with increasing and decreasing significant wave heights for Coal Oil Point. The results are shown for the **(A)** low, **(B)** mid and **(C)** high intertidal zones.

For the low intertidal zone, as the significant wave height was increased in the model the temperature decreased 0.56°C but remained within the high lethal range. When the wave height was decreased the temperature increased 1.26°C but remained within the high lethal range. As the wave height was increased for the mid intertidal zone the temperature decreased less than 0.0001°C and remained within the high lethal range. As

the wave height was decreased the temperature increased 0.19°C but remained within the high lethal range. The temperature for the high intertidal zone remained within the high lethal range. It increased with decreasing and increasing significant wave height in the model; however, the increase is extremely small (< 0.0001°C) for decreasing and increasing wave height) (Fig. 3.18).